2008

Small Molecules as Probes for Cell Division and Intracellular Transport

Ulf Peters

SMALL MOLECULES AS PROBES FOR CELL DIVISION AND INTRACELLULAR TRANSPORT

A Thesis Presented to the Faculty of

The Rockefeller University

in Partial Fulfillment of the Requirements for

the degree of Doctor of Philosophy

by

Ulf Peters

June 2008

SMALL MOLECULES AS PROBES FOR CELL DIVISION AND INTRACELLULAR TRANSPORT

Ulf Peters, Ph.D.

The Rockefeller University 2008

Cell-permeable small molecules that can act on their targets on fast time scales are powerful probes of cell division mechanisms and intracellular transport processes. Phenotype-based screens with chemical libraries have been used to identify such inhibitors. However, probes for most proteins are still not available, and the requirements on compound collections to yield such probes are not well understood. Here I present two approaches to find and use such probes.

First, in an attempt to find probes for cell division, I have shown that a small collection of 100 diaminopyrimidines yielded a range of cell division phenotypes, including changes in spindle geometry, chromosome positioning and mitotic index. Monopolar mitotic spindles were induced by 4 inhibitors including one that targets Polo-like kinases, evolutionarily conserved serine/threonine kinases. Using chemical inhibitors and high-resolution live-cell microscopy, I found that Polo-like kinase activity is needed for the assembly and maintenance of bipolar mitotic spindles. Inhibition of Polo-like kinase destabilized kinetochore microtubules while stabilizing other spindle microtubules, leading to monopolar spindles.

Second, I used pigment organelles in *Xenopus* melanophore cells, a specialized intracellular transport system for which the motor proteins driving movement, and primary signals regulating movement, are known, to identify inhibitors of intracellular transport. Screening of an unbiased commercial library yielded a compound, 37P11, that could be characterized as possible inhibitor of a yet unknown element in the regulation of organelle movement. From a collection of diaminopyrimidines, one compound, DAP-29, was identified that potentially targets cytoplasmic dynein, an essential motor protein in many transport processes. Both compounds showed activity in assays in a variety of other intracellular transport systems, highlighting their potential use as biological probes.

My findings indicate that development of new screening systems and further testing of compounds based on ‘privileged scaffolds’, such as diaminopyrimidines, can lead to powerful new probes for cell division and intracellular transport.

This thesis is dedicated to

My parents

Rainer and Ingrid Peters

ACKNOWLEDGMENTS

First and foremost, I would like to thank Dr. Tarun Kapoor for being a great mentor in all regards. My work would not have been possible without him.

Special thanks go to Jeffrey Kim, Dr. Joseph Cherian, Dr. Benjamin Kwok, and Dr. Michael Lampson, as members of the Kapoor laboratory that have been actively involved in my projects. Special thanks also to Dr. Vladimir Gelfand and members of his laboratory for the fruitful collaboration. Furthermore, I would like to thank all current and past members of the Kapoor laboratory for their help and advice.

Thanks would be given to my committee members: Dr. Tom Muir, Dr. Bruce Ganem, and Dr. Jack Taunton, for their help over the years as well as for reading and revising my thesis.

Without the technical support from the Rockefeller High Throughput Screening Resource Center, especially Dr. Charles Karan, and the Rockefeller Bio-Imaging Resource Center my work could not have been finished.

For financial and general support I would like to thank the Tri-Institutional Training Program in Chemical Biology as well as the Rockefeller Dean's Office.

TABLE OF CONTENTS

LIST OF FIGURES

LIST OF TABLES

LIST OF ABBREVATIONS

APC/C	Anaphase Promoting Complex/Cyclosome
ATP	Adenosine Triphosphate
BS-C-1	African Green Monkey Kidney Cell Line
BFA	Brefeldin A
cAMP	cyclic Adenosine Monophosphate
Cdk	Cyclin-dependent Kinase
DAP	Diaminopyrimidine
DIC	Differential Interference Contrast
DMSO	Dimethylsulfoxide
EC_{50}	Concentration Necessary for 50% of the Effect
ER	Endoplasmic Reticulum
GDP	Guanosine Diphosphate
GFP	Green Fluorescent Protein (enhanced)
IC_{50}	Concentration Necessary for 50% Inhibition
K-fibers	Kinetochore Fibers

LC/MS	Liquid Chromatography/Mass Spectrometry
MAP	Microtubule Associated Protein
mRNP	Messenger Ribonucleoprotein
MSH	Melanocyte Stimulating Hormone
PBD	Polo-box Domain
PKA	Protein Kinase A
Plk	Polo-like Kinase
Plk1	Polo-like Kinase 1 (etc.)
PtK	Rat Kangaroo Kidney Cell Line
PtKαT	Rat Kangaroo Kidney Cell Line stably expressing GFP-marked α-Tubulin
RNA	Ribonucleic Acid
RNAi	RNA Interference
SAR	Structure-Activity Relationship
s.d.	Standard Deviation
SFM	Serum Free Medium
Shh	Sonic Hedgehog

Smo	Smoothened
U20S	Human Osteosarcoma Cell Line
VR1	Vanilloid Receptor 1

1. Introduction

1.1. Small Molecule Inhibitors in Cell Biology

In cell biology, the idea that small molecules can be used to perturb the function of specific proteins has gained more traction in the last few years. This is an expected development, considering that many cellular functions are carried out by small molecules (nucleotides, steroid hormones, neurotransmitters) and that the use of small molecules has been a cornerstone of pharmacology. The main advantages of small molecules are: their rapid action, which might be just diffusion limited and allows a 'conditional' introduction at precise points in time, their potential reversibility, their tunable effects using different concentrations, the potential to easily use several inhibitors at once, and, in case of inhibitors of enzymatic activity, a modulation of activity without removal of the protein itself. Despite these clear advantages, identifying small molecules that bind specifically to a single protein remains a challenge, especially given that binding/active sites in homologous proteins can be very similar. In addition, small changes in chemical structure can affect the binding properties of small molecules greatly. This sensitivity usually prevents simple correlations or predictions to be made for suitable small molecules for a particular binding site, and often requires treatment of each small molecule as a unique case.

In cell biology the availability of genomic information has enabled more generalizable, but still specific, approaches with the use of genetic techniques such as gene knock-outs, RNA interference or genetic mutants. Essential

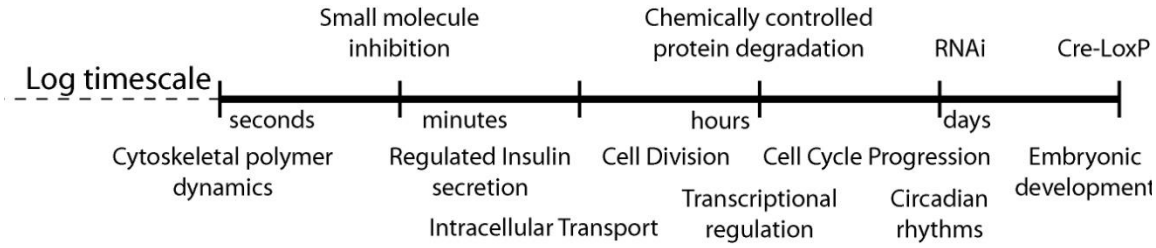

Figure 1: Overview over Time Scale of Biological Processes and Techniques for Their Perturbation

insights into cell biology have come from forward genetic approaches such as screening a library of mutants for phenotypic changes, coupled with the subsequent identification of the relevant protein, or reverse genetic approaches, such as protein knock-outs or knockdowns to study the resulting phenotype. However, these methods have drawbacks as well. Lethal knock-outs can be difficult to study, genetic mutants are typically not conditional and cannot be turned on or off at will, and knock-out/-down phenotypes can often be masked by functional compensation by a related gene. In addition, processes that can occur on a second or minute time scale such as intracellular transport can be difficult to study given that genetic techniques often require much more time (**Figure 1**).

While small molecules cannot replace genetic approaches in cell biology they can complement them by providing a general means of rapidly and conditionally inactivating proteins, as has been shown in numerous examples (see below). Since the number of small molecule inhibitors used in cell biology is still low, identifying new ones, as well as learning more efficient ways to find them, will benefit cell biology.

1.1.1. Small Molecule Inhibitors in Cell Division

During cell division, the genetic content of a cell is equally partitioned between two daughter cells (**Figure 2A-F**). Errors in this process are linked to developmental defects, and cell division gone awry is a hallmark of human diseases, such as cancer[1]. Cell division is a dynamic process that can be completed within an hour, a small fraction of a typical cell cycle[2]. Key processes, such as chromosome movements, occur at 1-6 microns/min, with individual

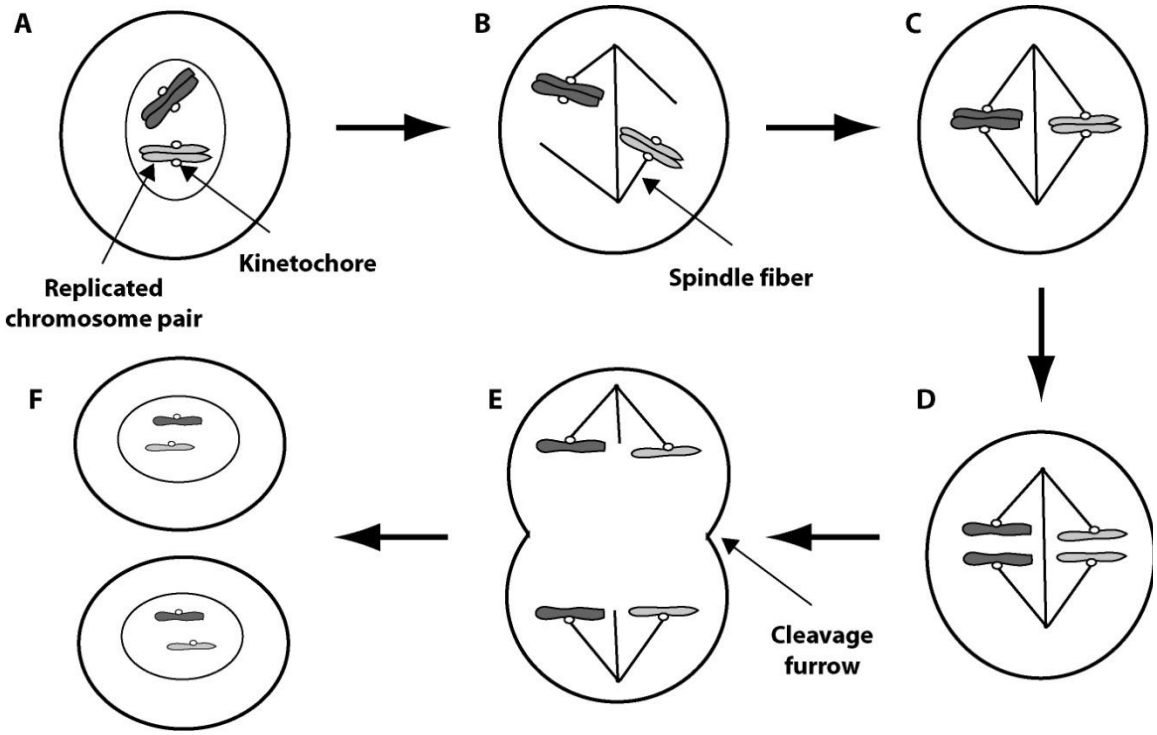

Figure 2: Overview of Mitosis

(**A**) Chromosomes are replicated before mitosis and sister chromosomes are held together. (**B**) After chromosome condensation and nuclear envelop breakdown the mitotic spindle forms and attaches to the chromosomes. (**C**) Chromosomes move to the center of the spindle and become aligned in metaphase. (**D**) Sister chromosomes separate at anaphase and move in opposite directions. (**E**) The cell divides as the cleavage furrow forms in cytokinesis between the separated chromosomes. (**F**) Two daughter cells with the exact copy of the genetic material at the end of cell division.

events, such as changes in directions of movement, taking seconds[3]. Therefore, error-free cell division requires a regulation of dynamic processes at specific cellular sites and at precise times. The molecular basis for this regulation is poorly understood.

Cell-permeable small molecules can target proteins on fast time scales, allowing inhibition or activation of function in live cells within minutes. This feature of small molecule inhibitors can be particularly useful in examining cell division dynamics, considering that all of cell division takes place in approximately 1 hour[4]. The mitotic spindle is a multi-component cellular machine that carries out DNA segregation during cell division. Several proteins required for mitotic spindle function represent potential targets for chemical inhibition. Microtubules, polymers of the cytoskeletal protein tubulin, provide a mechanical framework for mitotic spindle function[3]. The functions of tubulin in mitotic spindle assembly, chromosome movement, regulation of cell cycle progression, orientation of the cell division axis, and positioning of the cell cleavage plane have been revealed using compounds that directly target this protein[4]. Tubulin poisons are also effective chemotherapy agents used to treat diseases such as cancer, as inhibition of tubulin function blocks cell division and tumor growth[5].

A classic small molecule agent is the natural product colchicine (**Figure 3**). While it was known that colchicine induces mitotic arrest[2], the compound's mode of action was unclear. Shinya Inoue used it to treat cells in metaphase and observed a disappearance of the mitotic spindle fibers. The fibers could be recovered if the compound was washed out, even in the absence of protein

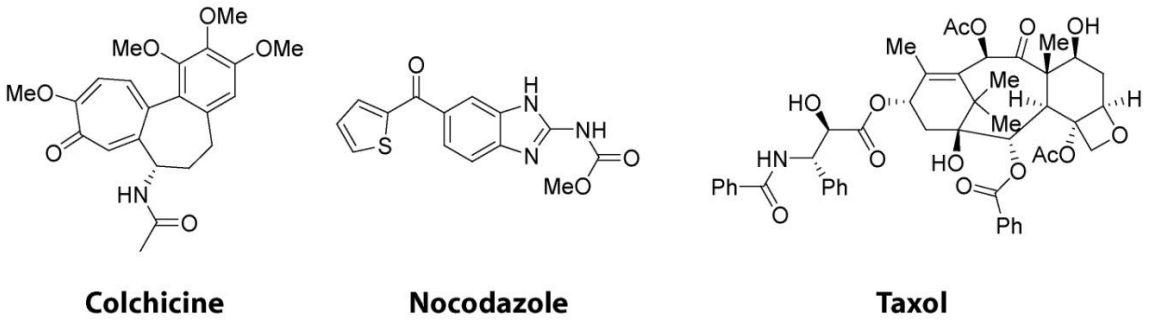

Figure 3: Chemical Structures of Small Molecules That Act on Microtubules

synthesis, implying that the spindle fibers are polymers made up from a pool of readily available monomers[6,7]. In addition, upon treatment with a low concentration of colchicine, chromosomes could be seen moving towards the pole, indicating that depolymerization of the filament might be coupled to chromosome movement[8]. A breakthrough in understanding the mechanism of colchicine came with target identification studies using a tritium label, which showed a reversible association with intracellular fibers called microtubules and led to the identification of the protein tubulin as the monomeric subunit[9].

Other microtubule depolymerizers like nocodazole have also found wide use in cell biology, for example to study transport processes or chromosome attachment in the absence of polymerized microtubules without affecting the monomeric protein. Interestingly, microtubule-stabilizing small molecules like taxol proved useful as well (**Figure 3**). Taxol stabilization of microtubules greatly affects their inherent dynamic properties. As a result, microtubules can still attach to kinetochores on chromosomes but are unable to create the necessary pulling forces to create tension across a kinetochore pair, assuming an attachment to

opposing poles in the mitotic spindle. Using this perturbation it was possible to show that a cell can recognize the absence of chromosome attachment (nocodazole treatment), but not necessarily the absence of tension (taxol treatment)[10-12].

Protein phosphorylation is a reversible modification essential in most signaling pathways. Kinases that are responsible for this modification are crucial components in cell division as well. Small molecule kinase inhibitors have proven to be useful probes. One such example is hesperadine, used to inhibit Aurora kinases, a class of proteins essential for cell division. Lampson et al. used this inhibitor to understand the role of Aurora kinases in the correction of chromosome attachment errors[13]. It was found that addition of hesperadine blocked error correction by stabilizing incorrect attachments, and after reactivation of the kinase by removal of the compound, the incorrect attachments became destabilized, clearly demonstrating the role of Aurora kinase in this process. The use of the small molecule combined with live-microscopy allowed them to look at a specific time in cell division, which was necessary since Aurora kinases have several roles throughout mitosis. In addition, the enzyme could be switched on and off with a high temporal control due to the reversibility of the small molecule.

At the end of cell division, following transport of chromosomes to the opposing poles, the cell physically divides into two daughter cells, in a process termed cytokinesis. Small molecules have helped to elucidate key aspects of this process. It was known from electron microscopy that a filamentous structure

existed around the cleavage furrow, termed microfilaments, but its identity was unclear (**Figure 4A**)[14]. Treatment with the small molecule cytochalasin led to its disruption and prevented furrow contraction in cytokinesis (**Figure 4B**). Interestingly, cytochalasin also blocked other forms of cellular or intracellular processes, such as cell motility and membrane ruffling[15,16]. Microfilaments were shown to be present in all of these systems. The use of colchicine demonstrated that such microfilaments seem to be unrelated to microtubules, leading to the conclusion that microfilaments were another crucial player in force generation in cells[16]. Treatment of purified actin fibers from muscle cells with cytochalasin led to a decreased viscosity, which suggested two conclusions: first, that the molecular target of cytochalasin is actin, and second, that the processes inhibited

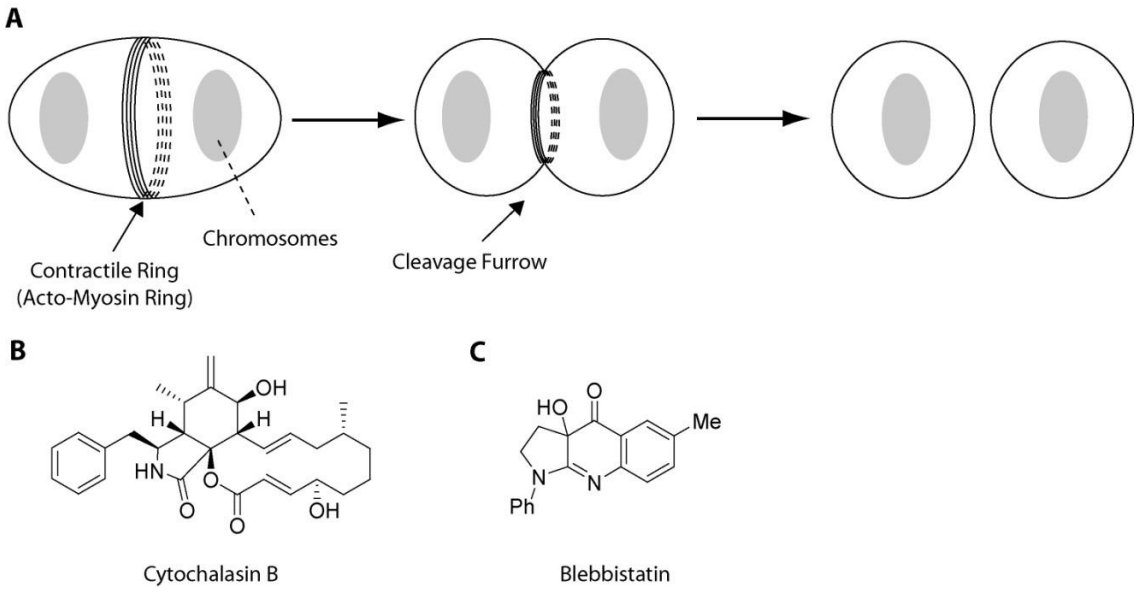

Figure 4: The Contractile Ring in Cytokinesis

(**A**) A ring of actin filaments and myosin II forms at the plasma membrane and contracts to divide the cell in half. (**B**) Chemical structure of cytochalasin B, a small molecule that targets actin. (**C**) Chemical structure of blebbistatin, a compound that targets myosin II.

by cytochalasin rely on actin for force generation. Therefore, the observed microfilaments contain actin as critical component. The molecular motor protein that works on the actin filaments in cytokinesis to allow contraction is myosin II. Recently a small molecule inhibitor of this motor protein, named blebbistatin, has been identified using a high-throughput screen (**Figure 4C**)[17]. Addition of blebbistatin to cells leads to a block in cytokinesis leaving components of the cleavage furrow in the correct position, but unable to carry out contraction. With cytokinesis arrested at this point, other small molecules could then be used to investigate the molecular requirements for furrow positioning without affecting preceding processes. For instance, it has been shown that signals from Aurora kinases as well as Rho kinases are necessary to localize myosin II to the cleavage furrow[17].

While small molecules have contributed crucial insights into cell division, the regulation of this highly dynamic process is still not well understood. Development of specific inhibitors for each protein involved, a continually growing list, would be ideal to answer the many outstanding questions. The identification of new small molecule inhibitors in cell division may also help to verify protein targets in diseases such as cancer, as the example of taxol and tubulin shows.

1.1.2. Small Molecule Inhibitors in Other Areas of Cell Biology

As the examples from cell division demonstrate, small molecules are valuable tools to study biological processes, with the potential to impact drug discovery. Since many processes in cell biology occur on a fast time scale, the use of small molecules has extended into areas as diverse as cell motility and migration[18],

aggresome formation[19], membrane transport[20], and nuclear export[21]. It should also be noted that although small molecules may not be the focus of a study they can play supporting roles such as inhibiting protein synthesis at precise points in time (cycloheximide), preventing degradation of proteins by certain pathways such as proteasome inhibition (MG132), or overriding DNA damage checkpoints (caffeine). The following examples demonstrate the versatility of small molecules and their applications.

Actin filaments are not only necessary during cytokinesis, but they are also essential as a cytoskeletal component in cell motility and migration. Therefore, the identification of actin as a target of cytochalasins, as described above, was important for this field as well. In a recent study, several small molecules have been used to better understand the interplay between actin, myosins and upstream signaling proteins in cell motility[22]. Using blebbistatin to disrupt myosin II, a kinase inhibitor that implicated Rho-kinase as responsible upstream signal, and calyculin A (**Figure 5**), a known phosphatase inhibitor, the authors were able to learn more about how a radially symmetric cell can initiate polarized cell motility in a certain direction.

Another area where small molecules have helped to gain a deeper understanding is vesicle secretion. Brefeldin A (BFA), a fungal metabolite, has played a crucial role (**Figure 5**). Treatment with BFA leads to the disassembly of the Golgi complex, a ribbon of stacked, flattened membrane cisternae and tubular extensions that is located near the microtubule organizing center. The Golgi functions to sort and concentrate membrane components moving from the

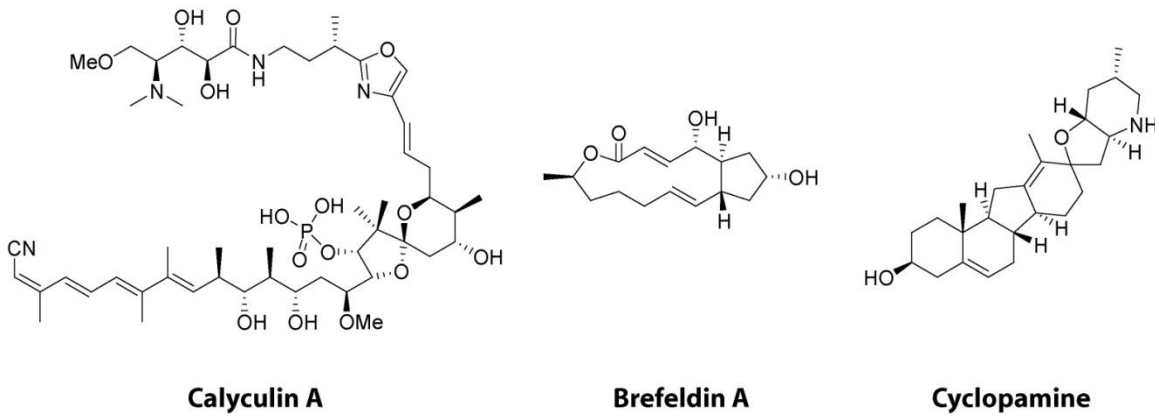

Figure 5: Chemical Structures of Small Molecule Probes for Different Areas of Cell Biology
Chemical structures of several natural products that have been used as small molecule inhibitors. Shown are the phosphatase inhibitor calyculin A, brefeldin A – a blocker of guanine nucleotide exchange in vesicle trafficking, and cyclopamine – an inhibitor of Smoothened.

endoplasmic reticulum (ER) to other organelles and is the center of a complex intracellular trafficking of lipids and proteins. Disassembly of the Golgi by BFA leads to its redistribution into other membrane compartments such as the ER. The resulting block of the secretion pathway allowed researchers to study dynamic processes such as retrograde transport within the membrane compartments[23]. The molecular target of BFA was also identified as a nucleotide exchange factor for small G-proteins involved in ADP-ribosylation, which help to assemble the 'coats' for vesicle trafficking. Interestingly, more recent studies including structural data have shown that BFA acts non-competitively by locking the ADP-ribosylation factor and its corresponding GDP-exchange factor into an inactive conformation of the complex thereby blocking nucleotide exchange and activation[24].

Small molecule inhibitors have proven valuable in studying developmental processes as well, as the example of the natural product cyclopamine shows

(**Figure 5**). This compound causes cyclopia in sheep[25] which resembled phenotypes seen of mutations in the sonic hedgehog gene (Shh), an important player in signal transduction pathways involved in patterning in many tissues[26]. The target of cyclopamine was identified as Smoothened (Smo), a transmembrane protein, that acts as an activator in the hedgehog pathway[27]. Using this inhibitor the role of Smo in the signaling pathway and its interaction partners could be better understood. Since the hedgehog pathway is involved in cancer as well, understanding the role of cyclopamine also opened a window for potential therapeutic intervention in this direction[28].

1.1.3. Alternative Strategies Using Small Molecules

In the examples described those far, small molecules have been used as direct effectors of native proteins. However, small molecules can also be utilized in more indirect ways to widen their applicability while still taking advantage of the temporal control they can provide.

The bump-hole approach, brought to prominence by the Shokat laboratory, combines the use of small molecules with protein engineering and has been especially successful with kinases. The method relies on the engineering of a functionally silent, but structurally significant, mutation in the ATP-binding pocket of the target kinase. In most cases this is achieved by a replacement of a conserved bulky residue with a smaller amino acid like glycine or alanine[29]. This generates a bigger pocket, the so called ‘hole’, ideally without greatly affecting the enzymatic activity. A non-specific small molecule inhibitor of the wild-type protein, often purine based, is chemically modified with substituents that

complement the mutation introduced into the active site, resulting in a ‘bump’ on the inhibitor. Due to steric clashes, the ‘bumped’ inhibitor should be unable to bind the wild-type active site, while being selective for the engineered protein (**Figure 6**). In the last step, the wild-type kinase needs to be replaced by the engineered one. This approach allows one to engineer specificity into inhibitors of conserved proteins like kinases and provide a means to specifically inhibit any protein of choice, given enough structural information and a suitable small molecule starting point. However, the replacement of the wild-type protein is not possible in all cases, and the changes in the active site of the engineered protein

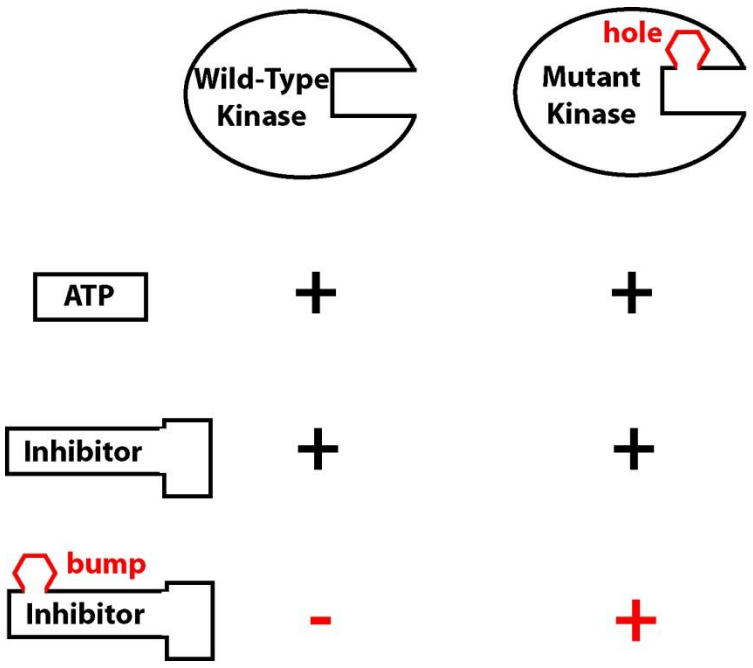

Figure 6: Schematic Overview over the Bump-hole Approach in Kinases

Kinase specific inhibition can be achieved by a combination of protein and small molecule engineering. Wild-type and mutant kinase both have enzymatic activity relying on binding to ATP. The unmodified inhibitor is not selective for either form of the kinase or for highly conserved binding active sites of other kinases. The ‘bumped’ inhibitor can only bind to the mutated kinase, providing selectivity over wild-type kinase and kinases with related active sites. + indicates binding to kinase.

can greatly affect enzymatic activity. The bump-hole approach has been successful in a number of examples such as determining the role of polo-like kinase (Plk) in cytokinesis[30], helping to understand the role of myosin Vb in membrane trafficking[31], and helping to identify substrates of specific kinases, e.g. cyclin dependent kinase 1[32].

Small molecules that function as dimerizers by mediating protein-protein interaction have proven useful as well. One classic example is the natural product FK506, which can induce the heterodimerization of the FK506-binding protein (FKBP) and a portion of the FKBP12-rapamycin-associated protein (FRAP)[33] (**Figure 7**). By using a dimer of FK506, called FK1012, a homodimerization of FKBP domains can be induced. If the FKBP-domains are attached to a protein of interest, oligomerization of this protein can be achieved in a FK1012 dependent manner. Using this inducible system, the Schreiber laboratory was able to oligomerize the Fas-receptor which is important in apoptotic signaling, and show that the dimerization of the receptor was sufficient

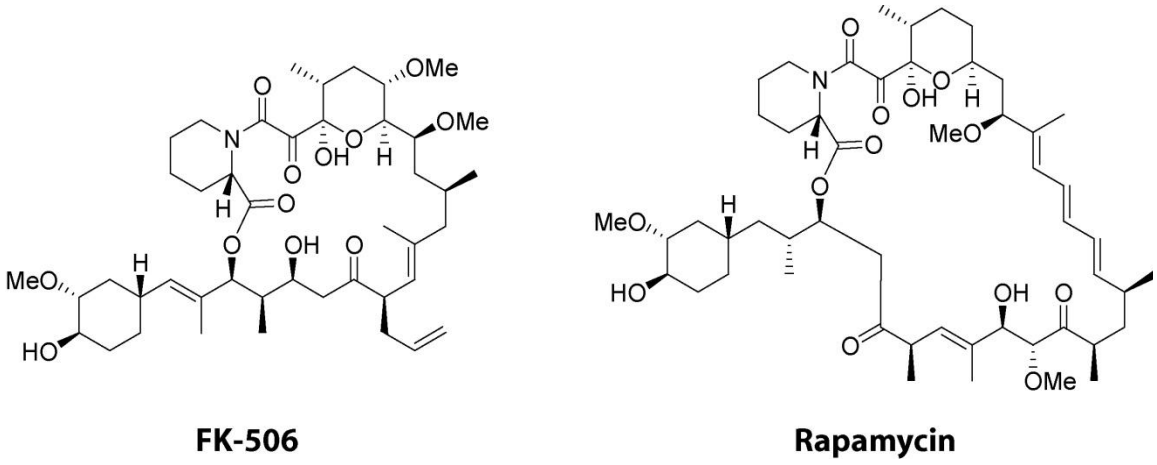

Figure 7: Structures of the Common Dimerizers FK-506 and Rapamycin

to induce apoptosis[34]. The idea of induced dimerization or oligomerization mediated by introduced protein domains is not limited to the studies of receptors. The Crews laboratory developed proteolysis targeting chimeric molecules (PROTACs) that consist of a ligand, for instance on FKBP ligand, and a short peptide sequence that can be recognized by ubiquitin ligase[35]. If the protein of interest is fused to a FKBP domain, the PROTAC can then bind to this fusion and recruit the ubiquitin ligase, leading to the ubiquitination of the target protein which marks it for degradation by the proteasome. Therefore, the PROTAC allows for induced protein degradation. Small molecule induced dimerization can be used in yet another way as a switch to activate or inhibit protein function, as the Muir laboratory has shown. Combining protein splicing, an editing process that removes a defined internal domain from a protein (intein), and fuses the flanking external domains (exteins), with induced dimerization allows for the rapid formation of a functional protein upon addition of the small molecule, resulting in conditional protein splicing[36]. Using rapamycin and its binding partners FKBP and FRAP in this system, formation of functional proteins could be induced in whole organisms[37] (**Figure 7**).

While all of the described alternative approaches for the use of small molecules hold promise, considering that one small molecule could work on a range of different proteins, they rely on protein engineering, which may not always be successful. Nevertheless, these techniques nicely complement the ‘classic’ small molecule approach and can be viable alternatives.

1.2. Finding Small Molecule Inhibitors

To find suitable small molecule probes, several key questions need to be addressed. What process/enzyme needs to be perturbed, and are there assays available to read out a perturbation? What part of chemical space should be searched for the small molecule? Most of the examples described here so far have been natural products that showed biological activity and therefore were analyzed further for their molecular target, their specificity, and their mode of action. While the approach to use 'nature' to design, synthesize, and screen small molecules has been very fruitful in the past, the advent of large scale chemical syntheses, especially combinatorial approaches and the wider availability of recombinant proteins, have led people to focus on generating and screening chemical libraries in order to find new small molecule probes and expand the scope of inhibitable proteins.

1.2.1. Available Compound Collection

Collections of natural products and extracts that take advantage of the natural biodiversity remain an important part in the discovery process of small molecule inhibitors. However, they are often difficult to isolate or synthesize in a large enough quantity, making target identification and biological application difficult.

Large libraries of compounds can and have been generated using combinatorial chemistry[38]. They might consist of compounds from a number of easily accessible scaffolds, often heterocycles that are chemically elaborated to produce compounds that contain sterically and/or electronically diverse

appendages at various positions. To expand the number of available scaffolds and achieve greater structural variety, diversity-oriented chemistry can be used as an alternative approach[39]. With the screening and testing of compounds from many different scaffolds against a range of targets, it became clear that a subset of the scaffolds are capable of binding to a variety of protein targets with high affinity[40]. These particular structural motifs are often referred to as 'privileged scaffolds'[40]. Libraries based on a 'privileged scaffold' have been successful in a number of examples, such as for 2,6,9-trisubstituted purines leading to inhibitors of kinases[41,42], and may hold promise as a general approach to identify small molecule probes.

With a large number of screens having been carried out, especially in industrial drug development, it has become clear that bioactive small molecules often follow certain rules regarding their chemical and physical properties. The 'Lipinski' rule of five states that an orally active drug should have: 1) no more than 5 hydrogen bond donors, 2) no more than 10 hydrogen bond acceptors, 3) a molecular weight under 500 g/mol, and 4) a partition coefficient log *P* of less than 5[43]. Although this rule refers to drug candidates and is not exclusive, it can provide a framework for a higher success rate, and is often followed for commercially available libraries. Compiling the results from many screens has also enabled access to compound collections consisting of previously identified bioactive compounds which may have activities in other areas as well.

1.2.2. *In Vitro* Screening Approaches Using Pure Proteins

If the protein target of interest is known and can be purified in sufficient quantity, screening for small molecules that modulate its activity is often carried out in an *in vitro* system. This approach has been especially successful with enzymes and receptors for two reasons. First, most of them have evolved to interact strongly and specifically with small molecules such a nucleotides, lipids, and steroid hormones, and therefore contain a suitable small molecule binding pocket. Second, readouts for a range of enzymatic activities and binding assays for small molecules, often based on fluorescent species, are available to allow for high-throughput screening.

Using pure proteins/peptides to find inhibitors of protein-protein interactions is possible as well, but due to the problems associated with this inhibition, such as the large binding interfaces and high number of protein-protein contacts, finding small molecule probes has not been as successful. An alternative to the classic screening of small molecule libraries in this regard are fragment-based discovery approaches[44-46]. They rely on using fragments, small organic molecules typically less than 200 Da, to screen for binding to a protein target. Active fragments, which usually have binding constants in the millimolar range, are then linked to generate larger sized compounds, which then can be screened for improved function. Because of the relatively low affinity of fragments, their discovery and characterization can be a challenge. Techniques such as structure-activity relationship (SAR) by NMR[45], which uses NMR as a screening tool but requires a solved protein structure, or tethering[46], which uses disulfide bonds to tether

fragments close to the protein site of interest, have been used to overcome these problems and have helped find inhibitors of protein-protein interactions[47,48]. Disrupting protein-protein interaction by targeting inhibitable allosteric sites away from the protein-protein interface is another viable alternative[49-51].

While pure proteins are required in these *in vitro* screens, a major advantage is that the target protein of the small molecule is known from the outset. Optimization by SAR, especially for potency, can be simply carried out in the established screening system. What is harder to address is the question of whether the small molecule probe is active in a biological system. Steps like adding high amounts of proteins like casein, to minimize non-specific protein binding by compounds, working in the presence of a low concentration of detergent to avoid inhibition by compound aggregation[52], or suitable library design to make bioavailability more likely, can help to increase the chances of the hit compound working *in vivo*, but these methods are not guarantees for success. In addition, the question of compound selectivity needs to be addressed as well, which holds true for all small molecule inhibitors.

1.2.3. Phenotype-based Screening Approaches

The alternative to *in vitro* screening for a known protein activity or binding interaction is to screen *in vivo* for a desired phenotype. This approach is related to classic forward genetic screening where instead of screening a library of mutants, a library of small molecules is used to affect a process of interest[53]. Compared to screening with pure proteins, it has two major advantages. First, the actual target protein does not need to be isolated or even known, and a direct

in vitro activity read-out assay is not necessary either. This allows insight into processes where not all the molecular players have been identified and offers a larger window of opportunity to find small molecules in. Second, by affecting the process *in vivo*, the hit compounds already show activity in a biological system giving them a higher chance to become useful biological probes.

Identification of the relevant protein target is still necessary to fully understand the mode of action of small molecule hits from phenotypic screens. This can often be a rate-limiting factor, but several target identification techniques are available. One of the classic approaches uses the small molecule or one of its analogues as bait to trap the protein. If the small molecule analog contains a tag, such as biotin, a fluorescent marker or a radioactive isotope, a covalent attachment of the compound to the protein, for instance by chemical or UV-crosslinking, can then be used to identify the protein by the introduced tag. The small molecule – protein interaction can also be used in affinity chromatography-based approaches, where the small molecule is immobilized via a linker to a solid support which is then used to enrich for its protein target. While covalent interaction is not necessary for affinity chromatography, the binding interaction needs to be sufficiently strong to achieve separation, often requiring affinities in the low micromolar or better range. While chemical derivatisation is not possible in all cases without significant loss of affinity, alternative strategies for target identification are available[53]. If the observed phenotype is fairly well understood, a candidate-based approach can be taken that tests for inhibition of likely target proteins. Data available from genome wide RNAi-based phenotypic screens or

from classic genetic screens can greatly aid in this process as more and more phenotypes are being described. Comparisons with already reported protein targets of chemically similar compounds can prove useful as well. In addition, designing suitable secondary screens to eliminate compounds with undesired modes of action and focusing on more well understood phenotypes should be helpful. If the screening system is amenable to large scale genetic techniques a suppressor screen of the phenotype induced by the small molecule can be carried out. This approach has been used for instance in the nematode C. elegans to help identify the protein target of the small molecule nemadipine A. All genetic mutants that suppressed the small molecule phenotype were linked to one specific calcium channel, and given this finding the authors were then able to show that nemadipine A is an antagonist of this channel[54].

As in the case of *in vitro* screens, the selectivity of the small molecules also needs to be addressed, keeping in mind that the observed phenotype may result from targeting several proteins, which may in turn also make non-chemical target identification approaches more difficult.

Of the biological systems amenable to high-throughput phenotypic screening, cell culture cells are the most common. The screen usually consists of the following steps. First, cells are plated into multi-well plates and incubated with the small molecules for an appropriate amount of time. Then the proteins or features of interest are made visible, most often fluorescently for instance by immunofluorescence using antibodies or tagging with a fluorescent protein, such as GFP. Depending on the desired read-out, either a plate reader or an

automated microscope can be used to acquire the data. Collecting microscopic images often provides additional information such as cellular localization or cell shape, and allows the detection of unexpected phenotypic changes more readily, but may require more refined analysis techniques. In addition, genetic techniques like RNAi, which is available for many cell types, can be used to complement phenotypic screening in tissue culture cells.

Besides the already mentioned example of blebbistatin[17] as an inhibitor or myosin II, the small molecule monastrol[55] was found in a phenotypic cell-based screen. Using phosphorylation of nucleolin as read-out for mitosis, compounds were selected which caused an increase in mitotic cells (**Figure 8A**). After a secondary screen that eliminated molecules that had an obvious effect on microtubules *in vitro*, which would lead to a mitotic arrest, the cellular phenotype of the remaining compounds was analyzed by immunofluorescence. Monastrol gave monopolar mitotic spindles, structures with only one pole with the chromosomes located radially around it (**Figure 8B,C**). Guided by the specific phenotype observed, the target of this small molecule could be identified as the mitotic kinesin Eg5, which is necessary for pole separation. Since its discovery, monastrol has been widely used in studies to understand the function of Eg5[56-58], as well as general tool in cell division, for instance to induce a mitotic arrest, to accumulate chromosome attachment errors[13], or to better understand the localization of the cleavage furrow in cytokinesis[59].

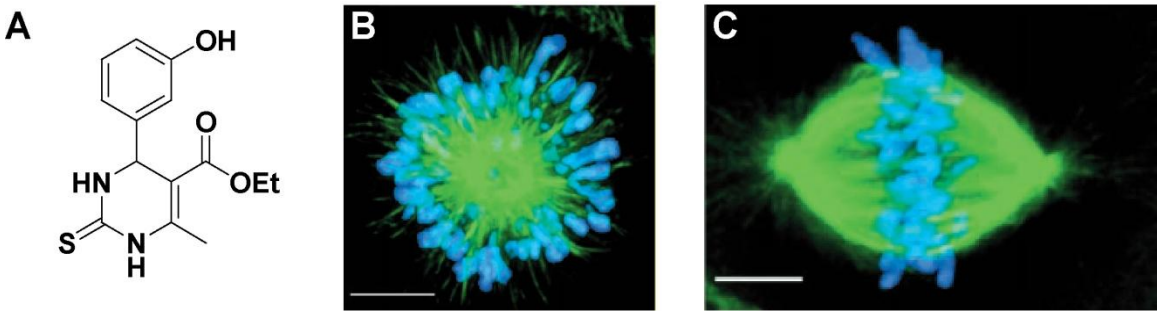

Figure 8: Monastrol, an Eg5 Inhibitor Discovered in a Cell-Based Screen

(**A**) Chemical structure of monastrol, a dihydropyrimidine. (**B**) Monopolar mitotic spindle are observed after monastrol treatment of BS-C-1 cells. Chromatin is shown in blue and α-tubulin in green. (**C**) Normal bipolar mitotic spindle as in cells treated with carrier (DMSO). Scale bars, 5 μm. Images were taken from [55].

While cell-based phenotypic screens still are more common, screening for phenotypes in whole organisms has proven successful as well. The studies at this point have traditionally used small organisms that are genetically tractable. One example is the aforementioned identification of nemadipine A as an antagonist of a calcium channel in the nematode C. elegans[54]. Another commonly used model organism is the zebrafish *Danio rerio*, where molecules that affect development[60], angiogenesis[61] or signaling[62] have been identified. While whole organism screens can easily address questions such as tissue specificity, cell-cell interactions in a their normal physiological context, and developmental processes, the throughput of the screens is usually lower than in cell culture, and phenotypes might be even harder to interpret than in single cells.

More and more cell lines and model organisms are becoming available. At the same time, improvements in imaging reagents and imaging technology are being

reached. Thus, phenotypic screening will continue to play important roles in small molecule discovery.

1.2.4. Inhibitor Specificity

While finding small molecule inhibitors can be approached in several different ways, one key question that needs to be addressed is their specificity for the intended protein target. Given the fact that small molecule binding sites are often highly conserved between members of a protein family, or even unrelated proteins, it is not unexpected that compounds can often act on multiple targets. The identification of the relevant off-targets is therefore crucial to be able to correctly correlate effects of the compound with inhibition of the desired protein.

One of the best studied examples addressing specificity of small molecules are inhibitors of kinases. Small molecules have been instrumental in understanding the functions of many kinases. A significant challenge to identifying specific, or selective, small molecule inhibitors is the highly conserved ATP-binding site contained within the ~500 kinases in humans. To assess the specificity of a kinase inhibitor several techniques can be used. Typically the compound is tested in an *in vitro* activity assay against a panel of available kinases to determine and compare potency among the panel members. Although this data gives an indication of specificity, it requires the isolation or recombinant expression of a large number of kinases. Furthermore, since the assay is carried out *in vitro*, factors that affect kinase activity such as native complexes of the kinase, local concentration, relevant physiological substrates, or alternative splice-forms of the kinase cannot be easily addressed[63]. Affinity chromatography

has also been used to identify kinase inhibitor targets and off-targets, employing an immobilized compound and subsequent analysis by mass spectrometry[64]. More recently binding assays to the ATP-site of kinases have been used to look at specificity, as well[65,66]. Expressed kinases are allowed to bind to an immobilized non-specific inhibitor. Free test compound is added, which may or may not affect this binding interaction, thereby reporting on specificity without the need to immobilize the compound of interest. An extension of this idea is the use of 'kinobeads', which are loaded with several non-specific inhibitors, and can be used to pull out a large number of kinases from cell extracts in the presence of absence of test compound[67]. Subsequent mass spectrometric identification of bound proteins can then give information on disrupted interactions and specificity. By employing this array of techniques, it has been found that all kinase inhibitors affect a varying number of off-target proteins.

The described *in vitro* assays for kinases can indicate whether the compound of interest is a promiscuous inhibitor or if it is selective. A correlation between potency and selectivity has also been found[63]. However, the assays usually cover only a subset of potential target proteins under *in vitro* conditions, making it necessary to address the specificity of compounds in the relevant biological context by additional means. The most valuable tool in this regard is a structurally unrelated chemical compound that targets the same protein[13,63,68]. This independent positive control is predicted to have different off-targets due to a different chemical structure. Observation of the same dose-dependent, *in vivo* phenotype in both cases would then help to confirm the correlation between a

small molecule, its relevant protein target, and the observed effects. Furthermore, measures such as working at the lowest inhibitor concentration possible can help to limit problems arising from off-target effects[63].

While the aforementioned techniques help to choose the most selective inhibitors available and minimize the potential risk of off-target effects, finding compounds that are highly specific for one kinase remains difficult. Approaches using protein and inhibitor engineering can get closer to this goal. One of them is the 'bump-hole approach' described earlier that allows the use of a bulky inhibitor that most likely does not target any other kinase. Another approach is the use of a reactive cystein close to the active site as one 'selectivity filter'. By equipping an inhibitor with an electrophilic group such as a haloketone that is properly positioned to react with the cystein, a highly potent irreversible inhibitor can be obtained[69]. Using this particular inhibitor as reactive probe to determine specificity, it was shown that only 2 kinases are covalently targeted in human cell lysate[69].

As the example of the kinase field illustrates, inhibitor specificity still remains a major factor to be considered when using small molecules. *In vitro* assays can help to improve and develop more specific inhibitors, but cannot rule out or address all off-target activities. Therefore, in an *in vivo* system, the use of inhibitors with different chemical structures, careful target validation, and comparison with phenotypes obtained from other experimental approaches are necessary to reliably correlate inhibition of the intended protein target with the biological effects observed.

There are many ways to find small molecule inhibitors, each associated with their advantages and disadvantages. Choosing the appropriate way to proceed mainly depends on the biological problem at hand and a careful choice should increase the chances of identifying a specific, biologically active probe.

1.3. Outlook

Small molecules as biological tools have helped to better understand dynamic processes in cell biology. But many questions still remain unanswered, mainly due to the lack of suitable small molecules. The work I present here addresses several aspects of this problem. First, I developed and utilized screens for small molecule inhibitors, in one case a phenotypic cell-based screen for cell division and in the other case a cell-based phenotypic screen for intracellular transport. Both screens gave promising hit compounds. Second, I designed compounds based on a ‘privileged scaffold’ to be used in the screens. These compounds were compared to compounds from commercial libraries to better understand the compound collection requirements to yield hits. Third, using small molecule inhibitors of Polo-like kinase 1 I was able to further elucidate its role during cell division. I hope that my work can serve as a step forward towards the goal of finding potent and selective effectors of functionally important proteins.

2. Probing Cell-division Phenotype Space and Polo-like Kinase Function Using Small Molecules

2.1. Introduction

As described earlier, small molecules have played crucial roles in understanding the intricate details of the highly dynamic processes in cell division, due to the exquisite spatio-temporal control they can deliver. However, the control and regulation of these processes is still poorly understood. In addition, while a large number of proteins required for cell division have been reported, and their knock-down phenotypes have been described[70,71], small molecule inhibitors for most of these proteins are not available. Further, the consequences of inhibiting their activities without directly reducing protein levels, a predominant mode of action for chemotherapy agents, are not known[68,72]. It is likely that small molecules that inhibit these proteins would be powerful tools to analyze the function of their target proteins during cell division, and would help to evaluate them as drug targets[4].

To identify small molecule inhibitors of cell division proteins, activity-based screens or cellular phenotype-based assays can be used. While both approaches have advantages and limitations as described previously, cellular phenotype-based screens have the potential to identify compounds that are active in cells and can lead to the discovery of new mechanisms[73]. An outstanding question is how diverse a collection of compounds must be screened

to identify inhibitors that target different proteins, using either method. Advances in chemical synthesis technologies are allowing large libraries to be generated[74]. Compound collections can be synthesized that either densely explore regions of chemical space occupied by a known bio-active compound, or that occupy other, yet untested, regions of this infinite multi-parameter space[75]. How effectively these different compound collections can span cell division phenotype space remains unclear.

2.2. The Screen

2.2.1. Compound Design and Synthesis

As a first step in addressing questions related to the extent and type of chemical diversity needed to span cell division phenotype space, I, together with Joseph Cherian, designed a chemical library based on diaminopyrimidines (hereafter, DAPs) (**Figure 9A**). DAPs represent a class of compounds that may be considered as a 'privileged scaffold'[40] as they are known to target different proteins, including reverse transcriptase[76], proton pumps[77] and kinases[78]. A range of amine substituents, such as alkyl, cycloalkyl, aromatic and heteroaromatics was commercially available and could be readily incorporated at the 2- and 4-position of the core pyrimidine to vary structure, polarity and hydrogen-bonding capacity. Of the large number of such DAPs, focus was put on a representative set of 100 compounds. Symmetric substitutions on the 2- and 4-position ($R_2 = R_3$) were avoided to achieve maximum diversity of functional groups within a small compound collection. The use of two readily available pyrimidines as starting materials allowed for variations at position-5 of the core.

The specifics of the compound collection are provided in the appendix (**Figure 36A-D**). Based on analyses of published work, 6 of the 99 compounds designed had been previously reported, but their cell division phenotypes were not known.

The chemical space occupied by the selected diaminopyrimidines was compared to that spanned by a commercially available compound collection, the Prestwick collection, which is selected for structural diversity, known safety and bioavailability in humans and over 85% of the compounds are marketed drugs (www.prestwickchemical.com). The 100 DAPs and ~880 Prestwick compounds were plotted along three vectors derived from principal component analysis of a 10-dimensional chemical descriptor matrix[79] (**Figure 9B**). The principal components shown account for over 97% of the variance of all the parameters

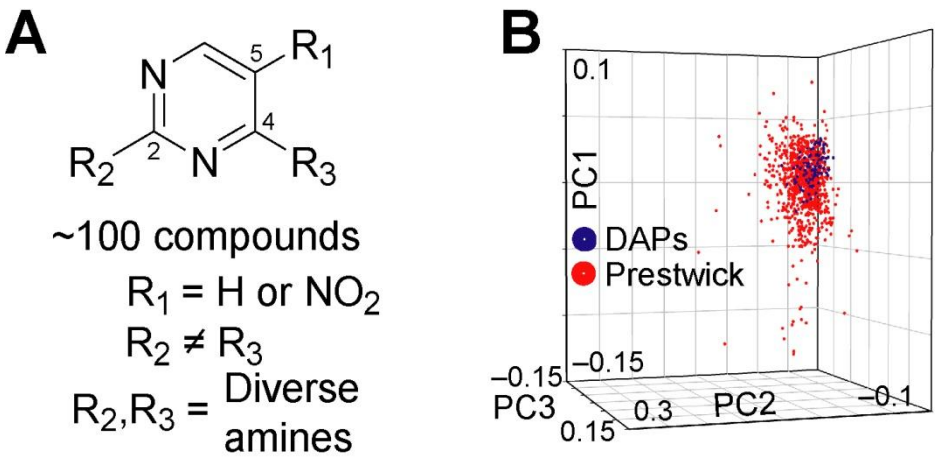

Figure 9: The Diaminopyrimidine Collection Maps into Chemical Space Occupied by Known Bioactive Molecules

(**A**) 100 compounds based on the diaminopyrimidine scaffold were synthesized. (**B**) Comparison of the chemical descriptor space occupied by a collection of known drugs and bioactive molecules, called the Prestwick collection, and the synthesized diaminopyrimidines. Three principal components covering over 97% of the variance in a 10-dimensional parameter space are shown.

used. This analysis reveals that the DAPs in the collection map to a sub-region of the chemical space spanned by the Prestwick compounds.

Compounds were synthesized by the sequential nucleophilic substitution of 2,4-dichloropyrimidines[78]. The products could be isolated in sufficient purity (>90% by LC/MS) and were generally obtained in 40-80% overall yield. 100 DAPs were synthesized and arrayed in formats compatible with high-throughput cell-based screens. Details of the chemical synthesis and characterizations are included in the Materials and Methods section.

2.2.2. Screen Setup and General Results

To analyze the effects of DAPs on cell division, I used BS-C-1 cells, a well-characterized mammalian cell line employed in screens for cell division probes[80]. Cells were treated with compounds (20 μM) for 4 hours, fixed and processed for immunocytochemistry. Images revealing the distribution of chromosomes and microtubules in compound-treated cells were acquired using an automated high-throughput microscopy system. To identify compounds that would be useful probes for mechanisms specific to cell division, the 16 compounds that severely altered microtubule organization in non-dividing cells, as compared to control cells (**Figure 10, Figure 11F,G**), were eliminated. As a control, I included in the DAP collection a compound that has been predicted to be a 'frequent hitter' that targets multiple kinases (**Figure 36D**). I found that this compound strongly perturbs interphase microtubule organization, cell shape and nuclear structure, consistent with general toxicity. Three other compounds yielded crystalline aggregates and were not examined further as this property is correlated with

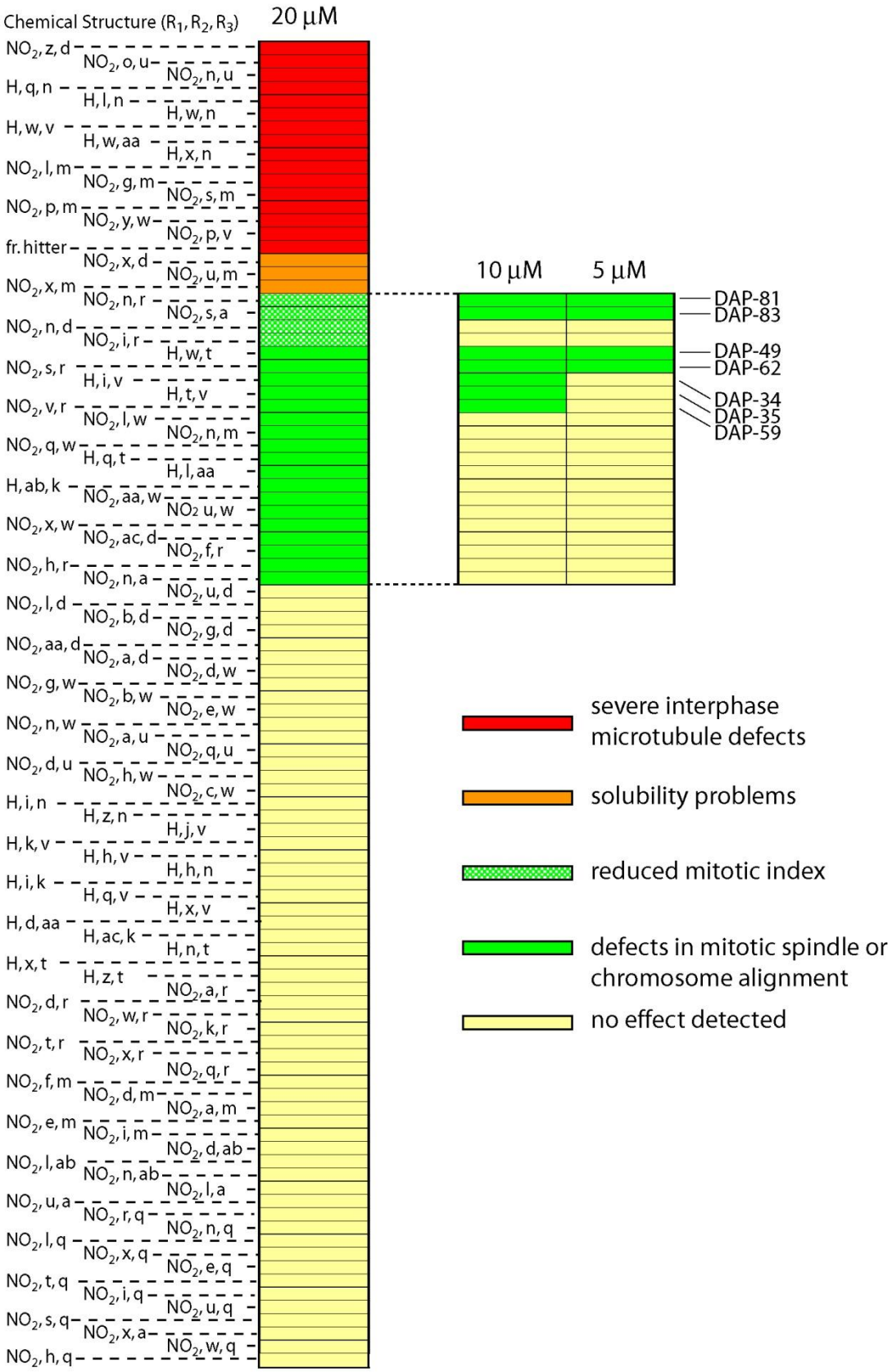
Chemical Structure (R_1, R_2, R_3)
20 µM
NO_2, z, d
NO_2, o, u
NO_2, n, u
H, q, n
H, l, n
H, w, n
H, w, v
H, w, aa
H, x, n
NO_2, l, m
NO_2, g, m
NO_2, s, m
NO_2, p, m
NO_2, y, w
NO_2, p, v
fr. hitter
NO_2, x, d
NO_2, u, m
NO_2, x, m
NO_2, n, r
NO_2, s, a
NO_2, n, d
NO_2, i, r
H, w, t
NO_2, s, r
H, i, v
H, t, v
NO_2, v, r
NO_2, l, w
NO_2, n, m
NO_2, q, w
H, q, t
H, l, aa
H, ab, k
NO_2, aa, w
NO_2 u, w
NO_2, x, w
NO_2, ac, d
NO_2, f, r
NO_2, h, r
NO_2, n, a
NO_2, u, d
NO_2, l, d
NO_2, b, d
NO_2, g, d
NO_2, aa, d
NO_2, a, d
NO_2, d, w
NO_2, g, w
NO_2, b, w
NO_2, e, w
NO_2, n, w
NO_2, a, u
NO_2, q, u
NO_2, d, u
NO_2, h, w
NO_2, c, w
H, i, n
H, z, n
H, j, v
H, k, v
H, h, v
H, h, n
H, i, k
H, q, v
H, x, v
H, d, aa
H, ac, k
H, n, t
H, x, t
H, z, t
NO_2, a, r
NO_2, d, r
NO_2, w, r
NO_2, k, r
NO_2, t, r
NO_2, x, r
NO_2, q, r
NO_2, f, m
NO_2, d, m
NO_2, a, m
NO_2, e, m
NO_2, i, m
NO_2, d, ab
NO_2, l, ab
NO_2, n, ab
NO_2, l, a
NO_2, u, a
NO_2, r, q
NO_2, n, q
NO_2, l, q
NO_2, x, q
NO_2, e, q
NO_2, t, q
NO_2, i, q
NO_2, u, q
NO_2, s, q
NO_2, x, a
NO_2, w, q
NO_2, h, q
10 µM
5 µM
DAP-81
DAP-83
DAP-49
DAP-62
DAP-34
DAP-35
DAP-59
severe interphase microtubule defects
solubility problems
reduced mitotic index
defects in mitotic spindle or chromosome alignment
no effect detected

Figure 10: Overview over Cell-Based Screening Results

The phenotypes associated with the 100 DAPs were clustered by similarity. Categories of phenotypes for the initial analysis (10x magnification, 3 independent screens, to score as a "hit" in a category the same phenotype had to be seen twice or more): (1) Severe microtubule disruption (red), (2) Compounds that form aggregates (orange), (3) Reduced mitotic index (light green). Scored if 2 or fewer mitotic cells per image (controls normally had ~10 mitotic cells). (4) Mitotic defects (green). These include spindle defects (2 or more cells per image field with perturbation) or chromosome alignment defects (5 or more cells per image field). (5) Compounds that did not meet the above criteria were considered inactive (yellow).The dose-dependence of the mitotic effects of the 22 compounds that either reduced the mitotic index or affected mitosis were determined (see inset). Phenotypes induced by compounds active at 10 μM were analyzed further using higher resolution microscopy (see **Figure 37A-F**). The corresponding chemical structure of each compound is abbreviated using the letter code provided in **Figure 36C**.

non-specific protein binding activity[81]. The 22 DAPs that perturbed cell division and did not strongly affect microtubule organization in interphase cells were examined further (**Figure 10**).

A wide range of cell division phenotypes, including changes in mitotic indices, mitotic spindles with perturbed or extra poles, bipolar spindles with perturbed architecture, monopolar spindles, improper chromosome alignment and defects in chromosome condensation were observed in treated cells (**Figure 11A-E**). The detailed results of the primary screen, including dose-dependence, are provided in the appendix (**Figure 37A-F** and **Table 1**).

It is noteworthy that most of the cell division phenotypic categories described in genome-wide RNAi screens are also observed in this screen[70,71]. It suggests that a small number of compounds covering a limited drug-like region of chemical space can effectively span cell division phenotype space.

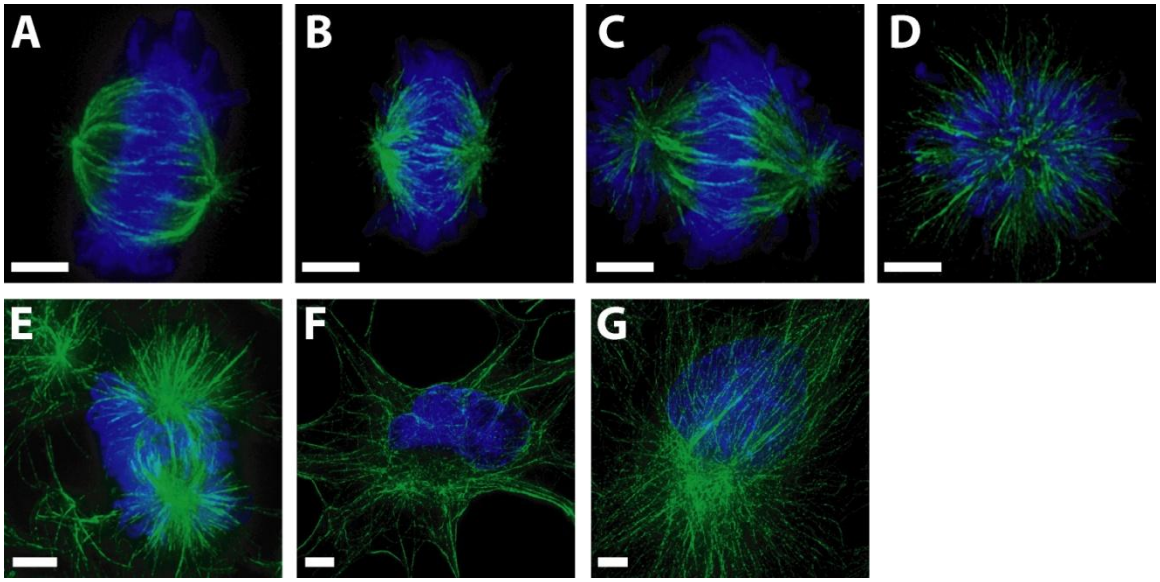

Figure 11: Cell Division Phenotype Space Is Effectively Spanned by a Small Collection of Diaminopyrimidines.

(**A-G**) BS-C-1 cells treated with diaminopyrimidines (4 h) were fixed and processed for immunofluorescence microscopy to analyze tubulin (green) and chromosome (blue) distribution. Cell division phenotypes observed for different compounds included: (**A**) unperturbed spindles as in untreated cells, (**B**) bipolar spindles of improper size, (**C**) chromosome alignment defects, (**D**) monopolar spindles, and (**E**) mitotic spindles with pole defects or extra poles. Severe microtubule organization defects were also seen (**F**). (**G**) Unperturbed interphase microtubule arrays in a control interphase cell. The images show maximum intensity projections of deconvolved image-series covering cell volumes. Scale bars, 10 μm.

2.2.3. Protein Targets of Compounds That Give Monopolar Spindles

Identifying the targets of compounds selected in cell-based screens can be difficult[82]. Therefore, while interested in finding the targets of the 22 DAPs that perturb mitosis, I focused on a cell division phenotype that is better understood than most others. Monopolar mitotic spindles, where chromosomes decorate a radial microtubule array, were observed in cells treated with 4 different DAPs (**Figure 37A-C**). High-resolution analysis revealed that two of these compounds

also altered chromatin condensation and therefore these compounds were not analyzed further. DAP-81, 2-[4-acetamidyl phenylamino]-4-[2-benzoyl phenylamino]-5-nitropyrimidine and DAP-49, 2-[benzothiazol-6-ylamino]-4-[indan-5-ylamino]-pyrimidine (**Figure 12A,B**), are compounds that increased the number of monopolar spindles in treated cells in a dose-dependent manner (for this phenotype EC_{50} 5 μM and ~30 μM, respectively) (**Figure 12C,D**).

As DAPs have been extensively analyzed, I first examined if the compounds that resulted in monopolar phenotypes had known targets. DAP-81 has been reported to target a member of an evolutionarily conserved family of serine/threonine kinases called Polo-like kinases (hereafter, Plks)[83]. Plks are implicated in many aspects of cell division, including cell cycle progression, mitotic spindle assembly, and cytokinesis[84]. Of the four members of the Plk family, Plk1 has been extensively characterized and its link to mitosis most firmly established[85]. As reported previously, DAP-81 inhibits Plk1 *in vitro* (**Figure 12E**, IC_{50} of 0.9 μM). Next, I tested whether DAP-49 also inhibits Plk1 to yield monopolar mitotic spindles, but no inhibition of kinase activity was observed at 100 μM (**Figure 12F**). Monopolar mitotic spindles are observed when cells have an improper number of centrosomes, microtubule organizing centers. This phenotype is also observed when centrosomes fail to separate[86]. Further analysis revealed that DAP-81 and DAP-49 do not change centrosome number in a 4-hour treatment (**Figure 13A-E**). Another possible target is the kinesin Eg5, a microtubule-based motor protein that plays an essential role in centrosome separation in eukaryotes[87]. Neither compound inhibited this protein in *in vitro*

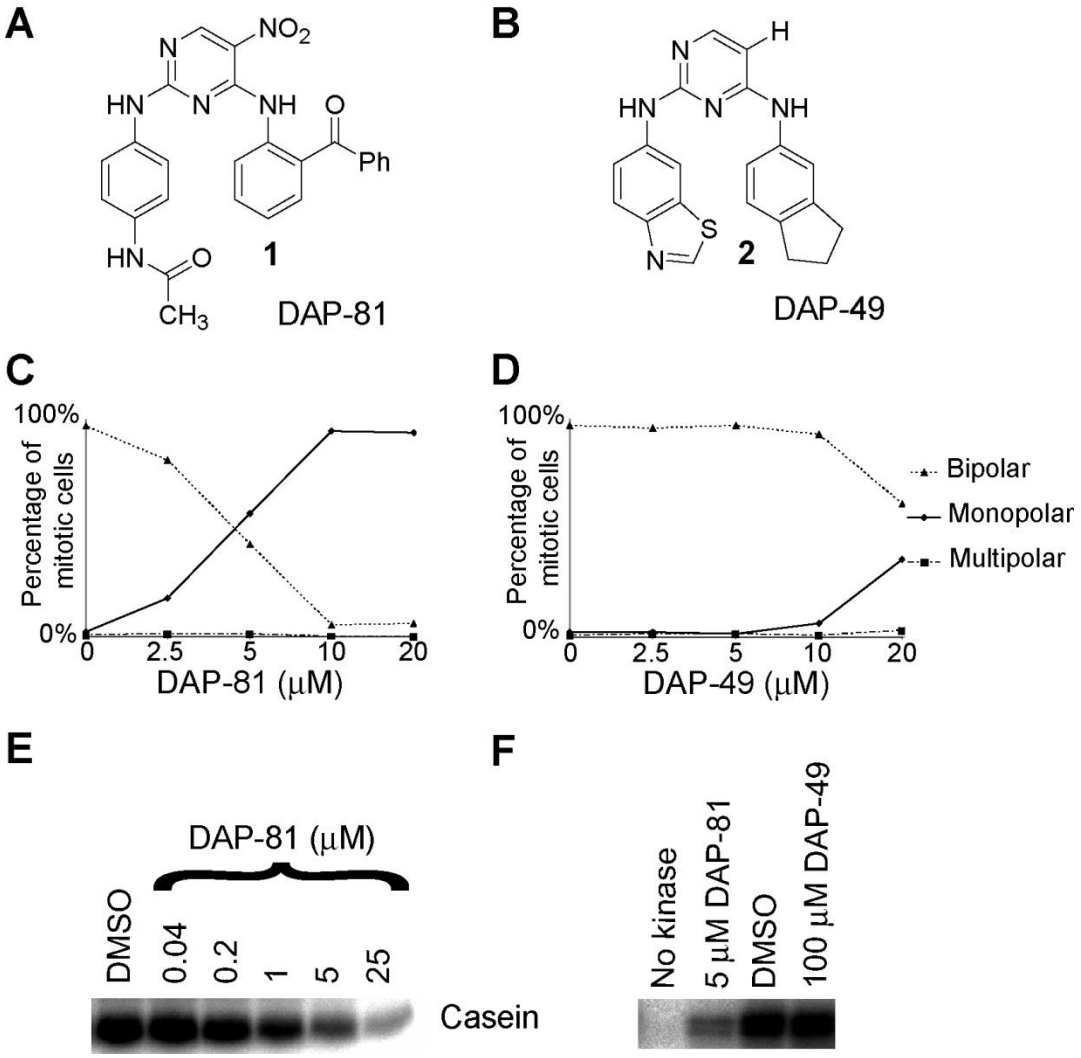

Figure 12: Monopolar Mitotic Spindles Are Induced by Two Diaminopyrimidines, Including One That Inhibits Polo-like Kinase 1 Activity *in vitro*.

(**A,B**) Structures of DAP-81 and DAP-49, compounds that induce monopolar spindles. (**C,D**) Quantification of mono-, bi- or multipolar spindles in treated cells (≥ 100 cells for each data point, n = 3). (**E**) Recombinant Plk can phosphorylate casein, as analyzed by the transfer of ^{32}P. DAP-81 inhibits this activity in a dose-dependent manner (IC_{50} = 0.9 ± 0.3 μM, n = 3, data was fit to a hyperbola). (**F**) DAP-49 (100 μM) did not change phospho-casein levels, when compared to controls and DAP-81 inhibited Plk1 kinase assays.

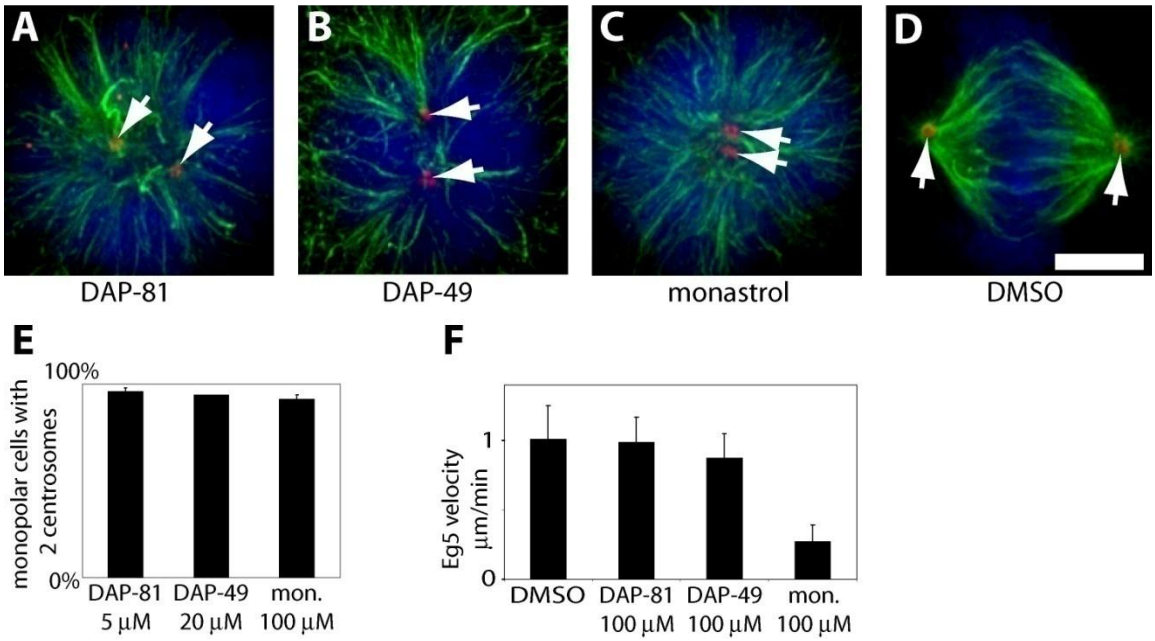

Figure 13: Monopolar Mitotic Spindles Induced by Two Diaminopyrimidines Do Not Result from Changes in Centrosome Number or Eg5 Inhibition.

(**A-D**) After 4-hour-treatment with either DAP-81 (5 μM), DAP-49 (20 μM), monastrol (100 μM) or vehicle (DMSO) BS-C-1 cells were fixed and processed for immunofluorescence. Images show DNA (blue), α-tubulin (green) and γ-tubulin (red). Arrows point at γ-tubulin stained centrosomes. (**E**) Percentage of monopolar cells with 2 centrosomes after treatment. The centrosome number in treated cells with monopolar spindles was determined using γ-tubulin as a centrosome marker. (≥ 50 cells per compound, *n* = 3). (**F**) Eg5 dependent microtubule gliding velocity was measured in the presence of carrier (DMSO), DAP-81, DAP-49 (100 μM each) (10 microtubules analyzed for each compound, *n* = 3). Monastrol (Mon.), an Eg5 inhibitor that induces monopolar mitotic spindles, was used as a positive control in the experiments. Error bars show s.d. The images show maximum intensity projections of deconvolved image-series covering cell volumes. Scale bar 5 μm.

microtubule sliding assays ruling it out as direct target of either DAP-81 or DAP-49 (**Figure 13F**). While the target of DAP-49 is not known, these data indicate that DAPs with similar chemical substitutions can induce the same cell division phenotype by targeting different proteins.

2.3. Plk Inhibitors as Probes for Cell Division

2.3.1. Polo-like Kinase in Mitosis

Besides the cyclin-dependent kinases (Cdks), which function as master regulators of cell division, attention has shifted towards other protein kinases that cooperate with Cdks to allow for proper regulation and coordination of this intricate process. Among them, the Polo-like kinases (Plks) play a crucial role. They are a family of serine/threonine kinases that were first described as mutant in the fruit fly *Drosophila melanogaster* (polo) that gave an arrest in mitosis with a monopolar like spindle[88,89], as well as in baker's yeast *Saccharomyces cerevisae* (cdc5)[90]. While there is only one Plk in fruit flies and baker's yeast, vertebrate species have several members, e.g. Plk1-4 in humans. They all have a similar structural organization with a kinase domain on the N-terminus and a polo-box domain(PBD) containing one or more so called polo-boxes (PBs) towards the C-terminus of the protein (**Figure 14**). The kinase domain is highly conserved and its activity can be regulated by phosphorylation, whereas the PBDs recognize phosphopeptides and are important in substrate recognition and specificity. Prior phosphorylation of a Plk substrate by a so-called priming kinase is often necessary to allow PBD binding and subsequent phosphorylation by Plk. Of the four members of mammalian Plks, Plk1 is the best studied and believed to carry out most mitotic functions associated with the single kinases Polo and Cdc5 in flies and yeast. Therefore I focused on this member of the protein family for the subsequent studies.

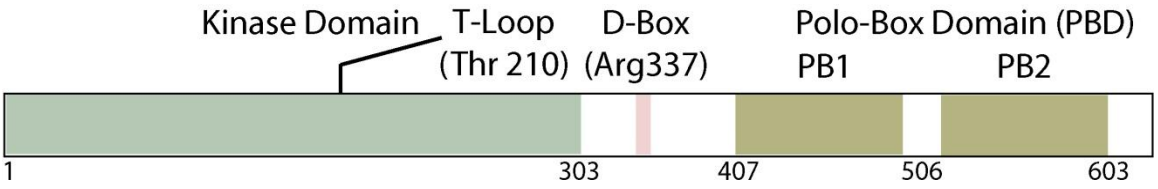

Figure 14: Domain Structure of Polo-like kinase

Plk can be divided into two main parts, the N-terminal kinase domain and the C-terminal polo-box domain (PBD), which contains two (or one in case of Plk4) polo boxes (PB). The linker region contains a D-box motif that is required for the degradation by the anaphase-promoting complex/cyclosome. The activating phosphorylation site Thr210 in the T-loop of the kinase domain is marked. Human Plk1 is used for annotation of residues. Figure adapted from Reference[84].

Before starting my studies, Plk1 had been implicated in a wide range of functions during mitosis. In mitotic entry, Plk1 had been shown to phosphorylate the Cdc25c phosphatase as well as Wee1 and Myt1 kinases, all resulting in the activation of the essential cyclin dependent kinase 1 (cdk1)/cyclin B complex (reviewed in [91]). Plk1 has also been shown to be involved in centrosome maturation, as the recruitment of γ-tubulin, an essential microtubule nucleator, is decreased with reduced Plk1 activity[92]. Furthermore, Plk1 seems to be necessary for the assembly of bipolar mitotic spindles, as demonstrated by the emergence of monopolar spindles and abnormal bipolar spindles upon antibody injection or depletion by RNAi[92-94]. In addition to these roles, Plk1 is also involved in the control of sister chromatid cohesion, by phosphorylation and subsequent removal of subunits of cohesin, a necessary protein in this process[95]. Furthermore, in later stages of mitosis, Plk1 has been implicated in the activation of the anaphase promoting complex (APC/C)[96,97]. A role for Plk1 in cytokinesis has also been suggested, consistent with its localization to the midbody, and its

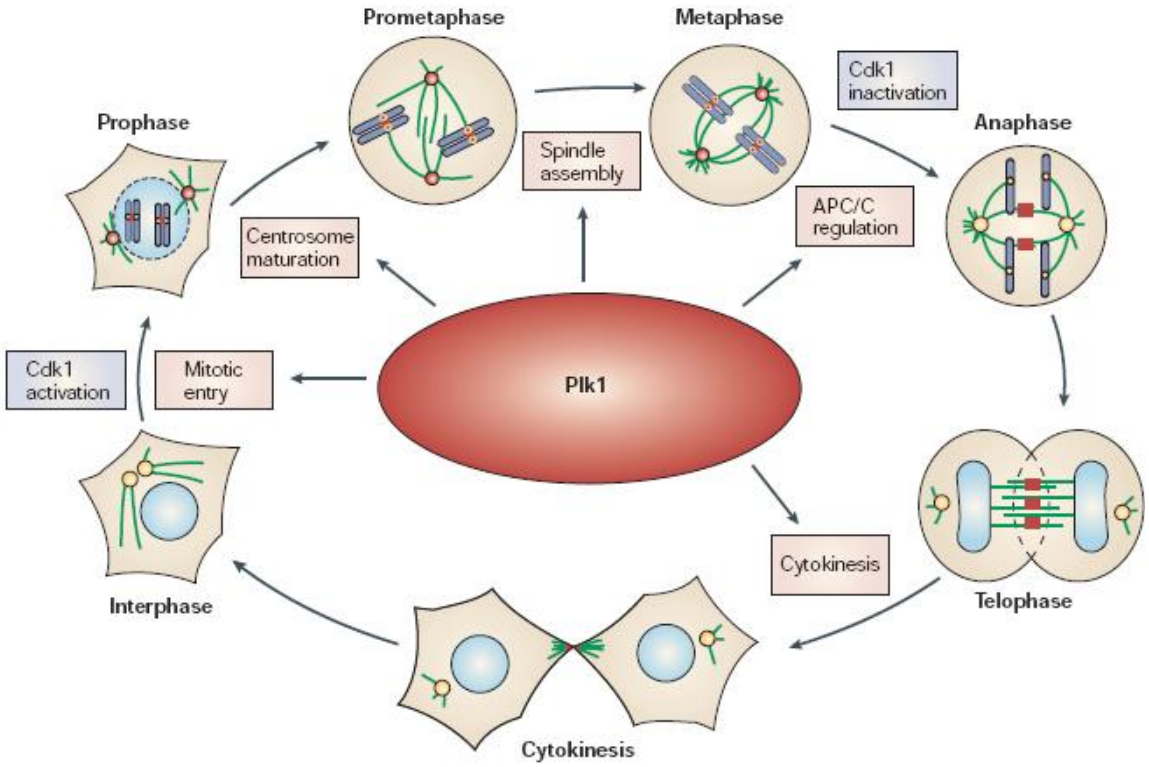

Figure 15: Different Roles of Plk1 in Mitosis

This figure was taken from Reference[84].

phosphorylation of proteins involved in cytokinesis, such as the motors Mklp1[98] and Mklp2[99], or NudC[100] and Rho exchange factor ECT2[101] (summary in **Figure 15**).

Giving the multiple functions of Plk1 throughout mitosis, determining its specific role in each phase can be difficult. In the case of slow acting perturbations of Plk1, such as depletion by RNAi, knock-outs or mutants, only cumulative effects of Plk1 perturbation can be seen. To dissect Plk1's role especially in later stages of mitosis, faster-acting techniques coupled with high-resolution observations are necessary, which small molecule inhibitors can potentially provide.

Consistent with its multiple functions throughout mitosis, Plk1 expression is linked to cancer progression and prognosis[85,102]. Overexpression of the kinase is seen in many tumors such as carcinomas, lymphomas and melanomas and it may be a negative prognostic marker[103]. Interestingly, mutations in Plk1 in human tumors are not very common. Supporting a role of Plk1 in cancer is the finding that depletion by RNAi or transfection with a dominant negative form of Plk1 can induce apoptosis in cancer cells without necessarily affecting normal cells[104-107]. More recently, the use of specific small molecule inhibitors for Plk1 showed promise in *in vivo* studies of tumor growth inhibition, further validating this kinase as potential cancer therapeutic target and encouraging the development of more small molecule inhibitors[108].

2.3.2. Available Inhibitors of Polo-like Kinase

In addition to DAP-81, different inhibitors for Plk had been reported at the time of the study, including a styryl benzylsulfone (ON01910)[109], and a benzothiazole-N-oxide (here named BTO-1, **Figure 16A,B**)[102,110]. Before these inhibitors could be used to examine Plk function in cellular contexts, the following issues needed to be addressed. First, the small molecules should be able to recapitulate key aspects of loss-of-function phenotypes using other approaches. Second, the compounds should inhibit phosphorylation of known Plk substrates in cellular contexts. Third, at concentrations where the compound induces mitotic phenotypes and inhibits substrate phosphorylation, the specificity of the compounds needs to be analyzed.

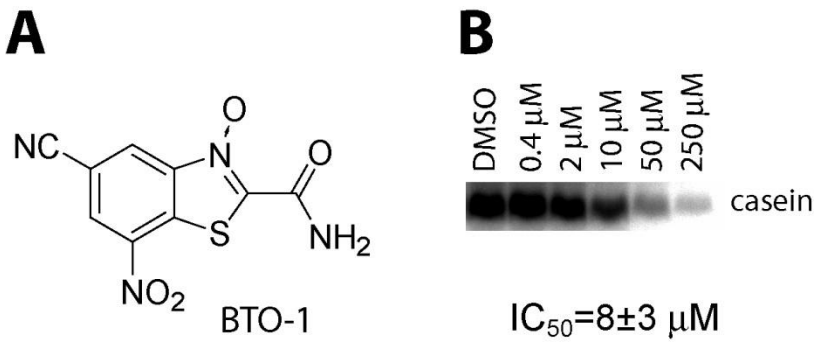

Figure 16: BTO-1 Inhibits Plk1 *in vitro*

(**A**) Chemical structure of BTO-1, a benzothiazole-N-oxide. (**B**) Recombinant Plk1 can phosphorylate casein, as analyzed by the transfer of ^{32}P. BTO-1 inhibits this activity in a dose-dependent manner (IC_{50} = 8 ± 3 μM, *n* = 3, data was fit to a hyperbola).

More recently, two additional small molecule inhibitors of Plk1, cyclapolin[111], a compound related to BTO-1, and BI-2536[112] have been reported and used in studies of Plk1 function. Results from these studies are briefly discussed later on.

2.3.3. Target Validation

Phenotypes Resulting from Chemical Inhibition and RNAi Treatment

Although the effects of depleting a protein using RNAi versus its chemical inhibition by small molecules are not necessarily expected to be identical, they can be reaffirming[68]. To compare the effects of chemical inhibition using BTO-1, ON01910 and DAP-81 to the loss of Plk function, human osteosarcoma cells (U20S) were treated with these compounds and direct comparisons to Plk1-RNAi treated cells were made. Confirming previous reports, Plk1-RNAi resulted in monopolar spindles with a reduced amount of γ-tubulin at their centrosomes[93,94](**Figure 17A,B**). Treatment with DAP-81 and BTO-1 for 4h resulted in monopolar spindles in a comparable fraction of mitotic cells as well,

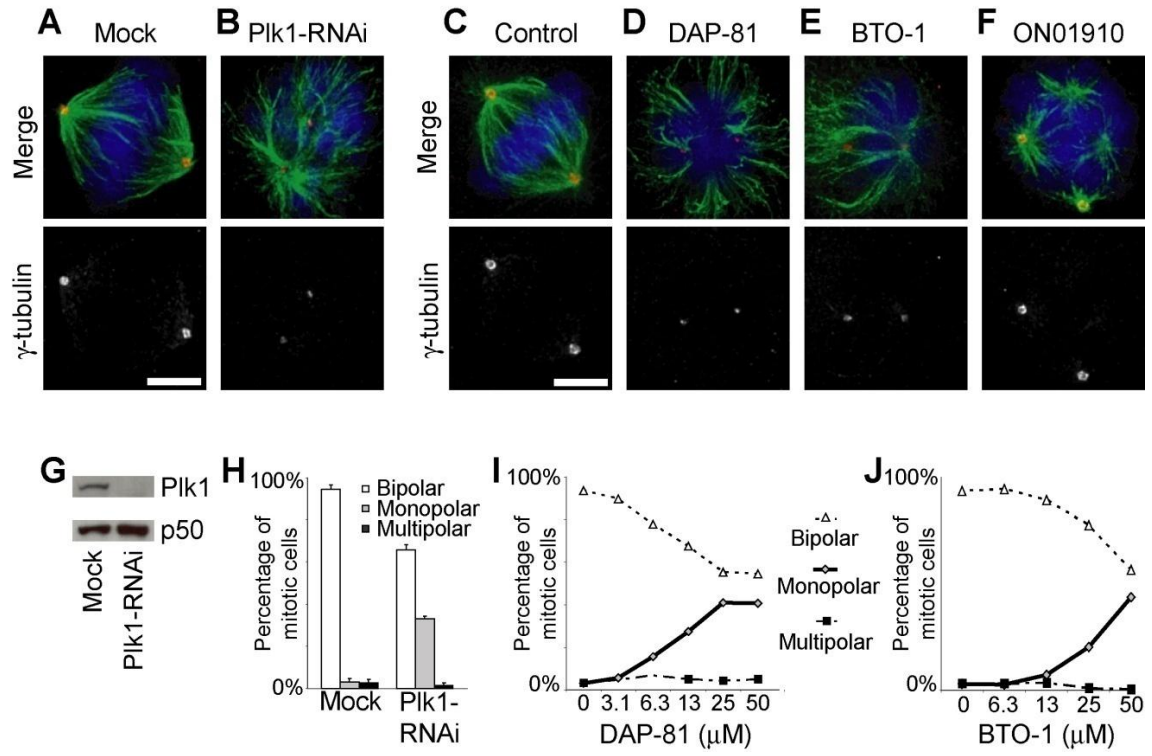

Figure 17: Comparison of Cell Division Phenotypes of Plk1-knock-down and Chemical Inhibitor Treatments.

(**A,B**) U20S cells were either mock-transfected , or transfected with RNA-oligos against Plk1 as previously described[94]. After ~45 hours cells were fixed and processed for immunofluorescence. (**C-F**) After treatment of U20S cells for 4 hours with carrier (DMSO), 25 μM DAP-81, 50 μM BTO-1, or 250 nM ON01910 the cells were processed as in (**A,B**). Overlays show DNA (blue), α-tubulin (green) and γ-tubulin (red). The distribution of γ-tubulin is shown separately. The images show maximum intensity projections of deconvolved image-series covering cell volumes. Additional images are provided as Supplementary Material. (**G**) Western blots for Plk1 knock-down after 45 hours (mitotic shake-off, p50 dynactin is used as a loading control). (**H**) Quantification of mono-, bi- or multipolar spindles in Plk1-RNAi transfected or mock-transfected cells is shown (≥100 cells for each data point, *n* = 3, error bar s.d.). (**I,J**) Quantification of mono-, bi- or multipolar spindles after 4h treatment with different concentrations of DAP-81 or BTO-1 (≥50 cells for each data point, *n* = 3). Scale bars, 5 μm.

along with a reduction of γ-tubulin at the centrosomes (**Figure 17C-E,H-J**). It is noteworthy that similar to the RNAi of Plk1 in this cell type, and from other

reports[93,94], variation in the inter-centrosomal distance was observed and centrosomes often dissociated from the center of monopolar microtubule arrays (**Figure 38A-E** for additional images). Treatment of U20S cells with ON01910 (250 nM) resulted in multipolar spindles, as reported previously for HeLa cells[109]. In addition, interphase microtubule organization was perturbed and a measurable reduction of γ-tubulin staining at centrosomes (4-hour-treatment) was not observed (**Figure 17F**). Due to these differences in the phenotypes observed in ON01910 treated cells versus DAP-81, BTO-1 and Plk1 RNAi-treated cells, only DAP-81 and BTO-1 were used in further experiments. Both of these inhibitors are predicted to target the nucleotide pocket of the kinase and are therefore not likely to be selective for a specific Plk family member. Based on my RNAi experiments, and the known roles of Plk-family members[84], I anticipate that these inhibitors will reveal phenotypes consistent with loss of Plk1 activity, particularly in the time-frame of my live-cell experiments (see below).

Inhibitor Activity in a Cell Line Expressing Fluorescent Tubulin

To take advantage of the temporal control over protein function provided by cell-permeable inhibitors, it is useful to match the perturbation time scales with high resolution analysis of cell division dynamics. A mammalian cell line stably expressing GFP-α-tubulin (PTKαT) has been established as a model system to examine microtubule and chromosome dynamics during mitosis using multi-mode microscopy[113]. Before chemical inhibitors and high-resolution imaging of PTKαT cells could be used to examine Plk function in mitosis, characterization of

the effects of DAP-81 and BTO-1 in this cell type was required. A dose-dependent increase in monopolar mitotic spindles was seen in treated cells (**Figure 18A,B**), with saturation at ~6 μM DAP-81 and ~20 μM BTO-1 (more than 90% of mitotic structures being monopolar). Perturbed bipolar spindles, which had reduced spindle pole separation, were observed at lower concentrations.

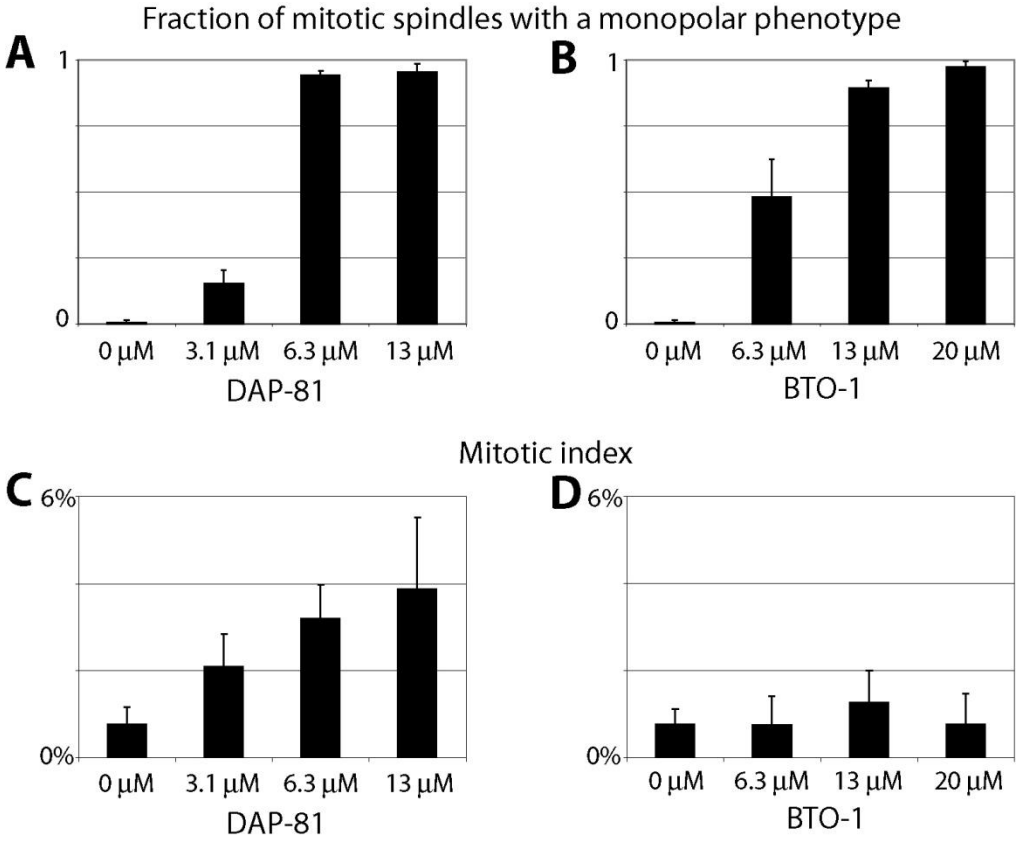

Figure 18: Quantitation of Monopolar Spindles and Mitotic Indices in DAP-81 and BTO-1 Treated PTKαT cells.

PTKαT cells were treated for 4 hours with DAP-81 or BTO-1 at different concentrations, fixed and immunostained for α-tubulin and DNA. (**A,B**) Mitotic spindles were analyzed and the fraction of monopolar spindles was determined (≥ 50 cells for each data point, *n* = 3, error bar s.d.). Saturation was observed at 6.3 μM DAP-81 and 20 μM BTO-1 with 94% and 97% of the mitotic spindles, respectively, being monopolar. (**C,D**) The mitotic indices were determined for both compounds (≥ 500 cells for each data point, *n* = 3, error bar s.d.).

Consistent with these spindle perturbations, a dose-dependent increase in mitotic index was seen for DAP-81 (**Figure 18C**). For BTO-1, the mitotic index did not change appreciably, suggesting that in addition to spindle perturbations, entry into mitosis may also be affected (**Figure 18D**, and data not shown).

Although data for monopolar spindles indicated that ~6 μM DAP-81 and ~20 μM BTO-1 may be saturating concentrations, I needed to ensure that Plk is inhibited in cells at these inhibitor concentrations. Cdc25C has been reported to be a Plk1 substrate and reagents for examining the phosphorylation of Cdc25C on serine-198 are available[114]. Quantitative immunofluorescence was used to analyze phosphorylation levels of Cdc25C in DAP-81 and BTO-1 treated PTK cells. A dose-dependent reduction in phospho-Cdc25C was observed, with saturation at ~6 μM for DAP-81 and ~13 μM for BTO-1 (**Figure 19A-E**). The observed differences in potency of either compound as compared to the data from the *in vitro* kinase assay are not unexpected. Factors such as using a native substrate and phosphatase activity in cells may contribute. Furthermore, differences in ATP concentration can also greatly affect the measured IC_{50} values, assuming competitive inhibition (Cheng-Prusoff equation)[115]. In summary, these data suggest that both inhibitors can block Plk kinase activity in cells at concentrations at which monopolar spindles were observed.

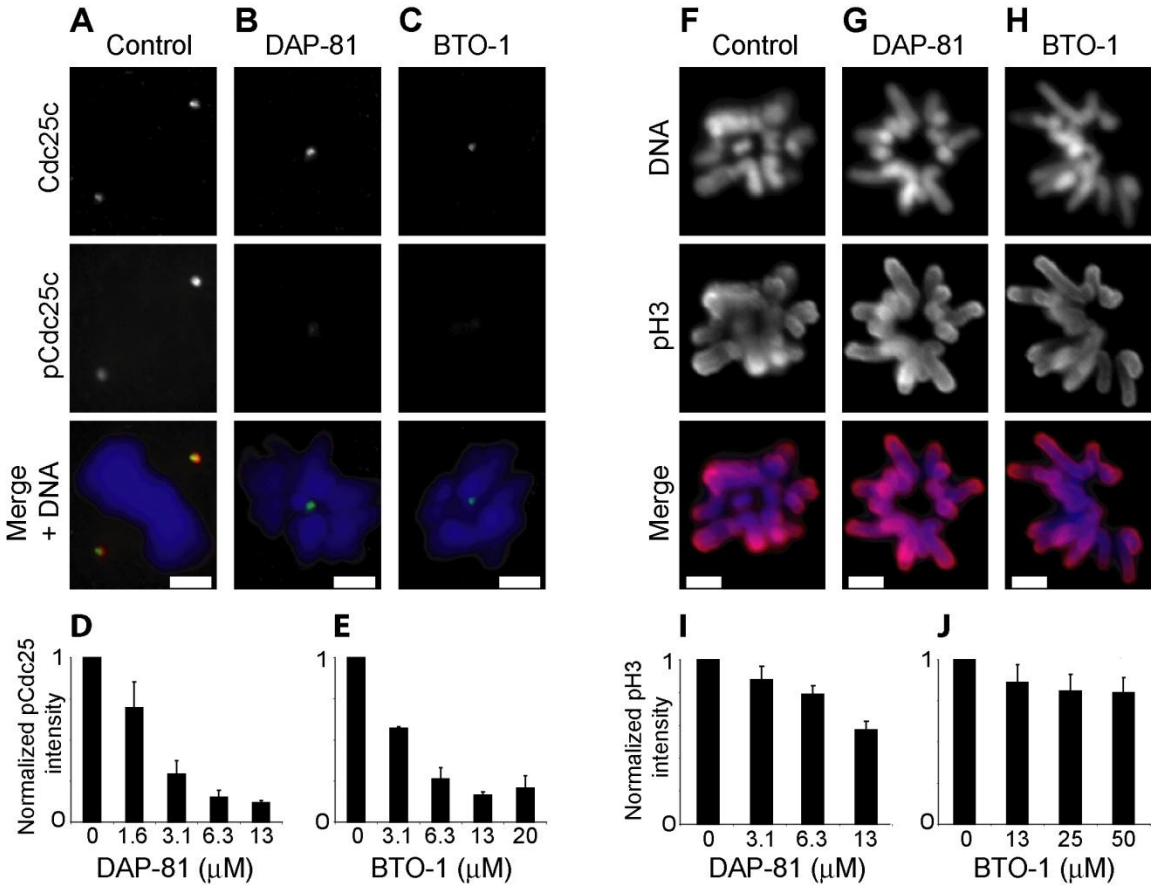

Figure 19: DAP-81 and BTO-1 inhibit the Phosphorylation of a Plk1 Substrate, Cdc25C, in Cells at Concentrations at which Phosphorylation of an Aurora B Kinase Substrate, Histone H3, Is Not.

(**A-E**) PTK cells were treated for 1 hour with carrier (DMSO), DAP-81 (6.3 μM) or BTO-1 (20 μM), fixed and processed for immunofluorescence analysis of Cdc25C, Cdc25C phosphorylated at Ser-198 (pCdc25C) and DNA. Overlays show Cdc25C (green), pCdc25C (red) and DNA (blue). (**D,E**) Quantification of phospho-Cdc25C levels at centrosomes, normalized to Cdc25C, in DAP-81 or BTO-1 treated cells. All scale bars, 5 μm. (**F-J**) Histone H3 phosphorylation at Ser-10 (pH3) was analyzed in treated PTK cells. Cells were arrested in mitosis using monastrol (100 μM), treated with MG132 (20 μM) and carrier (DMSO), DAP-81 (6.3 μM) or BTO-1 (25 μM) for 1 hour, fixed and processed for immunofluorescence. Overlays show DNA (blue) and pH3 (red). (**I,J**) Quantification of pH3 levels in cell treated with either DAP-81 or BTO-1. ≥ 20 cells per condition (*n* = 3). Error bars show s.d.

Examining the Specificity of Plk Inhibitors in PTKαT Cells

The specificity of chemical inhibitors is a key issue that can limit their usefulness as probes of cellular mechanisms. To test the specificity of Plk inhibitors in cellular contexts I examined effects on two key mitotic kinases, Aurora kinases and cyclin-dependent kinases (Cdks)[116]. Ser10 on histone H3 is a known Aurora B phosphorylation site[117]. Quantitative immunofluorescence was used to examine histone H3 Ser10 phosphorylation. At 6.3 μM DAP-81 or 25 μM BTO-1 I found about 20% reduction in H3 phosphorylation compared to control cells (**Figure 19F-J**). At higher concentrations a further reduction in the H3 levels with DAP-81 was seen, consistent with some off-target activity of the inhibitor in this cell type.

Aurora kinase inhibitors as well as Cdk inhibitors can drive cells out of mitosis, even in the presence of anti-mitotic agents that perturb microtubule polymerization or organization[117,118]. RNAi experiments have shown that loss of Plk function blocks cells in mitosis. Therefore, cells arrested in mitosis, by tubulin poisons or monastrol, would not exit mitosis upon treatment with a Plk specific inhibitor. Any off-target activity of a Plk inhibitor that blocks Aurora kinase or Cdk function would suppress the effects of other anti-mitotic agents. To use this assay as an additional test for specificity of Plk inhibitors, PTKαT-cells were accumulated in mitosis by monastrol treatment for 3 hours. Then either DAP-81 or BTO-1 were added and the mitotic state of individual cells was tracked by live imaging using phase-contrast microscopy. The Aurora kinase inhibitor

hesperadin and the Cdk inhibitor purvalanol A were used as controls in parallel experiments. As expected, hesperadin (500 nM) and purvalanol A (10 μM) led to mitotic exit within 90 minutes (9/18 cell and 12/15 cells, respectively)[13,117,118], whereas BTO-1 (20 μM) and DAP-81 (6 μM) treated cells remained in mitosis (cells exiting mitosis: 0/20 and 2/15, respectively). Together, these data indicate that at concentrations where DAP-81 and BTO-1 result in monopolar mitoses, inhibition of Aurora kinase or Cdk is not significant.

Exhaustive tests of inhibitor specificity are typically limited to *in vitro* analyses with non-physiological substrates. These tests for all known mitotic kinases were not readily accessible to me. Instead, I took advantage of an alternative strategy involving the use of different chemical inhibitors of Plks in parallel experiments. It can be assumed that chemically unrelated inhibitors are less likely to have overlapping off-target effects, if any, particularly in the context of a narrow window of cell biology. The use of this strategy to examine the function of the Aurora kinases in cell division has been reported[13]and more recently this strategy was generally suggested to address specificity[68]. Therefore, BTO-1 and DAP-81 were used in parallel experiments to further study Plk function in cell division.

2.3.4. Plk Inhibition Changes Microtubule Dynamics in Dividing Cells

Having validated the inhibitors in cellular context and addressed their specificity, I next used them to examine the effects of Plk inhibition in live cells with a focus on metaphase. The bipolar metaphase spindle is a steady-state structure that can maintain its shape and size for hours in the face of constant microtubule

turnover[2]. I used near simultaneous spinning-disc confocal and differential interference contrast (DIC) microscopy to study microtubule and chromosome dynamics in live PTKαT cells. Cells at metaphase, with established bipolar spindles, were located and DAP-81 was added (6.3 μM). Within minutes, the bipolar spindle started collapsing (3 cells of 6 imaged). In the 3 other cases, cells proceeded with chromosome segregation, most likely due to anaphase initiation prior to equilibration of compounds at inhibitory concentrations in the imaged cell. In subsequent experiments, addition of the proteasome inhibitor MG132 blocked anaphase. In every case (*n* = 15) DAP-81 treatment inhibited the maintenance of spindle shape. The two spindle poles moved closer together and the thick microtubule bundles attaching the poles to the chromosomes, called kinetochore-fibers (K-fibers), shortened. Over time, chromosomes that were aligned at the metaphase plate changed their positions to distribute around the unseparated spindle poles (**Figure 20A-L**). In the time-course of the experiment (1 hour, to limit photobleaching), every spindle imaged shortened, and 4 cells formed monopolar structures. The V-shape of the moving chromosomes indicated that pulling forces acted on chromosomes through K-fibers and that spindle connections were maintained during the disassembly of these microtubules after Plk inhibition (**Figure 20M**). Similar results were obtained in BTO-1 treated cells (**Figure 20N-W**, *n* = 7).

A striking difference between the initial bipolar spindle and the collapsing spindle was the persistence of microtubules that extended from the spindle poles to the cell periphery (*n* = 15). In untreated spindles, a highly dynamic set of

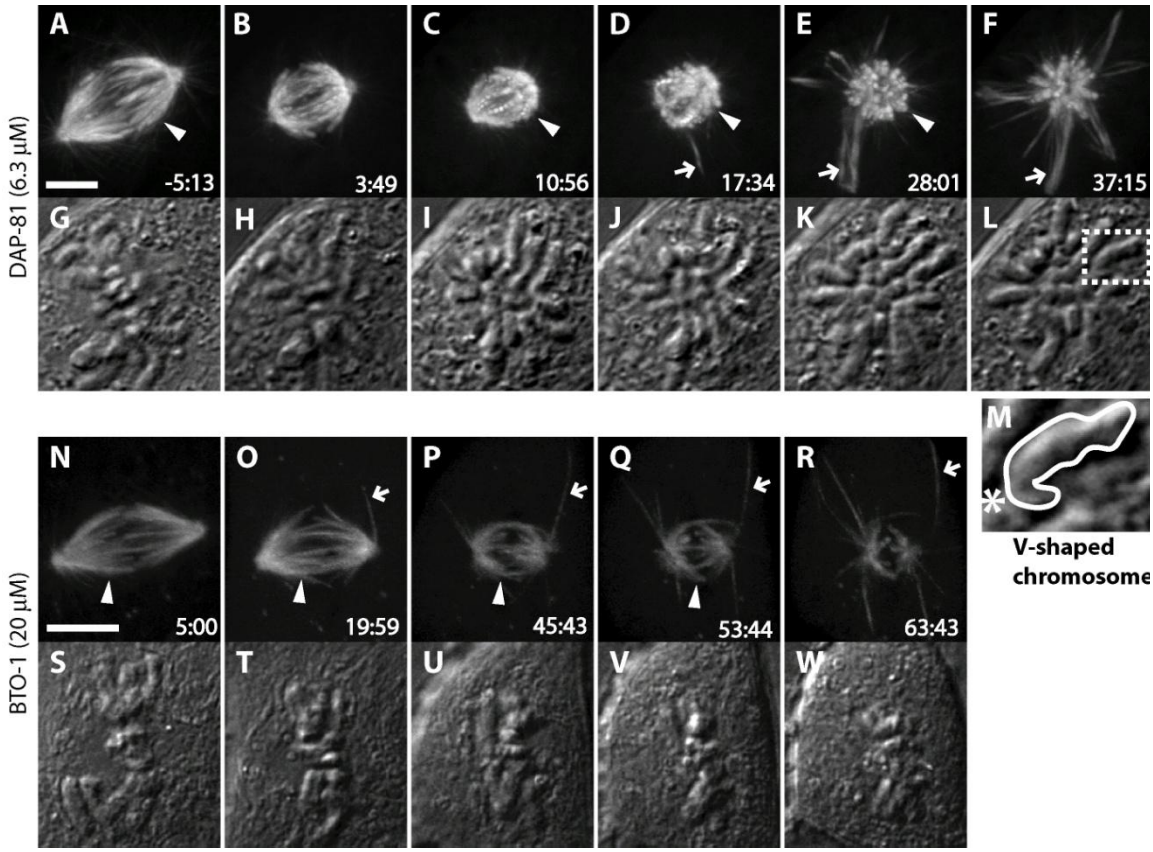

Figure 20: Polo-like Kinase Activity Is Required for the Maintenance of Spindle Bipolarity. GFP-α-tubulin expressing cells were imaged using near simultaneous 3D spinning-disc confocal microscopy and DIC, to track microtubule (**A-F,N-R**) and chromosome distributions (**G-L, S-W**), respectively. (**A-L**) A cell at metaphase with a bipolar spindle was located and DAP-81 (6.3 μM) was added (t = 0 min). The shortening of chromosome-associated microtubule fibers (arrow heads) and the formation of microtubule bundles, not associated with chromosomes and extending away from the spindle (arrows), are indicated. MG132 (20 μM) was used to accumulate metaphase spindles. (**M**) An example of a V-shaped chromosome observed in treated cells is highlighted (from outlined region in panel (**L**), asterisk marks the primary constriction). (**N-W**) In a parallel experiment, BTO-1 (20 μM) was added (t = 0 min) to cell at metaphase and microtubule and chromosome dynamics were examined. Time is in min:sec. Scale bars, 5 μm.

microtubules interacts with the cell cortex. This array is referred to as astral microtubules, which are typically single microtubules that cannot be readily resolved by light microscopy due to low fluorescence intensities and fast

movements in 3-D[86]. In cells treated with either inhibitor, some microtubule fibers that emanated from the spindle pole and made contact with the cell cortex were very intense in confocal sections, indicating that many microtubules were bundled to form these fibers. Analysis using kymography in DAP-81 treated cells showed that unlike astral microtubules in untreated cells, these fibers appeared to be stable over several minutes (**Figure 21A-H**). In collapsing bipolar spindles these microtubule bundles often were not straight, but buckled, suggesting that these fibers were likely pushing against the cell cortex[119]. Together, these data reveal that Plk function is required for the stabilization of chromosome-associated microtubule bundles and the maintenance of dynamic astral microtubules.

The normal shape and size of the bipolar spindle is maintained through a balance-of-forces generated at the cell cortex and at different sites within the spindle[120]. While the observed changes in microtubule dynamics were associated with the spindle collapse, it was unclear how the balance of forces maintaining spindle shape was perturbed. To examine this, I measured the distance between sister kinetochores on individual chromosomes, a read-out for spindle-generated forces acting at chromosomes (**Figure 21I-L**)[121,122]. In untreated bipolar spindles, the inter-kinetochore distance (centromere stretch) was 2.3 ± 0.5 μm. In the presence of nocodazole (33 μM), spindle microtubules were absent and as expected, inter-kinetochore distances were reduced to 1.4 ± 0.3 μm. In collapsing bipolar spindles in cells treated with DAP-81 or BTO-1, I found the inter-kinetochore distance to be 1.9 ± 0.3 μm and 2.3 ± 0.3 μm, respectively. Assuming that these inter-kinetochore distances are not at an elastic limit, such

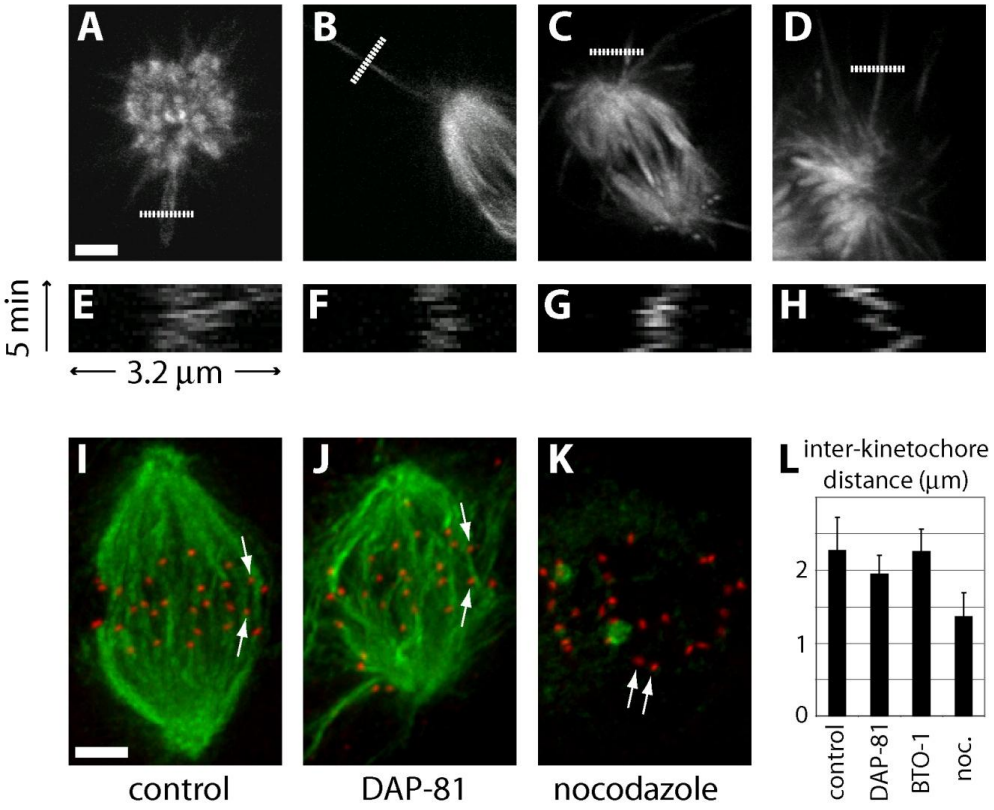

Figure 21: Plk Inhibition Leads to Collapsing Spindles with Stable Astral Microtubule Bundles without Loss of Centromere Tension.

(**A-H**) Stability of microtubule bundles pointing away from the chromosomes (astral microtubules) that formed after treatment with DAP-81 (6.3 μM) was assessed using kymographs, computer-generated montages prepared by aligning the same region imaged in a time-lapse experiment, such that the spatial and temporal components are presented in the x- and y-axes, respectively. For these experiments, inhibitor-treated PTK-α-tubulin cells were imaged by 3D confocal fluorescence microscopy at 20 second time-intervals for 5 minutes. (**A-D**) Mitotic spindles at the start of the recording. The regions used for preparing kymographs are indicated (white bar). (**E-H**) Kymographs for each cell (**A-D**). Stable microtubule bundles are visible as regions of fluorescence intensity that persist for several minutes. (**I-L**) Inter-kinetochore distances were measured in PTK-α-tubulin cells treated with carrier (DMSO), DAP-81 (6 μM), BTO-1 (20 μM) or nocodazole (33 μM) for 45 minutes. Cells were fixed and stained for α-tubulin (green) and CREST-antigen (red). Distances between kinetochore pairs in mitotic cells (center-center of CREST intensity) were measured in three dimensions using deconvolved image planes. (**I-K**) Representative images are shown as maximum intensity projections of deconvolved image-series covering cell volumes. Arrows indicate kinetochore pairs. (**L**) Average inter-kinetochore distances (≥67 kinetochore pairs total from ≥9 cells total for each compound, error bar s.d.). MG132 (20 μM) was used to accumulate metaphase spindles. Scale bars, 2.5 μm.

that they do not increase in response to higher forces, my data suggest that the forces acting on chromosomes are high in Plk inhibitor treated cells, but no greater than those acting in control spindles. Therefore, the spindle collapse is not likely to be a consequence of an increase in the polewards forces acting at chromosomes, but more likely to result from changes in the forces keeping spindle poles apart.

I next examined the consequence of activation of Plk in treated cells, after relief from chemical inhibition. Based on the chemical structure of DAP-81, I expected that the inhibition of the kinase activity would be reversible. To test this idea, the cell culture medium during live microscopy of DAP-81 treated cells was replaced with Plk inhibitor-free media. I observed that upon relief from inhibitor treatment, microtubule dynamics changed. The chromosome-associated K-fibers lengthened, and the astral microtubule bundles destabilized resulting in a typical dynamic astral microtubule array (**Figure 22A-E**, arrows). Furthermore, chromosomes repositioned at the metaphase plate at the center of the spindle (**Figure 22F-J**). Exchanging the medium to remove BTO-1 did not lead to a recovery, indicating that this inhibitor may act irreversibly. Based on the chemical structure of BTO-1 this is not unexpected and irreversibility of this class of inhibitors has also been observed by others[111]. These data suggest, that changes in microtubules dynamics and the associated changes in spindle geometry and chromosome-spindle attachments are dynamically maintained through Plk activity during metaphase.

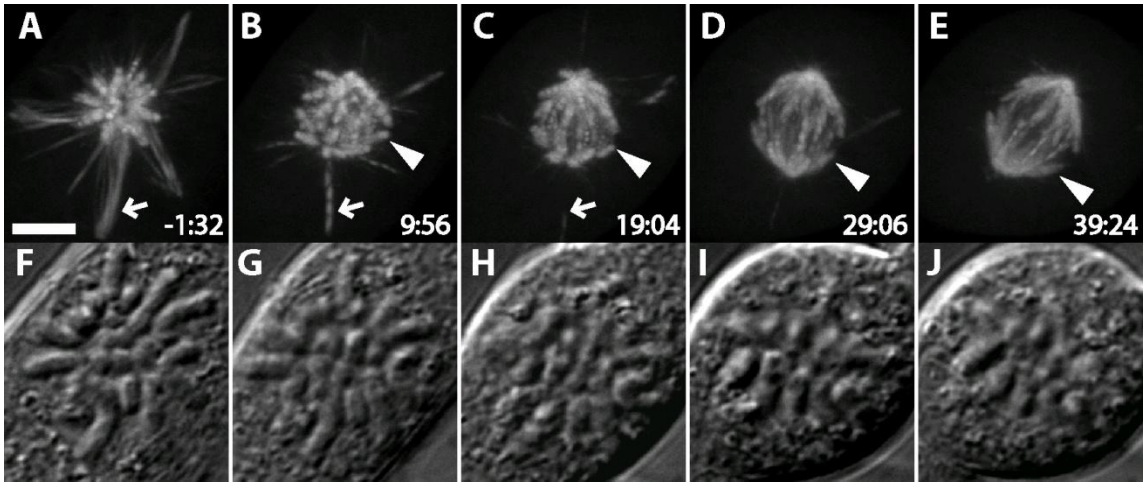

Figure 22: The Selective Stabilization of Astral Microtubules and the Destabilization of K-fibers Can Be Reversed by Plk Activation

GFP-α-tubulin expressing cells were imaged using 3D spinning-disc confocal microscopy and DIC, to track microtubule (**A-E**) and chromosome distributions (**F-J**), respectively. After treatment of a cell with DAP-81 (6.3 μM), the cell culture media was replaced with Plk-inhibitor free media (t=0 min). The chromosome-associated microtubule fibers (arrow heads) lengthened and the microtubule bundles extending away from the spindle and chromosomes (arrows) disassembled, leading to a bipolar spindle. MG132 (20 μM) blocked anaphase onset after relief from DAP-81 treatment. Time is in min:sec. Scale bar, 5 μm.

2.3.5. Discussion

The error-free segregation of chromosomes during cell division depends on the proper functions of a large number of proteins at specific times and cellular sites. The cell division phenotypes observed in cells treated with DAPs are expected to be linked to the functions of a subset of these proteins. Recent genome-wide protein knock-down screens and other RNAi studies have revealed the cell division phenotypes caused by the loss of a large number of proteins, and have linked many proteins to individual phenotypes[71]. For example, multipolar spindles are observed upon depletion of ch-Tog[123], RanBP2[124], Tpx2[125], and astrin[126].

Chromosome alignment defects are seen after RNAi of Aurora kinases[127], Cenp-F[128], Kid[129], and haspin[130]. Monopolar spindles can result from the loss of function of different proteins as well. Activity assays for proteins linked to this phenotype, such as Eg5 and Plk, have been useful in determining the mechanisms of action of small molecule inhibitors that induce monopolar spindles. Therefore knock-down data can help streamline the identification of the targets of compounds selected from phenotype-based screens. However, it requires that assays are available for the activities of different proteins whose functions are linked to a phenotype.

By combining the use of cell-permeable inhibitors that act on fast time scales with high-resolution microscopy I found that Plk contributes to the formation of bipolar mitotic spindles by differentially regulating the dynamics of microtubule populations in the cell. Previous studies have shown that K-fibers in mammalian cells are crosslinked bundles of ~28 microtubules that are believed to be more stable than other spindle microtubules[131]. This has been directly assayed in a number of different ways[3], including chemical perturbations, increasing pressure on cells or changing temperature. Centrosome-associated microtubules, called astral microtubules, represent a subset of spindle microtubules that are generally believed to be more dynamic and not bundled by cross-linking proteins[86]. Upon Plk inhibition, the normally stable K-fibers disassemble and the dynamic centrosome fibers get stabilized and bundled, indicating that Plk activity plays a key role in maintaining the spatial asymmetry in microtubule dynamics in dividing cells. While the emergence of stabilized astral microtubules is visible, their origin

is not clear. Three pathways could lead to their formation: centrosome-mediated nucleation, kinetochore-mediated nucleation, or nucleation mediated by existing microbules[132-135]. The absence of kinetochores on the end of the stabilized bundles indicates that kinetochore mediated nucleation is most likely not relevant. Differentiation between the two other possibilities is difficult and would require more detailed studies of microtubule dynamics in these bundles, which are beyond the scope of my work. Such spatially-specific regulation of microtubule polymerization has also been proposed for the role of Aurora kinases in the disassembly of incorrect chromosome-spindle attachments and the stabilization of the proper attachments[13]. In a similar fashion, Plk could affect the phosphorylation state of microtubule stabilizers or destabilizers in normal bipolar spindles, in a spatially specific manner to help establish the differentiation between stable K-fibers in the mitotic spindle and dynamic astral microtubules. Exactly which effectors of microtubules are involved is not yet clear, but further studies using small molecule inhibitors might help to identify relevant Plk substrates.

The bipolar spindles can collapse into monopolar structures upon Plk inhibition because of two different force-generating mechanisms. It is possible that the depolymerizing K-fibers, which are associated with unseparated sister chromatids, can generate a pulling force that draws the two spindle poles of a bipolar spindle together. Alternatively, hyper-stabilized astral microtubules could interact with the cell cortex to push the spindle poles together. While it is possible that both mechanisms contribute to the spindle collapse, the astral microtubule

bundles observed after Plk inhibition buckle upon cortical interactions, suggesting that pushing forces may be more important. Consistent with this hypothesis, I find that upon activation of Plk after relief from chemical inhibitor, bipolar spindle formation is closely linked to the disappearance of these stable microtubules. In addition, the observed tension across kinetochores in collapsing spindles indicates that spindle pulling forces are active, but not likely to be greater than in untreated cells. It is likely that combining microscopy studies with physical manipulation of the spindle and chromosomes will be necessary to unravel the roles of Plk in regulating the balance of forces that maintain spindle organization[87,121].

Small molecule probes for the different proteins that play key roles in cell division will help clarify the mechanisms required for the stable propagation of genomes. My studies suggest that one approach to obtain such probes is to explore thoroughly the chemical space around known bio-active compounds. Consistent with this idea, recent studies have shown that small changes in substitutions on kinase inhibitors can not only change their selectivity for different classes of kinases, but can also lead to inhibitors for completely unrelated proteins[63]. The hydroxyl modification of a Src-kinase inhibitor, which instead leads to carbonyl reductase inhibition, is a striking example how small changes in chemical structure can lead to divergent biological activity[136]. The number of different phenotypes observed in dividing cells treated with closely related diaminopyrimidines suggests that this scaffold can target several different proteins. In addition, a single phenotype can be induced by DAP-49 and DAP-81,

which target different proteins. I anticipate that further exploration of the chemical diversity of diaminopyrimidines will lead to new probes for cell division proteins. The fact that these compounds map to the chemical space occupied by drug-like molecules suggests that their further development into therapeutic agents could succeed. Current synthesis efforts generating diverse compounds should lead to other versatile scaffolds[74]. It will be important to test if other 'privileged scaffolds' can also effectively span cell division phenotype space.

2.3.6. Recently Reported Work Using Polo-like Kinase Inhibitors

After completing my studies on Polo-like kinase using DAP-81 and BTO-1, several new small molecule inhibitors have been reported and used to answer questions about Plk's role in cell division, with a particular focus on later stages of mitosis.

McInnes et al. used a benzothiazole related to BTO-1, termed cyclapolin 1, to answer questions regarding Plk at metaphase[111]. In addition to fixed cell experiments that resulted in abnormal bipolar mitotic spindles, Mcinnes et al. carried out live-cell experiments on Drosophila S2 cells that clearly demonstrated the collapse of bipolar spindles into monopolar spindles upon Plk inhibition, corroborating my findings. In addition they found that Plk inhibition led to a reduced recruitment of γ-tubulin to the centrosomes as well to a reduced ability of centrosomes to nucleate microtubules *in vitro*.

Lenart et al. employed BI 2536, a nanomolar and highly specific inhibitor of Plks, to look at Plk's role in mitotic entry as well as prophase and metaphase[112]. This

team found that inhibition of Plk led to a delay in mitotic entry but not a block, and that Plk activity was necessary to form stable microtubule attachments during prometa- and metaphase leading to a spindle-checkpoint arrest in its absence. As with the other reported compounds and my findings, the compound gave a monopolar spindle phenotype.

Continuing the work with BI 2536, Petronczki et al. reported interesting details about Plk's function in cytokinesis[137]. They added the small molecule inhibitor 20 minutes after metaphase in live-cell experiments and observed problems in cytokinesis, markedly the inability to assemble the actomyosin ring necessary for contraction. This may have been caused by localization defects of several proteins, since the authors showed that in the absence of Plk activity Plk itself, RhoA, its exchange factor Ect2 as well as Mklp2 failed to localize to the midzone.

I also provided BTO-1 and BI 2536 to collaborators to look at the role of Plk in anaphase and cytokinesis, areas I have personally not explored[138]. Ian Brennan in Aaron Straight's lab found that upon inhibiting Plk activity at anaphase onset, chromosome movement in anaphase A was unaffected, but the spindle elongation typical for anaphase B was inhibited. Focusing on cytokinesis, it was also shown that Plk activity was necessary for assembly of the contractile ring. Similarly to findings from other groups, it was shown that RhoA and its exchange factor Ect2 mislocalized, and that crucial components of the acto-myosin ring, like anilin, did not get properly recruited.

Comparable results were also obtained by Burkard et al. using a slightly different approach[30]. Knocking out the endogenous Plk1 and replacing it with an ATP-analog sensitive allele allowed the authors to control Plk1 activity by using an ATP-analog as a small molecule inhibitor. Employing this ‘bump-hole’ technique they showed that Plk1 activity was necessary for cytokinesis since cleavage furrow formation was blocked, accompanied by mislocalization of Plk1 as well as Ect2, in agreement with the aforementioned reports.

Using the advantage and availability of small molecule inhibitors the roles of Plk throughout mitosis could be better defined. In addition to its role in spindle maintenance, its roles in anaphase and cytokinesis are now better understood.

3. A Phenotypic Screen for Inhibitors of Organelle Transport

3.1. Introduction

3.1.1. Organelle Transport and Motor Proteins

Intracellular transport in the cytoplasm of eukaryotic cells is a fundamental biological process required for the correct distribution and positioning of organelles such as mitochondria or peroxisomes, and for macromolecular complexes, such as mRNPs and chromosomes in mitosis. In addition, intracellular transport processes can rapidly adjust and maintain the molecular architecture, which cannot be achieved with passive transport processes such as diffusion alone, on the typical length scale of eukaryotic cells.

To generate the forces necessary to move “cargo” in the viscous cytoplasm of cells, two major mechanisms are used: the polymerization and depolymerization of cytoskeletal subunits such as tubulin or actin, and the work provided by molecular motor proteins that use ATP-hydrolysis as energy source. These motors can be categorized into three classes: dyneins and kinesins, which move along microtubules, and myosins, which move along actin filaments[139].

To allow transport of a specific cargo to occur to a specific location within the cell at a precise point in time, prerequisites to create order within a cell, regulation of intracellular transport is essential. As one would expect, the regulation is complex and can occur on several different layers. First, specificity of the process can be

achieved by binding of the motor proteins to a defined set of cargoes, which is often mediated by adapter proteins, such as dynactin in the case of kinesin or dynein. This specificity can confer the proper targeting of organelles to certain sites within the cytoplasm, e.g. the transport of mitochondria to regions of increased ATP-usage. Second, the movement of cargo can be activated or inhibited depending on a certain physiological state of the cell, e.g. control of chromosome movement in mitosis [140,141], cessation of cytoplasmic organelle movement during cell division[142-144], as well as lipid droplet movement during embryonic development in Drosophila[145]. One of the most remarkable cases of regulated movement of organelles are pigment organelles (melanosomes) in the pigment cells (melanophores) of lower vertebrates (described below).

The study of factors involved in producing and regulating movement of cellular cargo remains one of the key challenges of cell biology. While many of the motor proteins are known, the mechanisms of their regulation and coordination are generally not well understood. Therefore, suitable methods for the identification of the molecular agents as well as detailed functional analysis in cellular contexts are of great importance.

Given the fact that intracellular transport processes occur on a fast time scale, small molecules coupled with live imaging microscopy would be well suited to better understand them. However, at the moment the available number of small molecules is limiting. For instance, as inhibitors of motor proteins only blebbistatin[17], which targets myosin II, and various inhibitors of mitotic kinesin Eg5 have been used significantly[55]. Therefore the identification of additional

small molecules that can lead to a better understanding of intracellular transport remains highly desirable. To achieve this goal, a screening system for inhibitors of intracellular transport would be beneficial.

3.1.2. The Xenopus Melanophore System

Pigment cells are a suitable system to study organelle transport, since their main physiological function is the coordinated redistribution and bidirectional movement of pigments in response to defined chemical signals. Pigment cells are generally referred to as chromatophores and can be classified into two major classes: cells that undergo pigment redistribution or structural changes that result in a physiological color change ('rapid color changes based on the intracellular mobilization of pigment-containing organelles'[146]) and pigment-producing cells where the pigment is transported to other cell types that take it up, resulting in a morphological color change ('color changes result from changes in the number and synthetic activity of integrumentary pigment cells'[147]). Pigment cells which contain black pigments are referred to as melanophores, in the case of the rapid acting cells common in invertebrates, fish, and amphibians, while the slow acting cells, common to birds and mammals, are referred to as melanocytes[146]. The organelles containing black pigment are known as melanosomes.

In the case of melanophores from the African Clawed Frog (*Xenopus Laevis*), the cells contain a large number of melanosomes in their cytoplasm that can either cluster around the center of the cell in the perinuclear region (aggregated state) or be homogeneously dispersed (dispersed state)(**Figure 23A**). The net effect of

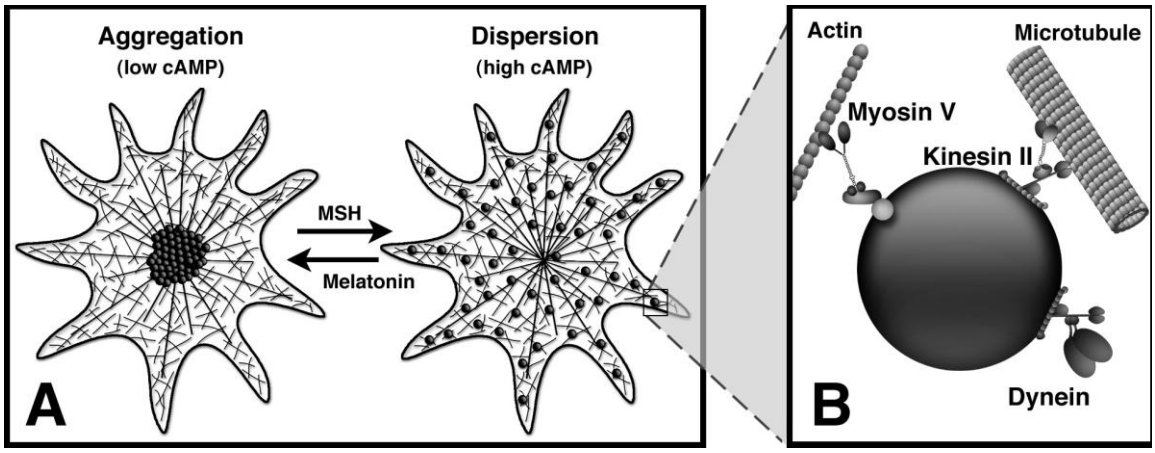

Figure 23: Hormones, Signals, and Motors Involved in Pigment Transport in Melanophores.

(**A**) Aggregation is induced by melatonin, which decreases the cAMP concentration, and dispersion by melanocyte-stimulating hormone (MSH). (**B**) Aggregation is performed by cytoplasmic dynein while dispersion requires two motors, kinesin II and myosin V. Figure adapted from Vladimir Gelfand.

the differences in pigment distribution in the skin is a lighter color in case of the aggregated cells and a darker color in the dispersed case.

To allow a switching between these two physiological states, hormones are used that affect the intracellular cyclic AMP (cAMP) level via a signaling cascade. Melatonin leads to a decreased level of cAMP, whereas melanocyte stimulating hormone (MSH) results in an increased level of cAMP, promoting aggregation and dispersion, respectively. A high-throughput screening approach in melanophores using the degree of dispersion as read-out can be envisioned, which is aided by the access to an immortalized Xenopus melanophore cell line[148]. Screening for inhibition of either direction of organelle movement is possible and enough cell-free extract for biochemical experiments as well as target identification studies can be obtained[149]. Furthermore, melanosomes are

easily observed in bright-field microscopy, and the obtained data can be easily subjected to computational analysis. Moreover, the melanophore system has been extensively studied as a model for organelle motility (reviewed in [150]) resulting in the following relevant findings for my work: (1) Correct movement of melanosomes requires the presence of microtubules and actin filaments as cytoskeletal components[151-153](**Figure 23B**). (2) Gradient purified melanosomes contain three types of molecular motor proteins on their membrane surface: heterotrimeric kinesin-II, a plus-end directed microtubule motor, cytoplasmic dynein, a minus-end directed microtubule motor, and myosin-V, an actin motor[149,152] (**Figure 23B**). (3) Movement of isolated melanosomes has been reconstituted *in vitro* [149,152,154]. (4) Components of the regulatory pathway from hormones and hormone receptors to protein kinase A (PKA) are well known[155]. In addition assays and reagents are available to determine whether a compound targets these proteins. Therefore, secondary screens can be used to select compounds that act downstream of PKA, a part of the signaling pathway not yet characterized (**Figure 24**).

This system provides several additional factors that are advantageous to a chemical screen. The organelle motility in melanophores relies on the relatively stable interphase microtubules, and is therefore much less sensitive to more subtle effects on microtubule dynamics, which are particularly seen in cell division screens[55,156]. Furthermore, inhibitors of vesicle formation and membrane fusion are not selected for in the case of melanophores, unlike a screen using

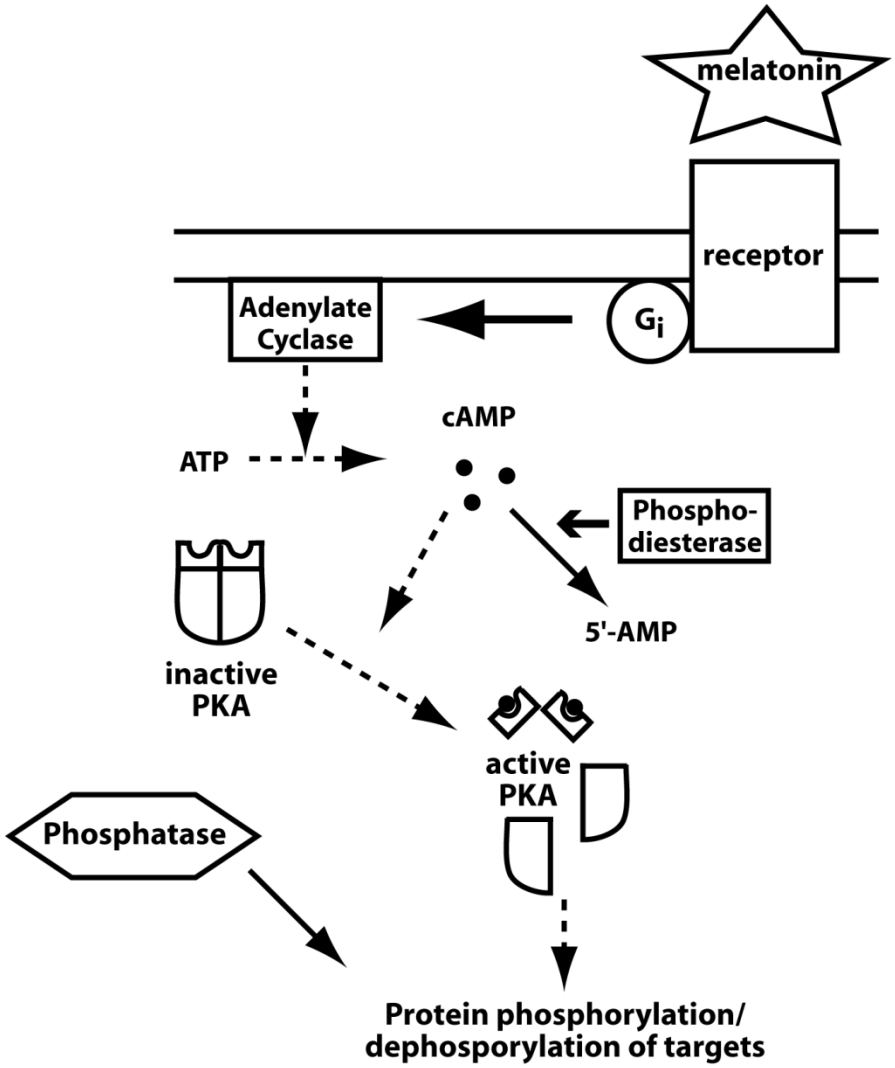

Figure 24: Signaling in Melanosome Aggregation

Protein dephosphorylation of unknown targets, which leads to aggregation of melanosomes, is dependent on a serine/threonine dependent phosphatase that becomes active when PKA is inactivated. G_i - inhibitory G-protein, cAMP – cyclic AMP, 5'-AMP – adenosine 5'-monophosphate. Solid arrows indicate active path, dashed arrows indicate inactive path. Adapted from Reference[155].

membrane transport between the endoplasmic reticulum and the Golgi apparatus as read-out[157].

While the advantages listed above make the melanophore system ideal to find inhibitors for organelle motility, the potential insights and compounds obtained

are expected to be applicable to the wider field of biological systems. Considering that many kinds of membrane organelles are associated with (at least) two microtubule based motor proteins of opposite polarities and a myosin[158-161], this assumption appears reasonable. Moreover, coordination of plus- and minus-end directed organelle movement on microtubules is not only observed in melanophores, but in other cell types as well[162-164]. In summary, the study of melanosome transport should uncover general mechanisms of organelle transport in eukaryotic cells.

In summary, establishing and using melanophores as a cell-based screening system for inhibitors of intracellular transport may be useful in identifying compounds that are of wider use in the field of intracellular transport and may help to gain a better understanding of this dynamic and highly regulated process.

3.2. The Screen

3.2.1. Screening for Inhibitors of Aggregation

With hormones available that either induce aggregation or dispersion in melanophores, melatonin and MSH, respectively, screening can be carried out for inhibitors of transport in either direction. Screening was focused on inhibitors of aggregation for two main reasons: The upstream signaling in aggregation is less complex: it relies only on PKA whereas dispersion can be influenced by PKA and protein kinase C[155], and aggregation mainly relies on the function of only one motor, cytoplasmic dynein. Both these facts help to simplify follow-up studies, especially considering that inhibitors of PKA and purified dynein were available.

In addition, a small molecule inhibitor of cytoplasmic dynein would be especially useful since this multisubunit motor protein participates in a large number of transport processes other than melanosome movement, such as positioning and assembly of the mitotic spindle, interflagellar and viral transport, as well as nuclear envelop breakdown[139].

The initial screen in a high-throughput format was developed and carried out by Michael Lampson in the laboratory. Briefly, melanophores are dispersed by treatment with MSH to obtained uniformly dispersed cells. Next, the screening compounds are added and after a short incubation period the melanosome aggregation is stimulated by treatment with melatonin. After fixation, the fields of cells can be imaged using an automated image acquisition set-up, followed by computational analysis with 'dispersion index' as readout (see **Figure 25**). This procedure can be carried out in a 384-well format, allowing a high throughput. (**Figure 25**)

3.2.2. Potential Targets of Active Compounds

Considering the inhibition of aggregation as the primary readout in the melanophore system, three major modes of action of the compounds can be envisioned, which need to be distinguished in follow-up screens. First, the compound could lead to an arrest of metabolic activity and therefore to a stop of ATP-dependent movement of aggregating melanosomes. Second, organelle movement could be inhibited in a more specific way by inhibiting either molecular motors directly, acting on the motor-cargo interaction, or affecting the necessary cytoskeletal components for motor activity. Third, the movement of melanosomes

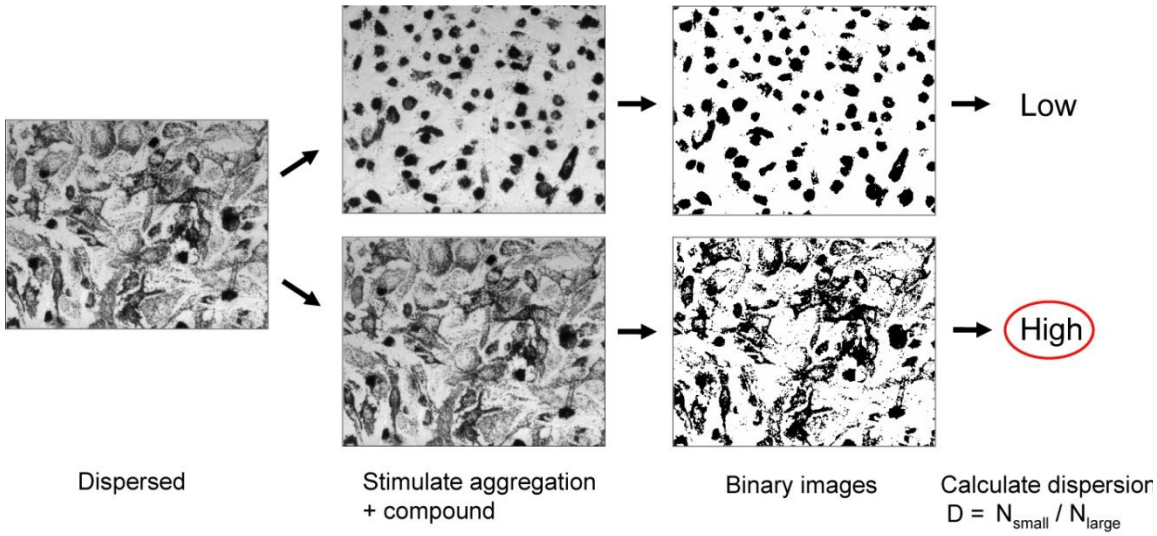

Figure 25: Inhibitors of Aggregation Can Be Identified by High-Throughput Imaging
The pre-dispersed cells are incubated with the test compound for 30 minutes followed by the treatment with melatonin to stimulate aggregation. After one hour the cells are fixed and images of the wells are acquired by an automated system. The images are then processed and inhibitors of aggregation can be detected and quantified by a high ratio of small objects (single dispersed melanosomes, N_{small}) versus large objects (aggregates of melanosomes in the perinuclear region, N_{large}), the ratio is referred to as dispersion index.

could be intact but their bias towards the perinuclear region is lost, indicating alteration of signaling events necessary for the coordination of movement. Of these potential target classes for compounds, two groups are of particularly relevant in understanding intracellular transport. The first are direct inhibitors of motor proteins, especially given the fact that only very few small molecule inhibitors are known so far[17,55]. The second group consists of compounds that act in the signaling pathway downstream of PKA, since this region is not well characterized[155]. A flow scheme for selecting these particular compounds of interest is shown below (**Figure 26**).

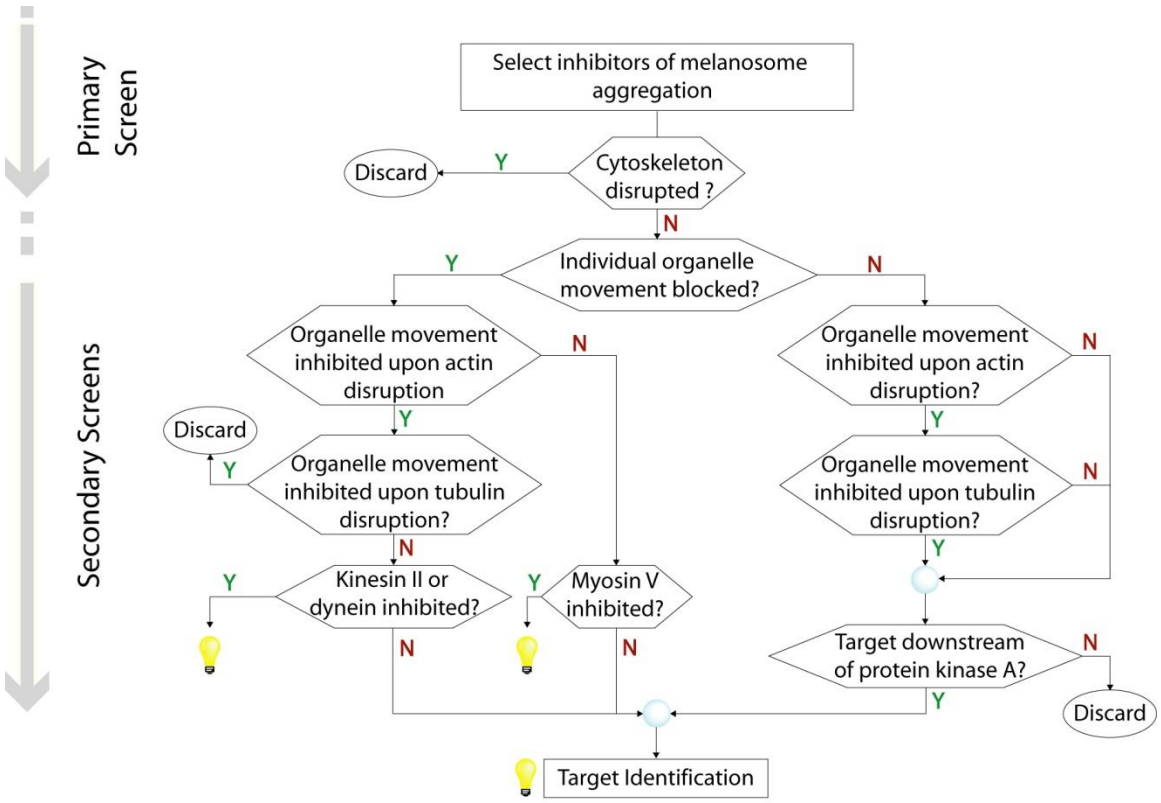

Figure 26: Flow Chart Outlining Potential Targets and Screening Strategies for Inhibitors of Aggregation

Light bulbs indicate satisfactory endpoints. Y- yes, N – no.

3.2.3. Selection of Compound Collections

The first primary screen used a commercial collection of 15000 compounds (Chemical Diversity, Inc., ”Chemdiv”) available through the Rockefeller University High-Throughput Screening Center. This collection contains about 125 combinatorial templates with up to 200 compounds per template. While this collection has no focus towards a particular class of target proteins it mostly consists of heterocyclic compounds that follow Lipinski’s Rule of Five[43] to increase the chance of finding small, cell-permeable, drug-like inhibitors.

In addition to an unbiased screen, the encouraging results from the DAP-collection in the screen for cell division phenotypes suggested that a biased approach using a ‘privileged scaffold’ might be successful as well. Therefore, compounds from the DAP-collection were tested in the melanophore screen. This should allow us to address several questions regarding the use of DAPs. First, is the hit rate increased in the case of DAPs as compared to an unbiased library? Second, are DAPs potentially useful inhibitors in the context of intracellular transport? Third, what is the cross-correlation between hits in both screens?

With a primary screen, follow-up assays and compound collections in hand, the identification of inhibitors of intracellular transport could be carried out.

3.3. Screen Results

3.3.1. Overview over Results from the “Chemdiv” Collection

The screen of the ~15000 compounds from the chemical diversity collection was carried out in triplicate for inhibitors of aggregation following the procedure outlined above. Compounds that showed activity in any of the screens were retested, leading to 156 confirmed hits from this library in the primary screen. After elimination of tubulin depolymerizers by evaluation of immunofluorescent tubulin stains, inhibitors were grouped into the two major classes: compounds that block aggregation by stopping organelle movement in cells, and compounds that block aggregation without stopping organelle movement. Compounds that did not stop movement most likely acted as regulators in the signaling cascade and were further differentiated as either upstream or downstream of PKA. For

this purpose, the compound's effect on aggregation was tested in the presence of a constitutively active PKA-inhibitor, PKI, a peptide that was transfected into melanophores. Overriding of the aggregation induced by PKI indicated that the compounds most likely acted downstream of PKA[165](**Figure 27A,B**). The summary of results is shown below (**Figure 28**).

A potential target for the 19 compounds that stopped organelle movement is cytoplasmic dynein. Dynein inhibition could be easily tested by an *in vitro* microtubule sliding assay using purified components from bovine brain[166]. In this assay the motor protein is immobilized onto a glass coverslip followed by addition of fluorescently marked microtubules that bind to the motor. In the presence of ATP the microtubules will 'slide' across the surface driven by dynein. None of the compounds, however, inhibited this dynein driven motion at concentrations of up to 125 μM.

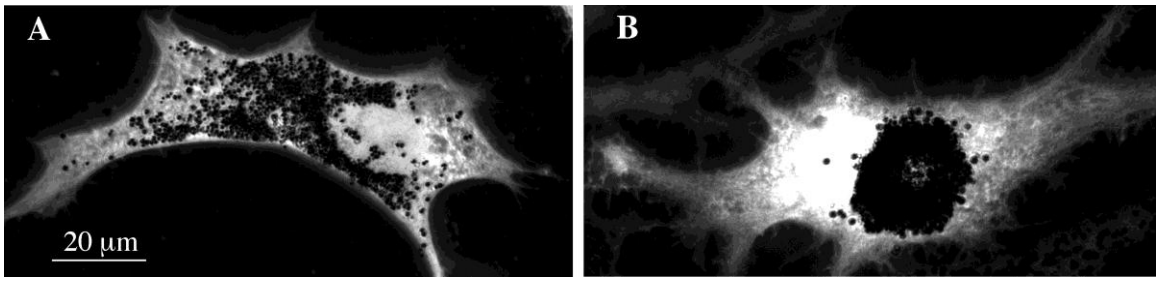

Figure 27: Compounds Downstream of PKA Induce Dispersion Even if PKA Is Inhibited.
Cells were transfected with a plasmid that encodes PKA inhibitor PKI and a tag[165]. Transfected cells were treated for 30 min with 20 μM compound (**A**) or DMSO (**B**) as control and fixed. The compound induces dispersion of melanosomes even in the cells with inhibited PKA. The image is a superposition of two images, brightfield (melanosomes) and immunofluorescence (tag). Figure courtesy of V.I. Gelfand.

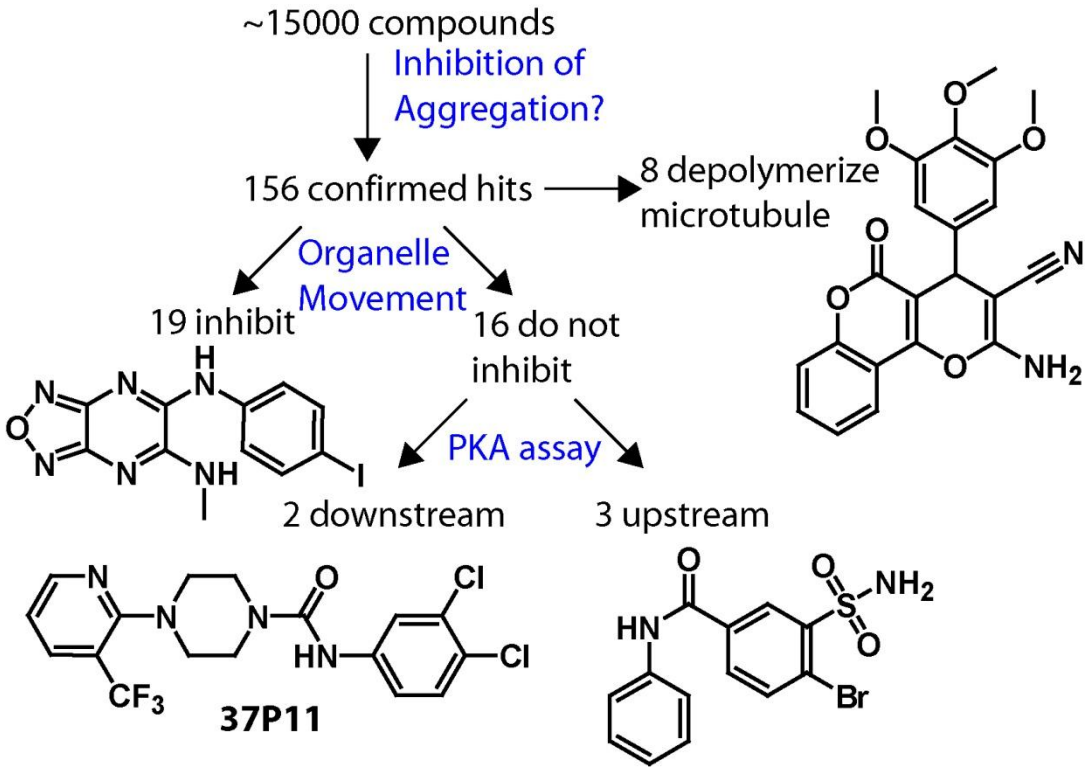

Figure 28: Overview of Results from the Screen of the Chemdiv Library

In addition to the number of compounds chemical structures of examples for each major class of hits are shown.

3.3.2. 37P11 Blocks Aggregation But Does Not Stop Organelle Movement

In the absence of a reliable assay for the testing of the direct inhibition of other motor proteins other than dynein, namely kinesin II, I focused my attention on the second class of hit compounds, the ones that did not stop organelle movement and therefore putatively acted on the signaling cascade. Of the compounds selected and tested, 37P11 appeared promising. It was able to overcome PKA inhibition, indicating that its primary target is downstream of this kinase. Furthermore, 37P11 has a modular chemical structure which should make it

easily amenable to analog synthesis for target identification studies (chemical structure see **Figure 28**).

Properties of 37P11 in Primary and Secondary Assays

For subsequent studies 37P11 needed to be characterized further in regard to potency as well as potential protein targets. Since the molecular target of this molecule was unknown, the cellular activity was the only relevant read-out for potency. A titration was carried out in triplicate in the primary assay yielding an IC_{50} value of 21 μM using the dispersion index as quantitation (**Figure 29A**). In addition, removal of the compound by washout in the same assay clearly demonstrated that the observed inhibition was reversible (**Figure 29B**). The inhibition of aggregation experiments were also carried out using live-cell microscopy, revealing a loss of bias towards aggregation despite relatively

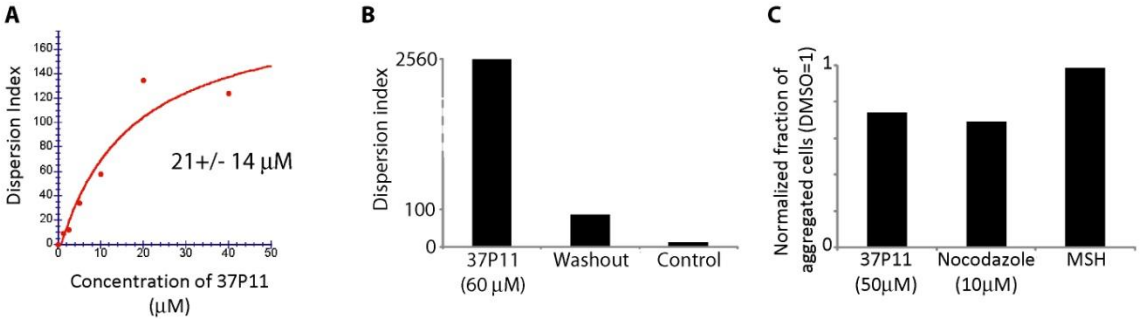

Figure 29: 37P11, a Reversible Inhibitor with an IC_{50} of 21μM, Acts Downstream of PKA

(**A**) Titration curve for 37P11 in the primary assay with dispersion index as read-out (experiment done in triplicate). (**B**) After removal of 37P11 (washout) the melanosomes are able to aggregate, the cells are nearly fully recovered as compared to the control case (DMSO). (**C**) Transfection of melanophores with PKI leads to tight aggregation. Treatment of cells with either 37P11 or nocodazole partially overcome that effect whereas MSH cannot, indicating that 37P11 acts downstream of PKA.

normal organelle motility (data not shown). As the next step, 37P11 was tested in the PKA inhibitor-assay (**Figure 27A,B**). Although the quantitation showed only a relatively modest effect of the compound in overcoming aggregation, the effect is comparable to that of nocodazole, which is known to depolymerize microtubules and to act downstream of PKA (**Figure 29C**). MSH, an upstream signal in aggregation shows no effect in the presence of PKA-inhibitor, as expected. These data indicate that 37P11 blocks aggregation without stopping the movement of melanosomes and that the target of 37P11 may be a regulatory protein downstream of PKA.

Design and Synthesis of 37P11 analogs for SAR Studies

After identification of 37P11 as compound that acts downstream of PKA, I was interested in determining its molecular target. Of note, very similar compounds are known as antagonists of mammalian vanilloid receptors, particular type I vanilloid receptors (VR1) also known as TRPV1 or capsaicin receptors[167-170]. This particular class of receptors are usually Ca^{2+}-channels that are expressed in neurons and play a role in signaling of noxious stimuli, including heat and pH[171,172]. They are the cellular target of capsaicin, the active component of hot peppers, but are also activated by a range of inflammatory mediators. Although, the VR1 class proteins are not expected to be present in Xenopus skin cells, it cannot be ruled out that 37P11 influences calcium signaling in the cells, leading to the observed changes in aggregation behavior.

To identify 37P11 targets, two important points regarding the compound needed to be addressed: a suitable attachment point in the molecule for an affinity linker

and an increase in potency of the compound. To achieve both goals I carried out a structure-activity relationship (SAR) study for 37P11. First, information from the primary screen was briefly analyzed. Among the compounds initially screened, only one additional library member belonged to the same template as 37P11, and it showed very similar activity to 37P11. Since it structurally resembles 37P11 closely, not much information could be obtained from this data point. For the detailed SAR study the molecule was divided into 4 parts: the pyridine ring, the piperazine ring, the urea linkage, and the phenyl ring (**Figure 30B**). Employing a modular tactic, the parts of the molecule were individually varied using different substitutions to see changes in activity and guide the design of more potent analogs. On either end of the molecule, larger functional groups, such as esters, silicon ethers or biotin, were also introduced to test if potential linkers for affinity probes would be tolerated. The designed analogs were then synthesized, mostly in a two step procedure, including a nucleophilic substitution on the pyridine ring followed by the urea-forming reaction of the corresponding isocyanate with the piperazine (**Figure 30A**). Of the more than 40 analogs synthesized and tested, none was significantly more potent in the primary assay than the parent compound, 37P11. Additionally, introduction of larger functional groups led to a loss of activity (**Table 2**, appendix). Accordingly, only compounds with relatively minor changes in molecular structure were among the ones that showed comparable activity to the parent compound (**Figure 30C**). In summary, while biologically active analogs of 37P11 could be found in the SAR-study, no introduced modification gave a significant increase in potency. Furthermore, no

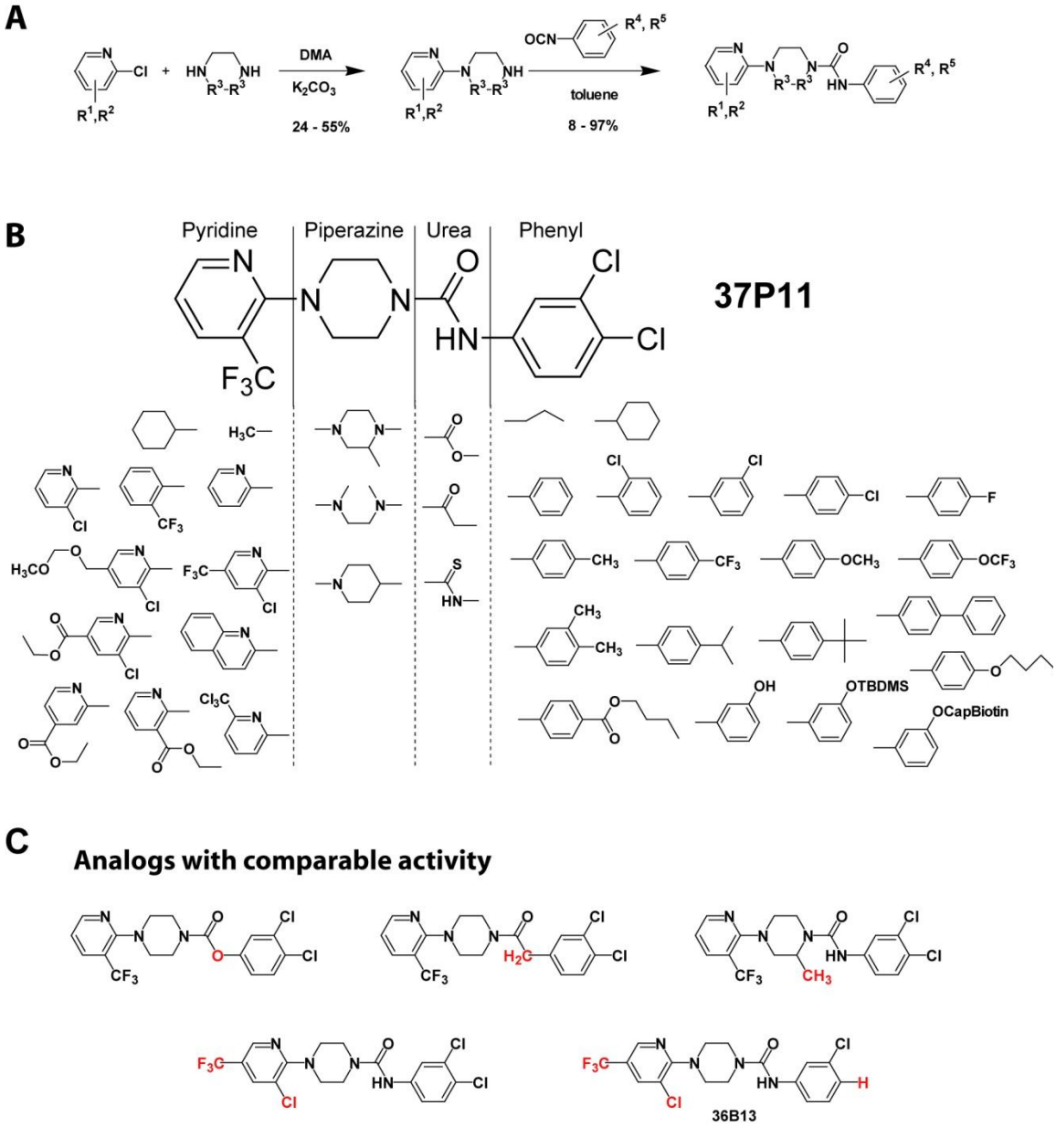

Figure 30: Analogs of 37P11 in SAR Studies

(**A**) General synthesis scheme for 37P11 and its analogs. (**B**) Overview over the 41 synthesized analogs of 37P11. Generally, only one part of the lead structure was changed at a time to the functional groups shown. (**C**) Structures of the 5 analogs that retained comparable activity to the parent compound 37P11. Among them is 36B13, another hit in the primary screen from the same template as 37P11. Changes to the parent compound are highlighted in red.

suitable attachment point for an affinity-based linker became apparent. In light of these results, target identification for this interesting compound did not appear feasible at this point in time.

Effects of 37P11 in Other Biological Contexts

Although target identification studies for 37P11 proved difficult, I was still interested in studying its effects in biological contexts other than melanosome movement. A closely related process is the bidirectional movement of lysosomes, another membranous organelle whose transport within the cell depends on dynein, a kinesin, and a myosin[158,161]. Lysosomes, as principal sites of intracellular digestion, are characterized by a low internal pH, allowing them to be stained with pH-sensitive fluorescent dye in living cells. Using this approach, I imaged and tracked lysosomes in Xenopus melanophores in the absence and presence of 37P11, to study the compound's effect on their motility. As readout the diffusion coefficient was determined (displacement^2/time), which is unaffected by the directionality of movement. While a high percentage of lysosomes in compound treated cells still showed a high diffusion coefficient, indicating active microtubule based transport, their number was somewhat reduced as compared to untreated cells (**Figure 31**). The difference seems to be an increased number of lysosomes with no or very slow apparent movement. Without the knowledge of the molecular target of 37P11, the interpretation of this data is difficult, but it might indicate that 37P11 is able to induce on increase in switching of lysosomes to the slow actin-based transport from the fast microtubule-based transport.

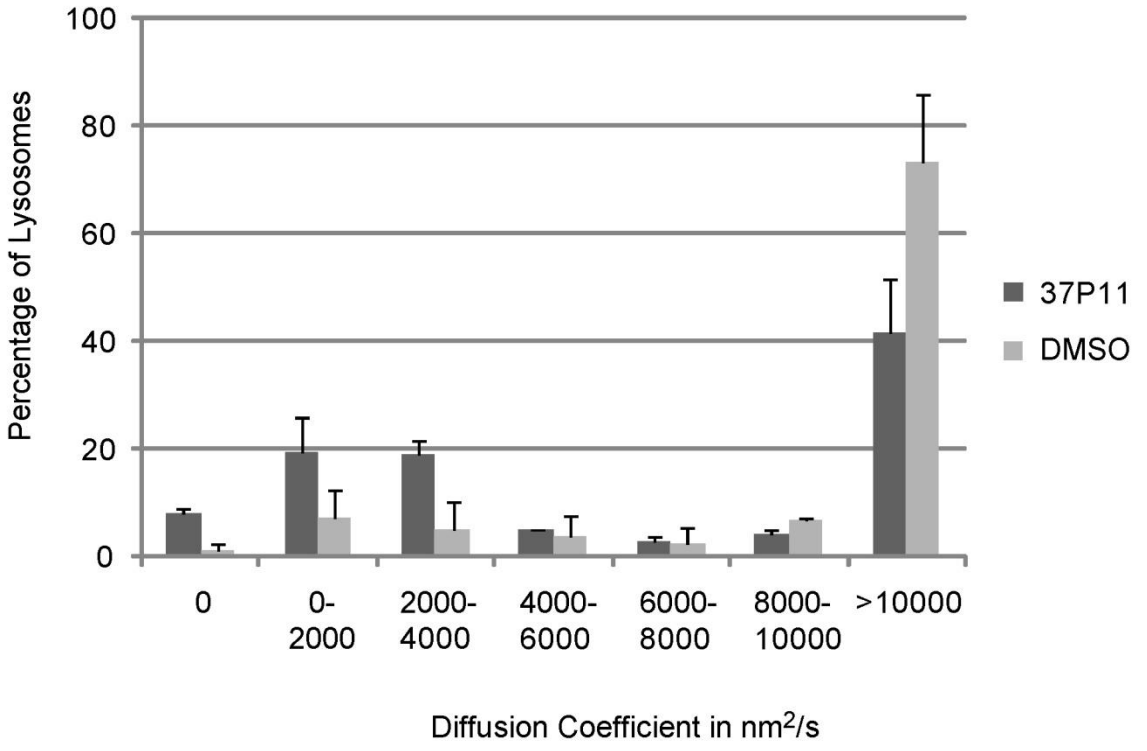

Figure 31: 37P11 Affects Movement of Lysosomes in Cells

Fluorescently labeled lysosomes were tracked in treated (37P11, 50 μM) or untreated (DMSO) live melanophores. Lysosome motility distribution is shown according to diffusion coefficient. At least 41 organelles (from more than 10 cells each) were tracked for each experiment. Error bar shows s.d. from two independent experiments.

Chromosomes in vertebrate cells show a regular oscillatory movement during mitosis, an intracellular transport process that can be easily observed. The switch in direction during the oscillation is usually abrupt, and has been termed 'directional instability'[173,174]. The exact mechanism for chromosome oscillation is not well understood, but a tug-of-war like mechanism is suspected to play a role. This would involve forces generated by motors as well as forces generated by microtubules[3,175-177]. For the analysis of chromosome oscillation in the presence of 37P11, PTK cells were treated with monastrol to generate monopolar cells

arrested in mitosis, and then incubated with 37P11. Time-lapse live-cell microscopy was used to image chromosomes and evaluate their movement over time. The movement of single chromosomes was then visualized using kymography (**Figure 32A,B**). While in the control cases all cells (12/12) showed chromosome oscillations, in the case of 37P11 chromosome oscillation was observed in only 7/15 cells (**Figure 32A,B**). This data indicates that 37P11 may also have an effect in this biological system, but the potential molecular target

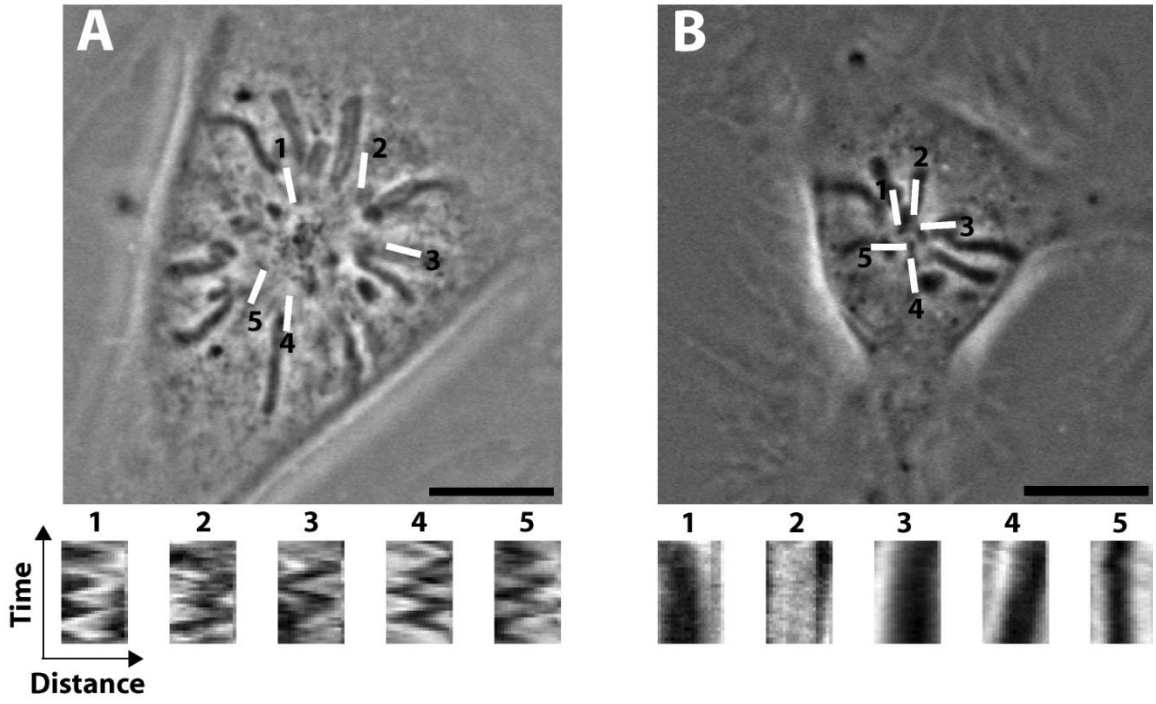

Figure 32: 37P11 Can Affect Chromosome Oscillations in Metaphase Cells

PTK cells were treated with monastrol (100 μM) for 30 min and then 37P11 or DMSO were added 30 min before imaging using a 40x phase objective. For visualization of the chromosome movement 31 frames with a 20s interval were taken. Plotting the intensities along a fixed line (distance) over all frames results in a kymographic image. (**A**) depicts a DMSO treated cell as an example of observable oscillations as clearly demonstrated by the zig-zag pattern in the corresponding kymographs. (**B**) One of the 37P11 treated cells (50 μM) that shows static chromosomes as seen by the straight lines in the kymographs. Regions for kymographic analysis are shown as white lines. Scale bars, 10 μm.

remains elusive. It cannot be ruled out, that the observed effect may be an indicator of general cytotoxicity of 37P11, given the fact that the cell division apparatus is very sensitive to perturbations of various kinds.

37P11 could be shown to be active in other biological contexts than melanosome movement but further studies would be needed to identify its exact role. Without fully understanding the role of 37P11 in melanosomes movement, an extension into other systems will remain difficult.

Conclusion

Identification of a number of small molecules that are active as inhibitors of aggregation showed that this screening approach is viable. One of the most promising compounds, 37P11, could be characterized as an inhibitor of a regulatory pathway, but as in many screens, target identification for the compound appeared to be the most difficult step and wasn't feasible. Although 37P11 showed activity in a range of different biological systems, in the absence of an identifiable target the compound has only limited value for further biological studies. In addition, the potential of off-target activities as suggested by the relatively high IC-value and known biological targets that could alter relevant calcium levels, are potential drawbacks, too. Therefore, 37P11 was not pursued further for biological application. Other identified inhibitors of melanosome aggregation from this unbiased library still hold promise for biologically active probes of intracellular transport.

3.3.3. Overview over Results from the Screen of the DAP Collection

The primary screen was carried out in triplicate in a high-throughput fashion using a subset of the DAP collection described earlier. Of the 53 compounds tested in the screen at 10 μM, 7 were identified and confirmed as hits. The observed hit rate of about 13% of the tested collection is surprisingly high, especially as compared to about 1% hit rate observed in the case of the "Chemdiv" library. On the other hand, the hit rate is more comparable to the one seen with the same compounds in the phenotypic screen for cell division phenotypes (41%). The somewhat lower number could be explained by several reasons, such as the lower compound concentration used in the case of the melanophores (10 μM vs. 20 μM), a higher sensitivity towards perturbations in cell division vs. in melanosome transport in interphase, or the difference in cell types used (Xenopus melanophores vs. BS-C-1 cells). Nevertheless, the considerably increased hit rate using the DAP-collection supports the assertion that it contains a bias towards biological activity. Since this 'bias' was observed in two different biological systems, the idea of screening 'privileged scaffolds' might prove viable on a larger scale.

Of the 7 hits, one compound strongly affected the interphase microtubule skeleton of melanophores and was not considered further. The remaining 6 compounds were tested in the organelle motility assay to reveal that 2 of them are able to stop organelle movement, indicating that they might target the involved motor proteins directly. The more potent compound of the two, DAP-29, was then selected for further testing of potential targets. Even without knowing

the precise molecular targets of the 7 compounds, it is clear that they fall at least into two different categories regarding the mode of inhibition of aggregation, which supports the idea that structurally related compounds (DAPs) can give the same phenotype by targeting different proteins.

Comparing the hit compounds from the melanophore screen as well as the screen for mitotic phenotypes, it is interesting to note that of the 7 compounds identified in the melanophore screen, 3 were not identified in the other screen, 2 scored as having mitotic defects, whereas the remaining 2 scored as effectors of the microtubule skeleton. This result illustrates that both screens seem to identify a different set of compounds with some overlap present.

3.3.4. DAP-29 as a Potential Inhibitor of Dynein Mediated Processes

DAP-29, a 2,4-diaryl diaminopyrimidine, was identified as an inhibitor of melanosome aggregation (**Figure 33A**). In contrast to 37P11, DAP-29 clearly belongs to the second class of compounds, which inhibits aggregation in the primary assay by stopping organelle movement. Therefore, the potency of DAP-29 can be easily determined using organelle movement in live cells. From the tracking data provided by my collaborator Vladimir Gelfand (Northwestern University), I determined the IC_{50} to be 6 μM, which is in agreement with the compound being a hit at the screening concentration of 10 μM (**Figure 33B,C**). In addition, removal of the compound from cells by replacing the medium (washout) led to a full recovery of melanosome movement indicating that the effects of DAP-29 are reversible (**Figure 33D**).

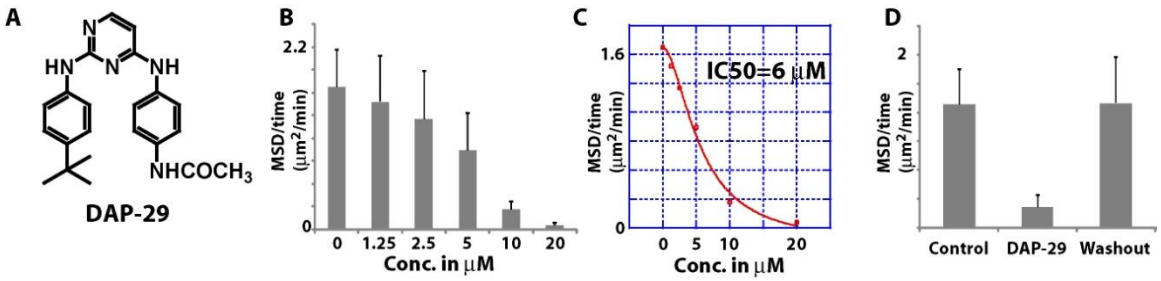

Figure 33: DAP-29 Reversibly Inhibits Melanosome Movement with an IC_{50} of 6 μM

(**A**) Chemical structure of DAP-29. (**B**) Dose response curve for melanosome movement in the presence of varying concentrations of DAP-29 using mean square displacement (MSD) per time (1s intervals) as measure. (**C**) IC_{50} was obtained using a logistic curve fit, as shown. (**D**) Melanosomes in cells treated with 20 μM DAP-29 showed a full recovery of movement after removal of the compound (washout), as compared to the untreated control (MSD per 4s period used). At least 14 melanosomes were tracked for each data point. Error bars show s.d.

Potential Protein Targets of DAP-29

Given the fact that DAP-29 can stop melanosome movement, its relevant protein target is expected to be closely associated with the transport process itself. This includes the essential motor proteins, namely heterotrimeric kinesin II, cytoplasmic dynein, and myosin V, as well as their tracks, microtubules and actin.

As first step, I evaluated the interphase microtubule skeleton of melanophores in the presence of the DAP-29 to see any potential effect. After treatment of the cells with 20 μM compound for 4 hours, a marked change occurred. The cells retracted somewhat, and a bundling of interphase microtubules seemed to occur (**Figure 34A**). While this rules out a strong depolymerizing effect of DAP-29 at relevant concentrations, it clearly indicates that microtubule architecture is affected, either by direct action of the compound on microtubules or by indirect

actions through microtubule associated proteins (MAPs). One of the relevant MAPs could be cytoplasmic dynein and the associated dynactin, since it has been reported that inhibition of their interaction can lead to problems in the interphase microtubule skeleton[178]. Of note, DAP-29 was found to affect interphase microtubules in the screen for mitotic phenotypes in BS-C-1 cells, corroborating the findings in melanophores. A specific assay to look for increased polymerization or depolymerization of purified microtubules in an *in vitro* setting (in the absence of microtubule associated proteins) was not conducted: however, it should be noted that no noticeable effects on microtubules themselves were observed in the microtubule sliding assays described below. This finding indicates that direct effects on microtubules are unlikely to be important at the compound concentration used. The treatment period of 4 hours might also be less relevant for effects seen in the screen on a 1 hour time frame.

To analyze whether the actin skeleton as well as the activity of the actin dependent motor myosin V are affected, the actin dependent transport in melanophores was tested in live cells (carried out by Vladimir Gelfand). This can be achieved similarly by organelle tracking as described above, but to separate the actin from the microtubule dependent part of melanosome motility, the microtubule skeleton was first depolymerized using nocodazole. Tracking of organelles in either DAP-29 treated or the untreated case showed very similar curves for the mean square displacement over time (**Figure 34B**). This finding indicates that neither actin nor actin-dependent transport by myosin V are significantly affected by DAP-29 in cells.

This result left inhibition of microtubule-based transport as the most likely explanation of the observed effects. To indicate whether DAP-29 can inhibit one of the relevant motors for this transport, cytoplasmic dynein or kinesin II, directly, microtubule sliding assays can be used. Cytoplasmic dynein could be isolated and purified from bovine brain for this experiment, however, kinesin II was not accessible. Therefore two other kinesins, conventional kinesin (kinesin I) and a member of the kinesin V family, Eg5, were used, which only allowed limited conclusions about effects of DAP-29 on the more relevant kinesin II. In all three cases, no strong effects of DAP-29 could be observed in the sliding assay at concentrations used in the primary screen (10 μM, data not shown). Interestingly, effects on microtubule sliding were clearly visible at higher concentrations (100 μM) with all three motor proteins (**Figure 34C-E**). This result may be interpreted in several ways. First, DAP-29 does not target cytoplasmic dynein or kinesin II directly and the effects seen at higher concentrations are due to off-target effects, potentially on tubulin. Second, DAP-29 targets cytoplasmic dynein, but because of differences in species of this multi-protein motor complex, this effect is only seen at higher concentration in the *in vitro* assay. Alternatively the higher potency in cells could be due to an accumulation effect. Third, the relevant target may be kinesin II, and because this protein is unavailable, it cannot be tested conclusively. While it is difficult to differentiate between these, and other alternative explanations for the observed results in *in vitro* assays, testing of the compound in other biological context may prove useful, especially to find out whether DAP-29 targets cytoplasmic dynein.

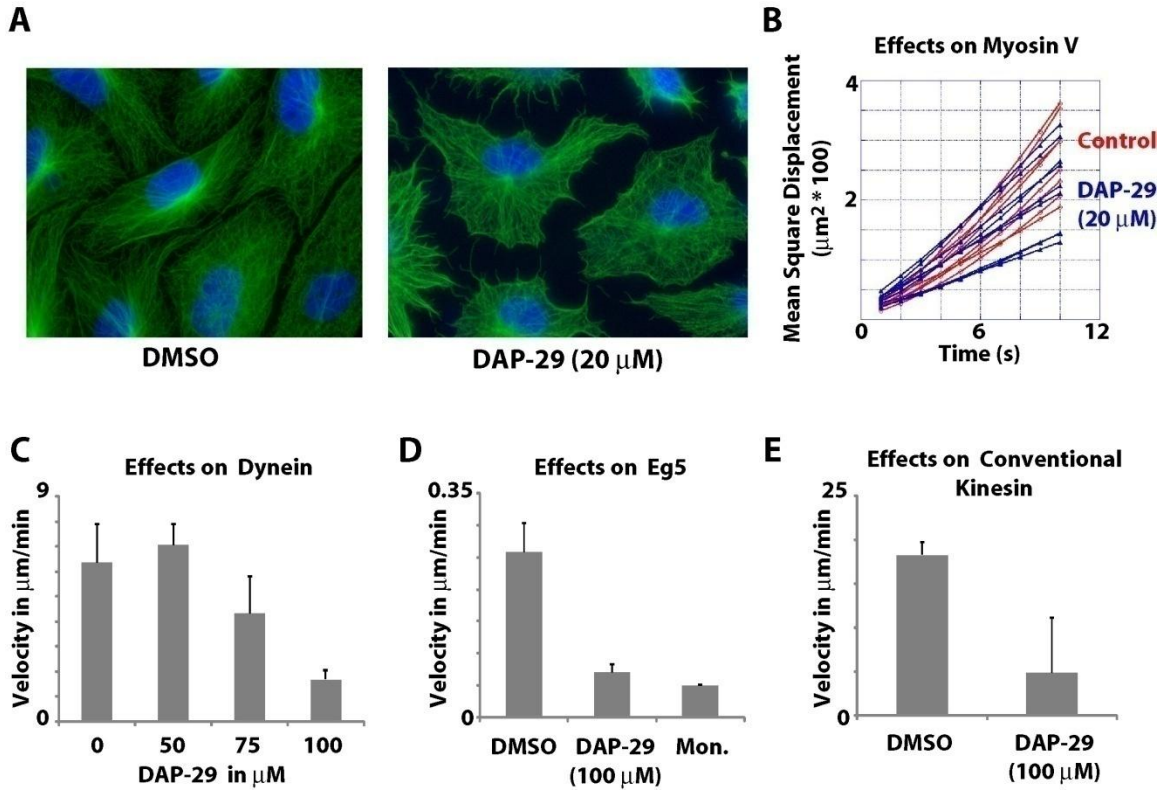

Figure 34: DAP-29 Effects on Microtubules and Several Motor Proteins

(**A**) Melanophores were treated for 4 h with either DMSO (control) or 20 μM DAP-29, fixed, and stained for α-tubulin (green) and DNA (blue). Color combined fluorescence images show an effect of DAP-29 on the interphase microtubule skeleton that includes bundling and cell retraction. (**B**) Tracking of melanosomes in live cells in the absence of microtubules (nocodazole depolymerized) showed no significant differences in the control and DAP-29 treated case (20 μM), demonstrating that myosin V mediated transport is unaffected (data from VG). (**C-E**) *In vitro* microtubule sliding assays were used to observe effects of DAP-29 on either cytoplasmic dynein, Eg5, or conventional kinesin, respectively. Strong effects on dynein motility were only seen at 100 μM DAP-29. At that concentration motility of Eg5, with monastrol as positive control, and conventional kinesin were also strongly affected. The sliding assays contained 1 mM ATP as nucleotide in duplicate. Error bars show s.d. from independent experiments.

DAP-29 in Other Biological Systems

The following studies, describing the effects of DAP-29 on other intracellular transport processes were carried out by collaborators in the laboratory of Vladimir Gelfand and therefore will be only briefly discussed here.

Sperm motility is dependent on active flagellar motion, which in turn is dependent on functioning axonemal dynein that slides microtubules against each other in an energy (ATP) dependent manner[179]. In the case of sea urchin the sperm can be easily collected and its movement studied. In the presence of 20 μM DAP-29 a shutdown of movement is observed, indicating that the compound might be targeting dynein. Since the flagellar movement does not depend on kinesin, this result suggests that among different alternatives dynein might be the more relevant target.

Similar to the movement of melanosomes, other cargoes are transported bidirectionally in the cytoplasm of cells. Among them are peroxisomes, organelles that carry out oxidative reactions using molecular oxygen, and messenger ribonuclear-protein complexes (mRNPs), that play important roles in gene expression[164]. In the case of peroxisome and mRNPs, their transport depends on cytoplasmic dynein and conventional kinesin[180,181]. Separate observation of both cargoes in Drosophila S2 cells, each can be visualized by fluorescently tagging specific proteins, in the presence of DAP-29 showed that their movement is inhibited (data shown for peroxisomes in **Figure 35**).

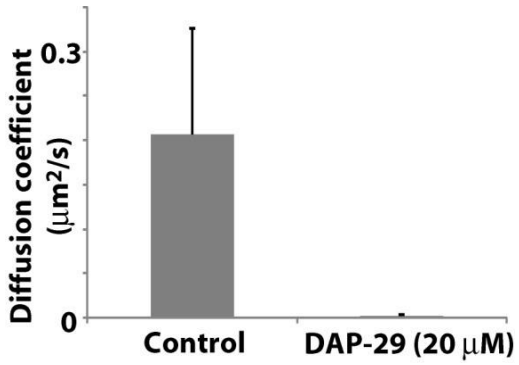

Figure 35: DAP-29 Affects Peroxisome Movement, Another Dynein Dependent Intracellular Transport System

Fluorescently labeled peroxisomes in Drosophila S2 cells were imaged and tracked to observe their movement in the presence of DAP-29. The diffusion coefficient was determined as mean square displacement per imaging interval (1 second). Actin based transport was disabled by addition of cytochalasin. At least 33 particles total from 5 or more cells were tracked for both conditions. Error bars show s.d. Experimental details as described in[178].

The observation that DAP-29 blocks movement in other microtubule dependent transport systems that depend on cytoplasmic dynein, but not on kinesin II, suggests the possibility that dynein might be a protein target of this compound. In addition, the clear activity of DAP-29 in other biological systems supports the idea that compounds identified in the melanophore screen can have general applicability to study intracellular transport processes.

Normal myosin V dependent motility in melanophores already indicated that DAP-29 does not act non-specifically on ATP-dependent transport processes, for instance by depleting ATP. To test this hypothesis further, actin-dependent membrane ruffling in the presence of DAP-29 was examined. No effect on this ATP dependent but dynein independent process was observed, indicating that

DAP-29 does not act non-specifically on all transport processes (data not shown).

It has become clear that DAP-29 effects dynein dependent processes in several *in vivo* systems, but does not seem to target dynein independent processes. This is intriguing, but not compelling, evidence that DAP-29 acts on cytoplasmic dynein as relevant target.

Summary

Identification of DAP-29 as an inhibitor of melanosome movement, possibly via inhibiting cytoplasmic dynein, further validates the screening approach using melanophores as model for intracellular transport. In addition, screening of compound collections based on a 'privileged scaffold' such as diaminopyrimidines appeared promising in the case of melanophores as well. DAP-29 biological activity in a range of dynein dependent processes correlates well with this motor protein or a closely related factor being the relevant target. Although conclusive evidence of direct targeting of dynein is missing at this point, further testing in additional biological systems and crosslinking studies might corroborate the finding in the future, and could also help to further address the specificity of the compound.

3.4. Conclusion

Phenotypic screening for inhibitors of intracellular transport in *Xenopus* melanophores proved successful, as inhibitors such as DAP-29 and 37P11 that target different aspects of organelle movement, show. Preliminary studies in

other biological systems indicate that these compounds are not active only in melanosome transport, but also in a wide array of intracellular transport processes. However, problems with target identification and validation need to be resolved before compounds from this screen can be fully utilized as biologically active probes.

Two different compound collections have been used in the screen: the unbiased library, and the collection based on a ‘privileged scaffold’. Both collections yielded interesting, biologically active compounds, indicating that both approaches can be successful. However, the use of a ‘privileged scaffold’ may be more effective, given the higher hit rate in the case of the DAPs.

Concluding Remarks

Phenotypic screens were used to identify small molecule probes of cell division and intracellular transport. In the process of this work, compounds based on a 'privileged scaffold' proved to be a viable starting point for small molecule discovery, implying that a broader use of 'privileged scaffolds' may lead to more effective screens. The work also reconfirms that, while target identification and compound specificity still remain major challenges in the field of small molecules, bioactive probes from phenotypic screens can provide powerful and valuable insights into biological processes. The further development of phenotypic screens and the continued exploration of chemical space should generate many more valuable small molecule probes.

4. Material and Methods

4.1. Phenotypic Cell-based Screen and Plk inhibitors

4.1.1. Chemical Synthesis and Characterization of DAP-library Members

Unless otherwise noted, materials were obtained from commercial suppliers and were used without further purification. Anhydrous grade solvents were purchased from Aldrich and used directly. Solvents were generally removed by distillation using a Büchi rotary evaporator attached to a vacuum pump. Obtained products were dried under high vacuum. Analytical thin-layer chromatography was performed on pre-coated silica plates (Whatman F254, 0.25 mm thickness); compounds were visualized by UV-light or by staining using anisaldehyde spray, potassium permanganate solution, or ammonium molybdate/ceric sulfate solution. NMR-spectra were recorded on a Bruker DPX 400 (400 MHz for ^{1}H) spectrometer. Chemical shifts (δ) are quoted in ppm and are referenced to the respective solvent ($CDCl_4$ δ=7.24, DMSO-d6 δ=2.50). LC/MS data was obtained using a Waters LC-MS ZQ 2795 spectrometer equipped with a Waters symmetry C18 2.1x50 mm column at a flow rate of 0.2 mL/min.

The members of the library were synthesized by sequential nucleophilic substitution of dichloropyrimidines. 3-Nitro-2,4-dichloropyrimidine (NDCP) and 2,4-dichloropyrimidine (DCP) were used as the starting materials.

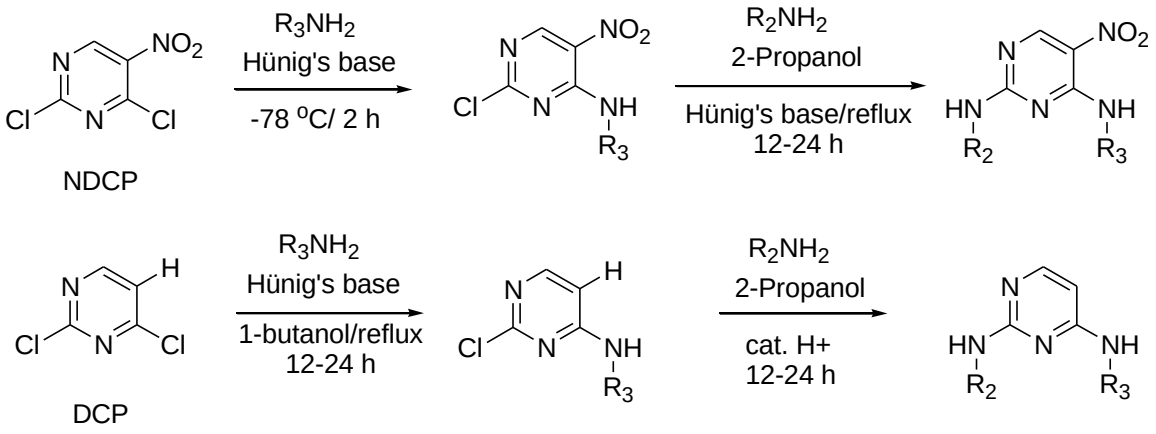

Typical procedure (adapted from[78,83])

For DCP-derivatives:

Step I: To a solution of the DCP (20 mmol, 3 g, 1 eq.) in 20 mL 1-butanol was added Hünig's base (24 mmol, 4.2 mL, 1.2 eq.) and amine/aniline (20 mmol, 1 eq.). The resulting mixture was heated at reflux for 24 h. Then the reaction mixture was cooled, evaporated and the residue crystallized from ethyl acetate to afford the monosubstituted chloropyrimidine derivative.

Step II: To a solution of the monosubstituted chloropyrimidine (0.2 mmol) in 2-propanol (4 mL) was added the amine/aniline (0.2 mmol) and ethereal HCl (0.2 mL) and the mixture heated to reflux for 24 h. After cooling the mixture to room temperature, the precipitate was filtered, washed with ether and dried *in vacuo*. In cases were no precipitate formed upon cooling, cold ether was added to the reaction mixture to induce precipitation.

For NDCP derivatives:

Step I: To a solution of NDCP (2.6 mmol, 0.5 g, 1 eq.) in THF (4 mL) was added Hünig's base (3.1 mmol, 0.54 mL, 1.2 eq) and cooled to -78 ^{o}C. A solution of the amine/aniline (2.6 mmol, 1.0 equiv) in 1 mL THF was then added dropwise. At the end of 2 hours, the mixture was allowed to warm to room temperature and poured into water. The obtained precipitate was filtered, washed with water and dried. In cases where no solid was formed, the product was extracted using chloroform, followed by removal of the solvent *in vacuo* and drying.

Step II: The resulting monosubstitued pyrimidine derivative (0.2 mmol, 1 eq.) was dissolved in iso-propanol (4 mL) and Hünig's base (0.2 mmol, 35 μL, 1 eq.) was added. Then the corresponding amine/aniline (0.2 mmol, 1 eq.) was added and the mixture was heated to reflux. After 24 hours, the mixture was cooled to room temperature and diluted with cold ether to induce precipitation. The product was isolated by filtration, washed with ether and dried *in vacuo*.

All library members were analyzed by LC/MS. ^{1}H-NMR data for selected compounds discussed in the text are shown.

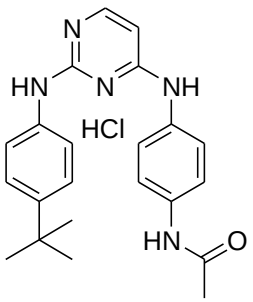

DAP-29. 4-[4-acetamidophenylamino]-2-[4-*tert*-butyl-phenylamino]-pyrimidine hydrochloride

^{1}H-NMR (400 MHz, DMSO-d6): δ 10.66 (bs, 1H), 10.25 (bs, 1H), 9.98 (s, 1H), 7.89 (d, J = 6.9 Hz, 1H), 7.54 (bs, 4H), 7.40 (s, 4H), 6.39 (d, J = 7.1 Hz, 1H), 2.04 (s, 3H), 1.31 (s, 9H); LC/MS (m/z) 376 (M+1).

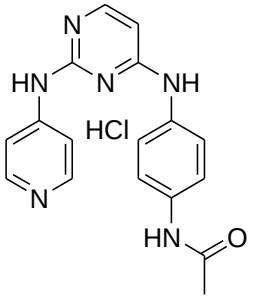

DAP-32. 4-[4-acetamidophenylamino]-2-[pyridin-4-ylamino]-pyrimidine hydrochloride

^{1}H-NMR (400 MHz, DMSO-d6): δ 10.27 (bs, 1H), 10.01 (s, 1H), 9.07 (d, J = 7.7 Hz, 2H), 8.92 (s, 2H), 8.34 (d, J = 5.9 Hz, 1H), 7.65 (d, J = 8.8 Hz, 2H), 7.55 (m, 2H), 7.02 (d, J = 7.8 Hz, 2H), 6.84 (d, J = 5.9 Hz, 1H), 2.05 (s, 3H); LC/MS (m/z) 321 (M+1).

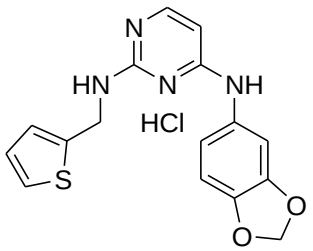

DAP-34. 4-[benzo[1,3]dioxol-5-ylamino]-2-[thiophen-2-ylmethylamino]-pyrimidine hydrochloride

^{1}H-NMR (400 MHz, DMSO-d6): δ 10.62 (bs, 1H), 8.69 (bs, 1H), 8.23 (bs, 1H), 7.83 (d, J = 7.1 Hz, 1H), 7.43-7.23 (m, 2H), 7.09-6.91 (m, 4H), 6.28 (d, J = 6.1 Hz, 1H), 6.03 (s, 2H), 4.73-4.71 (m, 2H), 4.25 (bs, 1H); LC/MS (m/z) 327 (M+1).

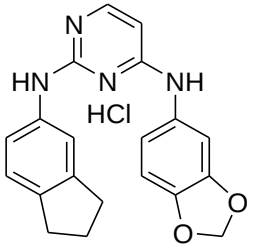

DAP-35. 4-[benzo[1,3]dioxol-5-ylamino]-2-[indan-5-ylamino]-pyrimidine hydrochloride

^{1}H-NMR (400 MHz, DMSO-d6): δ 10.63 (bs, 1H), 10.29 (bs, 1H), 7.88 (d, 7.0 Hz), 7.4-7.14 (m, 4H), 6.97-6.89 (m, 2H), 6.36 (d, J = 7.0 Hz, 1H), 6.04 (s, 2H), 2.87-2.83 (m, 4H), 2.06-2.02 (m, 2H); LC/MS (m/z) 347 (M+1).

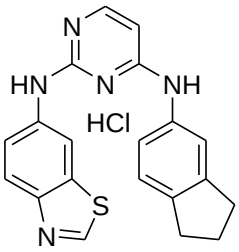

DAP-49. 2-[benzothiazol-6-ylamino]-4-[indan-5-ylamino]-pyrimidine hydrochloride

^{1}H-NMR (400 MHz, DMSO-d6): δ 10.88 (s, 1H), 10.83 (s, 1H), 9.36 (s, 1H), 8.39 (bs, 1H), 8.09 (d, J = 8.7 Hz, 1H), 8.00-7.98 (m, 1H), 7.57 (d, J = 8.7 Hz, 1H),

7.44 (s, 1H), 7.27-7.19 (m, 2H), 6.49 (d, J = 6.7 Hz, 1H), 2.86 (t, J = 7.3 Hz, 2H), 2.69-2.67 (m, 2H), 2.09-1.98 (m, 2H); LC/MS (m/z) 360 (M+1).

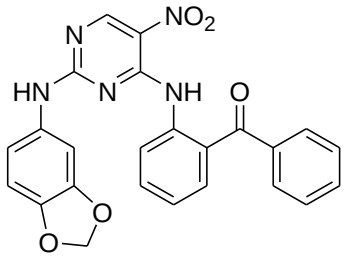

DAP-59. 2-[2-(benzo[1,3]dioxol-5-ylamino)]-4-[2-benzoyl phenylamino]-5-nitro-pyrimidine

^{1}H-NMR (400 MHz, DMSO-d6): δ 11.22 (s, 1H), 10.35 (bs, 1H), 9.00 (s, 1H), 8.09 (m, 1H), 7.68-7.38 (m, 8H), 7.25 (s, 1H), 7.00-6.98 (m, 1H), 6.80-6.78 (m, 1H), 6.01 (s, 2H); LC/MS (m/z) 456 (M+1).

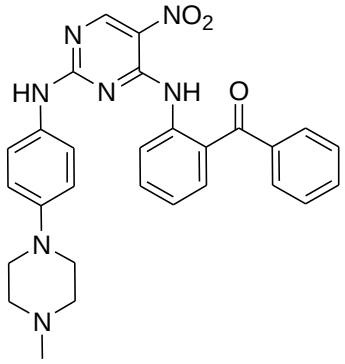

DAP-62. 4-[2-benzoyl phenylamino]-2-[4-(4-methyl-piperazin-1-yl)-phenylamino] 5-nitropyrimidine

^{1}H-NMR (400 MHz, DMSO-d6): δ 11.25 (bs, 1H), 10.28 (bs, 1H), 8.99 (s, 1H), 8.13-8.11 (m, 1H), 7.72-7.37 (m, 12H), 6.88-6.81 (m, 2H), 3.24-3.13 (m, 8H), 2.29 (s, 3H); LC/MS (m/z) 511 (M+1).

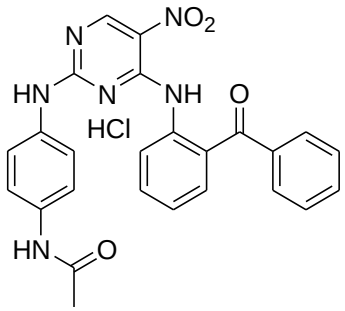

DAP-81. 2-[4-acetamidyl phenylamino]-4-[2-benzoyl phenylamino]-5-nitropyrimidine hydrochloride (previously reported in[83])

^{1}H-NMR (400 MHz, DMSO-d6): δ 11.15 (bs, 1H), 10.38 (bs, 1H), 9.87 (s, 1H), 9.00 (s, 1H), 8.07 (m, 1H), 7.66-7.44 (m, 12H), 2.03 (s, 3H); LC/MS (m/z) 469 (M+1).

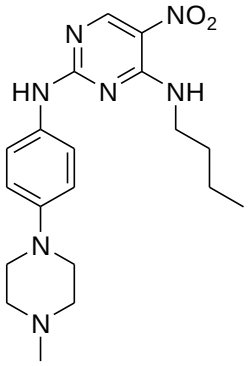

DAP-83. 4-[butylamino]-2-[4-(4-methyl-piperazin-1-yl)-phenylamino]-5-nitropyrimidine

^{1}H-NMR (400 MHz, DMSO-d6): δ 10.15 (bs, 1H), 8.93 (s, 1H), 8.86-8.84 (m, 1H), 7.65-7.63 (m, 2H), 6.90 (d, J = 9.0 Hz, 2H), 3.57-3.52 (m, 2H), 3.27-3.10 (m, 8H), 2.24 (s, 3H), 1.64-1.59 (m, 2H), 1.40-1.33 (m, 2H), 0.91 (t, J = 7.3 Hz, 3H); LC/MS (m/z) 387 (M+1).

The 'frequent hitter'[182,183] was synthesized as previously described.

4.1.2. Library Analysis for PCA

For chemical descriptor space analysis, OMEGA (Optimized Molecular Ensemble Generation Application, Openeye Scientific) was used to generate 3-dimensional conformers and output poses of each compound. They were then processed by VIDA (Openeye Scientific) to calculate the following 10 descriptors: partition coefficient (LogP), polar surface area (PSA), molecular weight, number of atoms, number of bonds, formal charge, number of carbons, number of hydrogens, number of rigid bonds, and number of rotatable bonds. Principal component analysis of the parameter set for all compounds was performed using R (r-project.org) to calculate the three components that spanned the greatest proportion of variance.

4.1.3. Cell Culture, Antibodies, siRNA and Chemical inhibitors

BS-C-1 cells (monkey epithelial kidney) and U20S cells (human osteosarcoma) were cultured in Dulbecco's modified Eagle's medium (DMEM; Invitrogen, Carlsbad, CA) with 10% fetal bovine serum (Sigma, St Louis, MO) and penicillin–streptomcyin (100 U/ml and 100 μg/ml, respectively; Invitrogen), at 37°C in a humidified atmosphere with 5% CO_2. PTK and PTKαT cells (rat kangaroo kidney) were maintained similarly using Ham's F12 medium (Invitrogen, Carlsbad, CA) instead of DMEM.

For fixed cell experiments, cells were transferred onto 10 mm round no. 1.5 glass coverslips and grown in 100 mm Petri dishes. For live-cell recordings, cells were transferred onto square 22 mm no.1.5 coverslips and grown in 100 mm Petri dishes.

Antibodies used for immunofluorescence microscopy were against α-tubulin ([mouse, FITC-DM1α, Sigma, 1 μg/mL] or [rat, MCA77g, Serotec, 0.5 μg/mL]), γ-tubulin (mouse, GTU-88, Sigma,1:5000), Cdc25C (mouse, DCS193, Calbiochem, 1 μg/mL), phospho-Cdc25C (Ser 198, rabbit, Cell Signaling, 1:100), human CREST antiserum (a gift from W. Brinkley, Baylor College of Medicine, Houston, TX) and phospho-histone H3 (Ser 10, rabbit, Upstate Biotechnology, 1 μg/mL). The appropriate secondary antibodies were purchased from Jackson ImmunoResearch Laboratories. DNA was labeled with Hoechst 33342 (Sigma, 1 μg/mL). Antibodies used for Western blotting were against Polo-like kinase 1

(mouse, sc17783, Santa Cruz Biotechnology, 0.4 μg/mL) and p50 (rabbit, D74620, Transduction Laboratories, 0.25 μg/mL).

The siRNA experiments in non-synchronized U20S cells were performed using Oligofectamine in Opti-MEM I (Invitrogen) medium following the manufacturer's instructions (Invitrogen). The siRNAi duplex targeting human Plk1 was described previously[94] and water was used for mock transfection (control). 45 hours after transfection, cells were either stained for immunofluorescence or cells from a mitotic shake-off (nocodazole-treated, 1 μg/mL, 16 hours) were lysed for Western blot analysis.

BTO-1[110,184] and ON01910[185] were synthesized as previously described.

Immunofluorescence

BS-C-1 cells in the screen were treated for 4h with the respective compounds and then fixed at 37°C with 4% formaldehyde in 100 mM PIPES at pH 6.8, 10 mM EGTA, 1 mM magnesium chloride and 0.2% Triton X-100 for 10 minutes. After fixation, cells were blocked in TBS with 0.1% Triton X-100 and 2% bovine serum albumin (BSA), and stained for α-tubulin in the same medium. DNA staining was carried out subsequently in TBS with 0.1% Triton X-100. Images for presentation were acquired as Z-stacks with 0.2-µm spacing using a 100x, 1.35 NA objective on a DeltaVision Image Restoration Microscope (Applied Precision Instruments, Issaquah, WA and Olympus, Melville, NY), and processed by iterative constrained deconvolution (SoftWoRx, Applied Precision Instruments).

Maximal intensity projections of the entire Z-stack are shown. For visualization of γ-tubulin the cells were fixed for 10 minutes in methanol at -20°C.

U20S cells, either from the RNAi knock-down experiment or after 4-hour-treatment with the chemical inhibitor, were fixed for 10 minutes in methanol at -20°C and then blocked and stained as described above. Images for presentation were acquired as described above using the Deltavision Image Restoration Microscope.

Quantitative Aspects of Immunofluorescence

For quantitation of phospho-H3 staining PTK cells were treated for 4 hours with 100 μM monastrol. Then the cells were incubated for 1 hour with test compound, 20 μM MG132, and monastrol. After fixation with formaldehyde and staining, images were acquired on a Carl Zeiss Axioplan 2 microscope with a 40x 0.75 NA objective. Phospho-H3 immunofluorescence intensity was measured using MetaMorph software (Universal Imaging, Downington, PA) and normalized to the control (n = 3, ≥ 20 cells for each data point). For each mitotic cell, Hoechst fluorescence was used to define the chromosome region, and total phospho-H3 immunofluorescence was measured in that region using the integrated intensity function. Background fluorescence, estimated from intensity measurements in regions with no DNA, was subtracted.

For quantitation of Cdc25C and phospho-Cdc25C staining PTK cells were treated for 1 hour with the respective compounds, pre-extracted with MTSBx (4 M glycerol, 100 mM K-PIPES, 1 mM EGTA, 5 mM $MgCl_2$, 0.5% triton X-100, pH

= 6.9) and fixed with methanol at -20°C for 10 minutes. The subsequent blocking was carried out as described above. After staining for Cdc25C, phospho-Cdc25C, and DNA, images were acquired on a Carl Zeiss Axioplan 2 microscope, with either a 63x 1.4 NA objective (for presentation) or a 40x 0.75 NA objective (for quantification). Phospho-Cdc25C immunofluorescence intensity on centrosomes was quantified in mitotic cells using MetaMorph software (Universal Imaging, Downington, PA) and normalized to the Cdc25C intensity on the same centrosome using previously described methods (n = 3, ≥ 20 cells for each data point)[186]. The intensity ratio for the control (DMSO) was set to 1.

For quantitation of inter-kinetochore distances, PTKαT cells were treated for 1 hour with MG132 (20 μM) and then for 45 minutes with the respective compound in the continuing presence of MG132. Cells were fixed for 10 minutes in methanol at -20°C and then blocked and stained as described above. Image planes covering the cell volumes were acquired using the DeltaVision Image Restoration Microscope. The distance between the centers of CREST antigen intensity of a kinetochore pair, was directly measured in three dimensions using SoftWoRx (Applied Precision Instruments). Only pairs of kinetochores for which attachment to opposite poles could be clearly detected were included (except with nocodazole) in the quantitation (≥ 67 kinetochore pairs total from ≥ 9 cells total for each compound).

4.1.4. Screening Procedure

For the screen, BS-C-1 cells were plated in a 384-well format using a Matrix Technologies wellmate multidropper 48 hours before the experiment. Compounds were added by pin transfer to solution plates and then transferred to the almost confluent cells using the MiniTrak V liquid handling robot (Perkin Elmer) to give a final concentration of 20 μM, and 10 or 5 μM as required. After a 4-hour-incubation fixation and staining (see above) were performed using a wand aspirator (VP scientific) and a multichannel pipettor (Matrix technologies) for liquid handling. One image per well (blue channel for DNA and green channel for α-tubulin) was acquired using the Discovery-1 (Molecular Devices) automated microscopy system with a 10x Nikon objective. Analysis of the images by visual inspection led to the identification of active compounds (detailed description of criteria in **Figure 37**).

4.1.5. Kinase Assay

Polo-like kinase 1 activity was assayed in kinase buffer (50 mM Tris [pH 7.6], 10 mM $MgCl_2$, 5 mM DTT, 2 mM EGTA, 0.5 mM Na_3VO_4, 20 mM NaF, 20 mM β-glycerophosphate). 3 μg casein, 100 ng of recombinant *Xenopus* Polo-like kinase 1 (expressed and purified similarly as described before[187]), and the appropriate amount of compound in DMSO (5% final) were added to half the reaction volume (10 μL), and allowed to incubate for 30 minutes on ice. Then 10 μL of kinase buffer containing cold ATP (50 μM final) and γ-^{32}P-ATP (2.5 μCi final) was added.

Reactions were mixed, incubated for 15 minutes at 30°C, stopped by the addition of Laemmli sample buffer. Proteins were resolved by SDS-PAGE (12.5%). Gels were dried, and exposed to a phosphorimager screen. Gel bands were quantified with Image Gauge software (Fujifilm).

4.1.6 Live cell imaging

Cells on 22x22 mm coverslips were mounted in a Rose chamber for imaging using L-15 medium without phenol red supplemented with FBS, antibiotics (see above), and 20 μM MG132 (if indicated). Chemical inhibitors were introduced either during the initial mounting or added later by medium exchange. If MG132 was used, cells were pre-incubated with it in 35 mm dishes for 30 minutes to 1 hour. For reversibility tests inhibitor containing media were exchanged with media containing the appropriate amount of carrier (DMSO) instead of compound.

Confocal GFP fluorescence time-lapse sequences were acquired on a Carl Zeiss Axiovert 200M microscope equipped with a *z*-motor and a 100x 1.4 NA objective. Experiments were performed at 37°C using an air curtain (Nevtek, Burnsville, VA). Z-stacks (seven sections separated by 1.0 μm) of GFP fluorescence were taken with an Orca ER cooled CCD camera (Hamamatsu, Hamamatsu City, Japan) coupled to a Yokogawa spinning disk confocal QLC100 unit. Illumination was achieved with an argon laser (Solamere, Salt Lake City, UT) at 488 nm. A single DIC image was taken immediately after each GFP stack. MetaMorph

software (Universal Imaging) was used for acquisition and analysis. Maximal intensity projections of GFP-tubulin z-stacks and single DIC images are shown for selected timepoints. A 2x2 lowpass filter was applied to all DIC images for presentation. Kymographic analysis was carried out using the kymograph tool of MetaMorph software (Universal Imaging, Downington, PA). Phase-contrast microscopy was carried out under the same live-imaging conditions using a 40x 1.3 NA phase objective.

4.2. Intracellular Transport Screen

4.2.1. Cell Culture and Cell-based Assays

Cell Culture of Melanophores

Xenopus melanophores[148] were cultured in 0.7X L-15 medium (Gibco/Invitrogen) supplemented with 4% fetal bovine serum (Sigma, St Louis, MO), penicillin–streptomcyin (100 U/ml and 100 μg/ml respectively; Invitrogen), 5 μg/mL insulin, and 0.29 mg/mL glutamate at 25°C in a humidified atmosphere in the dark. Serum free medium (SFM) has the same composition without containing serum. For cell freezing and to reduce the number of pigments to allow easier tracking or imaging the cells can be maintained in 1 mM phenylthiourea (PTU) which inhibits pigment biosynthesis. To induce dispersion melanocyte-stimulating hormone (MSH, M-4135 Sigma, 100 nM active concentration) was used, to induce dispersion melatonin (10 or 20 nM active concentration) was used.

Immunofluorescence in Melanophores

Staining for tubulin and DNA was carried out as described for BS-C-1 cells in section 4.1.3. using PTU-treated melanophores.

PKA-inhibitor assay

Melanophores were plated on 25x25 mm square, poly-lysine coated coverslips and transfected 1 day later either with GFP-pNP210 or GFP-pNP211, the active and inactive form of a PKA-inhibiting peptide, respectively, using FUGENE-transfection reagent (Roche diagnostics) according to manufacturer's guidelines[165]. Two or three days after transfection, the growth medium was exchanged with SFM, incubated for 1 hour, and then the respective compound was added in SFM. After 1 hour of incubation with compound, the cells were fixed with 3.7% formaldehyde in PBS, and mounted for imaging. The aggregation state for GFP-expressing cells was then determined by optical inspection for quantitation.

Lysosome Imaging and Tracking in Melanophores

PTU-treated melanophores were plated on 25x25 mm square, poly-lysine coated coverslips one or two days before the experiment. After washing twice with SFM and incubation for 1 hour in SFM, the respective compound was added (0.1% DMSO final) in SFM. After 25 min incubation a solution containing compound and Lysotracker Red DND 99 (100 nM final, Invitrogen) was added, followed by additional 5 min incubation. Then the cells were washed five times with SFM, mounted and sealed. Imaging was carried out on a Nikon Eclipse U2000 microscope with a plan-APO 60 1.4 NA objective. A 100W halogen light source

was used for epifluorescence to minimize phototoxicity. 100 images per field were captured every 0.2 s with a 0.1 s exposure time using an Orca-II-ER cooled charge-coupled device camera (Hamamatsu Photonics, Japan). Tracking was carried out by customized software (Ontash & Ermac, River Edge, NJ), and the obtained data was binned according to the diffusion coefficient.

Melanosome Tracking in Melanophores

Imaging and tracking was carried out in the Gelfand laboratory as previously described[188]. For the studies of melanosome movement in the absence of microtubules, nocodazole was added as depolymerization agent.

Chromosome Oscillation in PTK-cells

PTK cells were maintained and plated on coverslips as described for PTKαT cells in section 4.1.3. After incubation with 100 μM monastrol for 30 minutes, the compound was added (either 60 μM 37P11 or DMSO as carrier) and incubation was continued for 30 more minutes. Next, the coverslips were mounted in a Rose chamber, monopolar mitotic cells were located and then imaged for 10 minutes in 20 second intervals using a Ph3 40x Plan-NEOFLUAR 1.30 objective on a Carl Zeiss Axiovert 200M microscope under phase contrast conditions.

4.2.2. Screening Procedure

The cells (*Xenopus laevis* melanophores)[148] were plated 2 days before the experiment in a 384-well format (~100000 cells per well) using Corning Costar black walled, clear bottom plates. A Matrix Technologies wellmate multidropper

was used for liquid handling. For the experiment the cells were initially washed twice with 50 μl of serum free medium (SFM). After incubation with SFM for 45 minutes at room temperature in the dark, the cells were incubated with MSH (100 nM) in SFM for 1 hour to achieve full dispersion. The cells were then washed thrice with SFM to remove MSH and the compound of interest (at 20 μM for Chemdiv or 10 μM for DAPs) in SFM was added. Preparation of compound and hormone stock solutions was carried out by pin transfer using the MiniTrak V liquid handling robot (Perkin Elmer). After 30 min incubation, melatonin (20 nM final) was added to each well to induce aggregation. This mixture was allowed to incubate for 1 hour at room temperature in the dark, then the cells were fixed with 3.7% formaldehyde in phosphate buffered saline (PBS) for 45 minutes at which point the media was exchanged for PBS and each plate was stored in the dark at 4^{o}C, ready for imaging.

Image acquisition was performed using the Discovery-1 automated imaging system. The wells were usually imaged 5 times each at 20x using this system with a 5 ms transmitted light exposure, 2x2 binning, with an image spread that covered each well entirely. The images were analyzed using Metamorph software (Universal Imaging, Downington, PA) by thresholding to define the pigment occupied areas, and then dividing the number of small objects by the number of large objects to determine the dispersion index (DI). Definition of small and large objects used pixel area as well as shape factor. Individual cut-offs per plate for the DI were determined according to internal controls (nocodazole, MSH-treated, untreated/DMSO). The screens were carried out in triplicate.

4.2.3. Chemical Synthesis and Characterization of 37P11 analogs

Chemical synthesis procedures were carried out as described in section 4.1.1.

Synthesis of 37P11 analogs were generally carried out as previously described[167] in a two-step procedure, a nucleophilic substitution on a chloropyridine by a piperazine followed by the reaction of the free amine of the piperazine derivative with the appropriate isocyanate to yield the urea linked final product.

Exemplary procedure for the synthesis of 37P11:

Step 1:

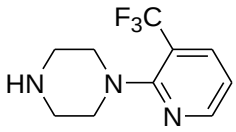

1-(3-Trifluoromethyl-pyridin-2-yl)-piperazine:

A *N*,*N*-dimethylformamide (30 mL) solution of 1.82 g (10 mmol) of 2-chloro-3-trifluoromethylpyridine and 0.86 g (10 mmol) of piperazine was stirred for 10 minutes at room temperature. Then 4.15 g (30 mmol) of anhydrous potassium carbonate were added and the resulting suspension was stirred for 1.5 hours at 140 ^{o}C. After cooling, 100 mL of water were added and the mixture was extracted 3 times using 65 mL ethyl acetate, each. The combined organic layers were then washed two times with 50 mL brine, dried over sodium sulfate and concentrated *in vacuo* to give a light orange oil. The crude was purified by

column chromatography on 60 g silica gel using a 95:5 chloroform:methanol solvent system to give 1.18 g (5.1 mmol, 51%) of a yellowish oil.

^{1}H-NMR (400 MHz, $CDCl_3$): δ 8.41 (d, J = 4.7 Hz, 1H), 7.83 (dd, J_1 = 1.5 Hz, J_2 = 7.8 Hz 1H), 6.95 (dd, J_1 = 4.8 Hz, J_2 = 7.7 Hz, 1H), 3.26-3.23 (m, 4H), 3.01-2.99 (m, 4H); LC/MS (m/z) 232 (M+1).

Step 2:

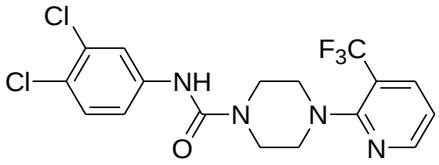

37P11, 4-(3-Trifluoromethylpyridin-2-yl)-piperazine-1-carboxylic acid (3,4-dichlorophenyl)-amide:

A toluene solution (1 mL) of 94 mg (0.5 mmol) of 3,4-dichlorophenyl isocyanate dissolved was added dropwise over 5 min to 116 mg (0.5 mmol) of 1-(3-trifluoromethyl-pyridin-2-yl)-piperazine (from step 1) in 1 mL of toluene. A white precipitate started to form almost immediately and the reaction mixture was stirred for 14 hours at room temperature. The solvent was then removed *in vacuo* to give a white solid. Purification of the crude by column chromatography on 60 g of silica gel using chloroform as solvent yielded 161 mg (0.385 mmol, 77%) of a white solid as final product.

^{1}H-NMR (400 MHz, $CDCl_3$): δ 8.44 (d, J = 3.7 Hz, 1H), 7.88 (d, J = 7.6 Hz, 1H), 7.55-7.54 (m, 1H), 7.29 (d, J = 8.7 Hz, 1H), 7.18 (d, J = 8.7 Hz, 1H), 7.06-7.02

(m, 1H), 6.60 (bs, 1H), 3.62-3.60 (m, 4H), 3.31-3.29 (m, 4H); ^{13}C-NMR (100 MHz, $CDCl_3$): δ 159.4, 154.5, 151.2, 138.5, 137.2, 137.2, 132.5, 130.3, 126.2, 121.6, 119.2, 117.8, 117.4, 50.4, 44.1; LC/MS (m/z) 419 (M+1).

The following analogs have similar potency as 37P11 (see **Table 2**) and their characterization data is shown as example for all analogs.

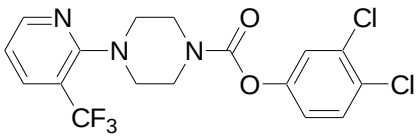

UP-II-95, 4-(3-Trifluoromethylpyridin-2-yl)-piperazine-1-carboxylic acid 3,4-dichlorophenyl ester

The compound was prepared from the piperazine derivative (step 1) by treatment with triphosgene followed by 3,4-dichlorophenol to yield the carbamate linkage.

^{1}H-NMR (400 MHz, $CDCl_3$): δ 8.46 (bs, 1H), 7.89 (d, J = 7.1 Hz, 1H), 7.40 (d, J = 8.7 Hz, 1H), 7.28 (bs, 1H), 7.07-6.99 (m, 2H), 3.77-3.69 (m, 4H), 3.29 (bs, 4H); ^{13}C-NMR (100 MHz, $CDCl_3$): δ 159.7, 152.9, 151.2, 150.0, 137.2, 137.2, 132.7, 130.5, 129.2, 124.0, 121.4, 118.1, 50.6, 44.7, 44.1; LC/MS (m/z) 420 (M+1).

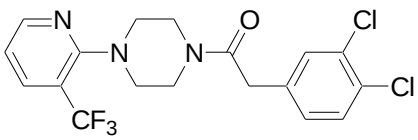

UP-II-115, 2-(3,4-Dichloro-phenyl)-1-[4-(3-trifluoromethylpyridin-2-yl)-piperazin-1-yl]-ethanone

The compound was prepared from the piperazine derivative (step 1) by treatment with the corresponding acid chloride to yield the amide linkage.

^{1}H-NMR (400 MHz, $CDCl_3$): δ 8.42 (bs, 1H), 7.87 (d, J = 6.8 Hz, 1H), 7.39-7.35 (m, 2H), 7.10-7.04 (m, 2H), 3.76-3.69 (m, 4H), 3.58 (bs, 2H), 3.21-3.16 (m, 4H); LC/MS (m/z) 418 (M+1).

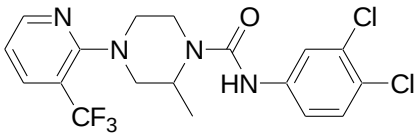

UP-II-132, 2-Methyl-4-(3-trifluoromethylpyridin-2-yl)-piperazine-1-carboxylic acid (3,4-dichloro-phenyl)-amide

The compound was prepared as described in the general procedure using 1-methylpiperazine.

^{1}H-NMR (400 MHz, $CDCl_3$): δ 8.45 (d, J = 3.6 Hz, 1H), 7.89 (dd, J_1 = 1.6 Hz, J_2 = 7.8 Hz, 1H), 7.55 (d, J = 2.5 Hz, 1H), 7.26 (d, J = 8.8 Hz, 1H), 7.19 (dd, J_1 = 2.5 Hz, J_2 = 8.8 Hz, 1H), 7.06 (dd, J_1 = 4.8 Hz, J_2 = 7.8 Hz, 1H), 6.80 (s, 1H), 4.34-4.32 (m, 1H), 3.88-3.85 (m, 1H), 3.49-3.34 (m, 3H), 3.20 (dd, J_1 = 3.6 Hz, J_2 = 12.4 Hz, 1H), 3.02-2.96 (m, 1H), 1.34 (d, J = 6.7 Hz, 3H); ^{13}C-NMR (100 MHz,

$CDCl_3$): δ 160.3, 154.4, 151.2, 138.7, 137.1, 137.1, 132.4, 130.1, 126.1, 121.8, 119.6, 118.0, 117.8, 54.6, 51.3, 47.9, 39.3, 15.7; LC/MS (m/z) 433 (M+1).

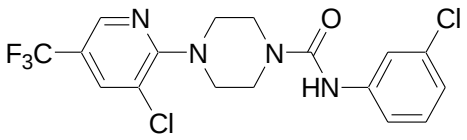

37B13, 4-(3-Chloro-5-trifluoromethylpyridin-2-yl)-piperazine-1-carboxylic acid (3-chloro-phenyl)-amide

The compound was prepared analogously to 37P11.

^{1}H-NMR (400 MHz, $CDCl_3$): δ 8.39 (s, 1H), 7.78 (s, 1H), 7.43 (s, 1H), 7.18-7.15 (m, 2H), 6.99-6.98 (m, 1H), 6.72 (bs, 1H), 3.63-3.61 (m, 4H), 3.52-3.50 (m, 4H); LC/MS (m/z) 419 (M+1).

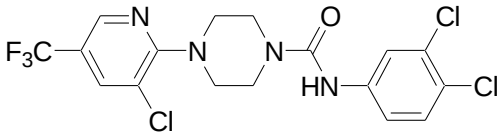

UP-II-139, 4-(3-Chloro-5-trifluoromethylpyridin-2-yl)-piperazine-1-carboxylic acid (3,4-dichlorophenyl)-amide

The compound was prepared analogously to 37P11.

^{1}H-NMR (400 MHz, $CDCl_3$): δ 8.39 (d, J = 1.1 Hz, 1H), 7.79 (d, J = 2.0 Hz, 1H), 7.59 (d, J = 2.5 Hz, 1H), 7.32 (d, J = 8.7 Hz), 7.18 (dd, J_1 = 2.5 Hz, J_2 = 8.7 Hz, 1H), 6.42 (s, 1H), 3.66-3.63 (m, 4H), 3.55-3.53 (m, 4H); LC/MS (m/z) 453 (M+1).

4.2.4. Motility Assays

Motility assays were carried out as previously described[189], briefly:

The motor protein in BRB80 (80 mM Pipes, 1mM $MgCl_2$. 1 mM EGTA, pH=6.8 with KOH, ~7 μL) was allowed to bind onto a glass coverslip in a flow chamber. After blocking with 0.5 mg/mL of casein in BRB80 for several minutes (20 μL), fluorescently marked microtubules (X-rhodamine) obtained from GMPCPP seeds were added to bind to the motor protein (~10 μL). Next motility buffer (BRB80, 1mM $MgCl_2$, 1 mM ATP, oxidation mix [glucose oxidase, catalase, glucose and β-mercaptoethanol]) containing the compound of interest in DMSO (usually 1% total) was added and the movement of microtubule was observed by time-lapse microscopy. To calculate sliding velocities, 10 or more microtubules were randomly chosen and the distance traveled during the timelapse was measured. The following motor proteins/constructs were used in the assay: Eg5 full length at 0.18 mg/mL[189], human conventional kinesin K560 at 0.09 mg/mL[190], and cytoplasmic dynein isolated from bovine brain at ~0.07 mg/mL[166].

APPENDIX

A

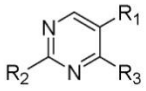

100 compounds

B

R_1 =	H	NO_2
	26	73

C

Fragment		R_2	R_3
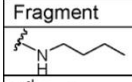	a	4	5
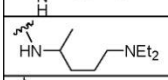	b	2	-
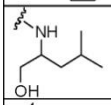	c	1	-
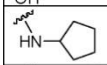	d	6	10
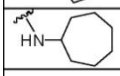	e	3	-
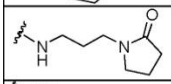	f	2	-
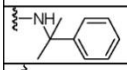	g	3	-
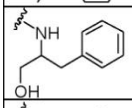	h	5	-
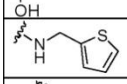	i	6	-
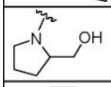	j	1	-
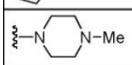	k	2	3
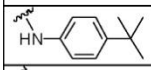	l	8	-
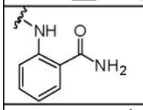	m	-	12
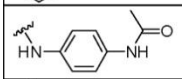	n	9	7
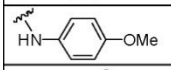	o	1	-
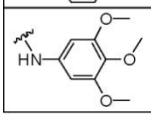	p	2	-

Fragment (cont.)		R_2	R_3
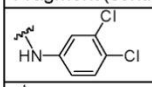	q	6	11
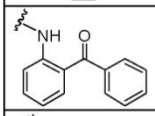	r	1	13
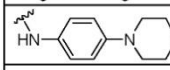	s	4	-
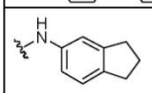	t	3	5
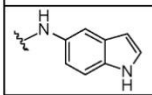	u	5	5
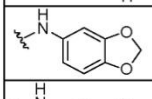	v	1	9
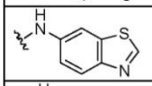	w	6	13
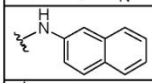	x	9	-
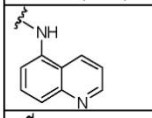	y	1	-
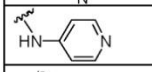	z	3	-
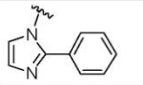	aa	2	3
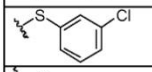	ab	1	3
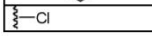	ac	2	-

D

"Frequent hitter"

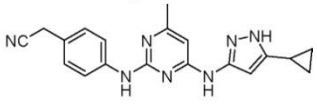

Figure 36: Composition of the Diaminopyrimidine Library.

(**A-C**) Core structure and substituents. Each substituent at R2 and R3 is coded with a letter. Number of compounds in the collection with the respective substituents is shown. (**D**) Chemical structure of a reported “frequent hitter” that was included in the collection [182].

Table 1: Primary Screening Data for Active DAPs

Name	Chemical Structure	Primary Screens			Combined Result	Detailed Analysis
DAP-8	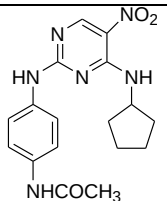	2	2	1,2	Reduced mitotic index	/
DAP-10	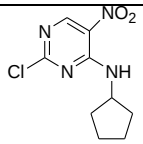	/	4	3	Spindle/ Chromosome	/
DAP-15	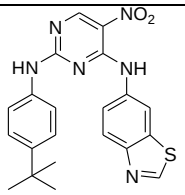	3	3	/	Spindle/ Chromosome	/
DAP-16	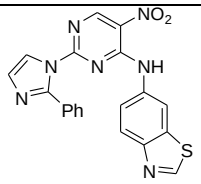	5	/	3	Spindle/ Chromosome	/
DAP-17	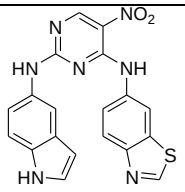	/	3	6	Spindle/ Chromosome	/
DAP-18	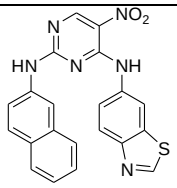	/	5,6	6	Spindle/ Chromosome	/

DAP-20	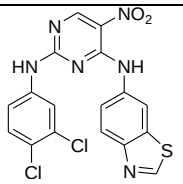	3	5	5	Spindle/ Chromosome	/
DAP-34	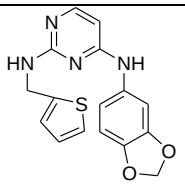	/	5	3	Spindle/ Chromosome	**Figure 37D**
DAP-35	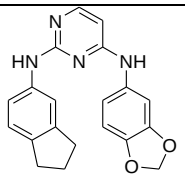	/	5	6	Spindle/ Chromosome	**Figure 37E**
DAP-41	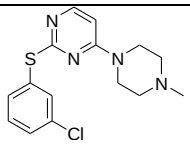	3	5,6	/	Spindle/ Chromosome	/
DAP-46	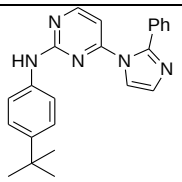	/	1,5	3	Spindle/ Chromosome	/
DAP-49	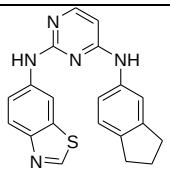	/	5,6	1,3	Spindle/ Chromosome	**Figure 37B**
DAP-51	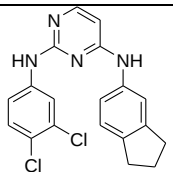	/	6	3,6	Spindle/ Chromosome	/

DAP-55	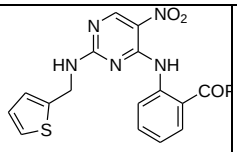	/	2	2	Reduced mitotic index	/
DAP-57	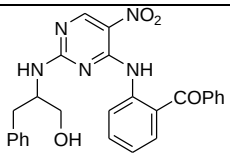	3	6	2	Spindle/ Chromosome	/
DAP-59	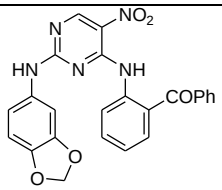	3	5	/	Spindle/ Chromosome	**Figure 37D**
DAP-62	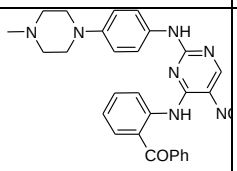	3,5, 6	3	3,5, 6	Spindle/ Chromosome	**Figure 37A**
DAP-65	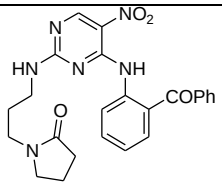	6	6	/	Spindle/ Chromosome	/
DAP-67	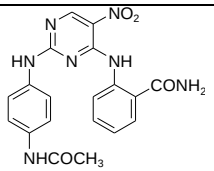	6	3	/	Spindle/ Chromosome	/

DAP-81	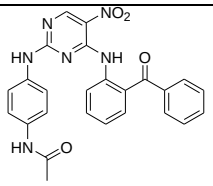	3	1,2	2	Reduced mitotic index	**Figure 37A**
DAP-83	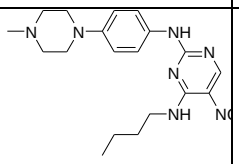	5,6	2	2	Reduced mitotic index	**Figure 37C**
DAP-97	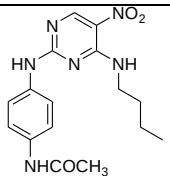	6	/	3	Spindle/ Chromosome	/

For analysis of the primary screen (done in triplicate at 20 μM compound concentration) fields of cells were analyzed by visual inspection of 10x images. Phenotypes were then assigned according to following categories: 1 – strong effects on interphase microtubules, 2 – greatly reduced mitotic index, 3 – monopolar mitotic spindles, 4 – spindles with aberrant poles/extra poles, 5 – abnormal spindles (other than 3 or 4), 6 – chromosome alignment defects in control-like spindles, 7 – increased number of cells in anaphase/cytokinesis, 8 – greatly increased mitotic index, 9 – visible compound aggregates. If a compound scored at least 2 out of 3 times in one category (categories 3-6 were considered as one category for this purpose referred to as spindle/chromosome alignment defects) the compound was considered a respective hit. Shown in the table are all compound that scored as hit in the screen and do not fall in category 1 or 9. Detailed analysis of these hit compounds revealed a range of mitotic phenotypes. A more detailed description of mitotic phenotypes of a subset of compounds is given in **Figure 37**.

Figure 37

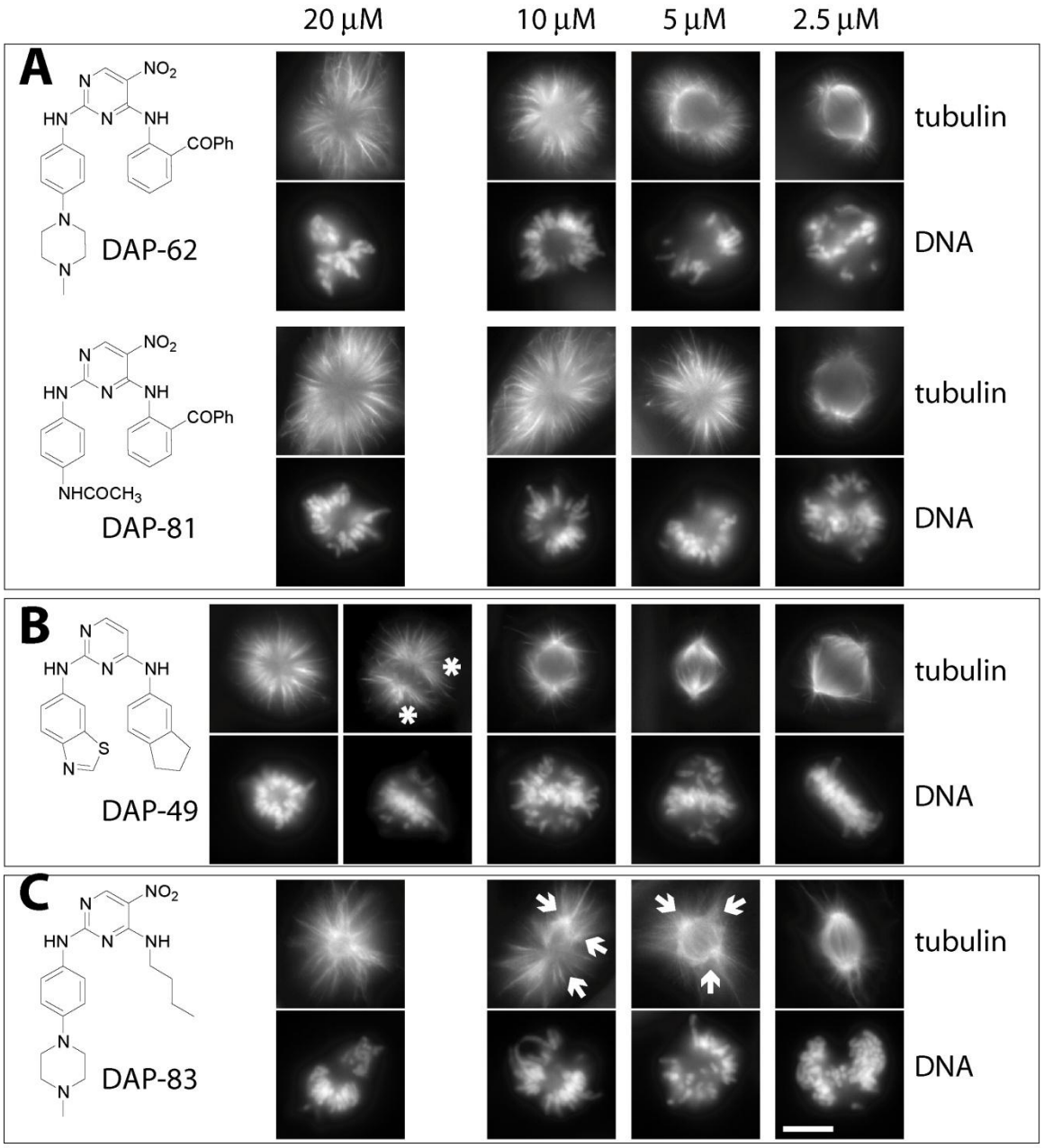

arrows: spindle pole defects or extra microtubule foci (poles)
asterisks: seperated microtubule asters with no central spindle (with no clear antiparallel microtubule overlap)

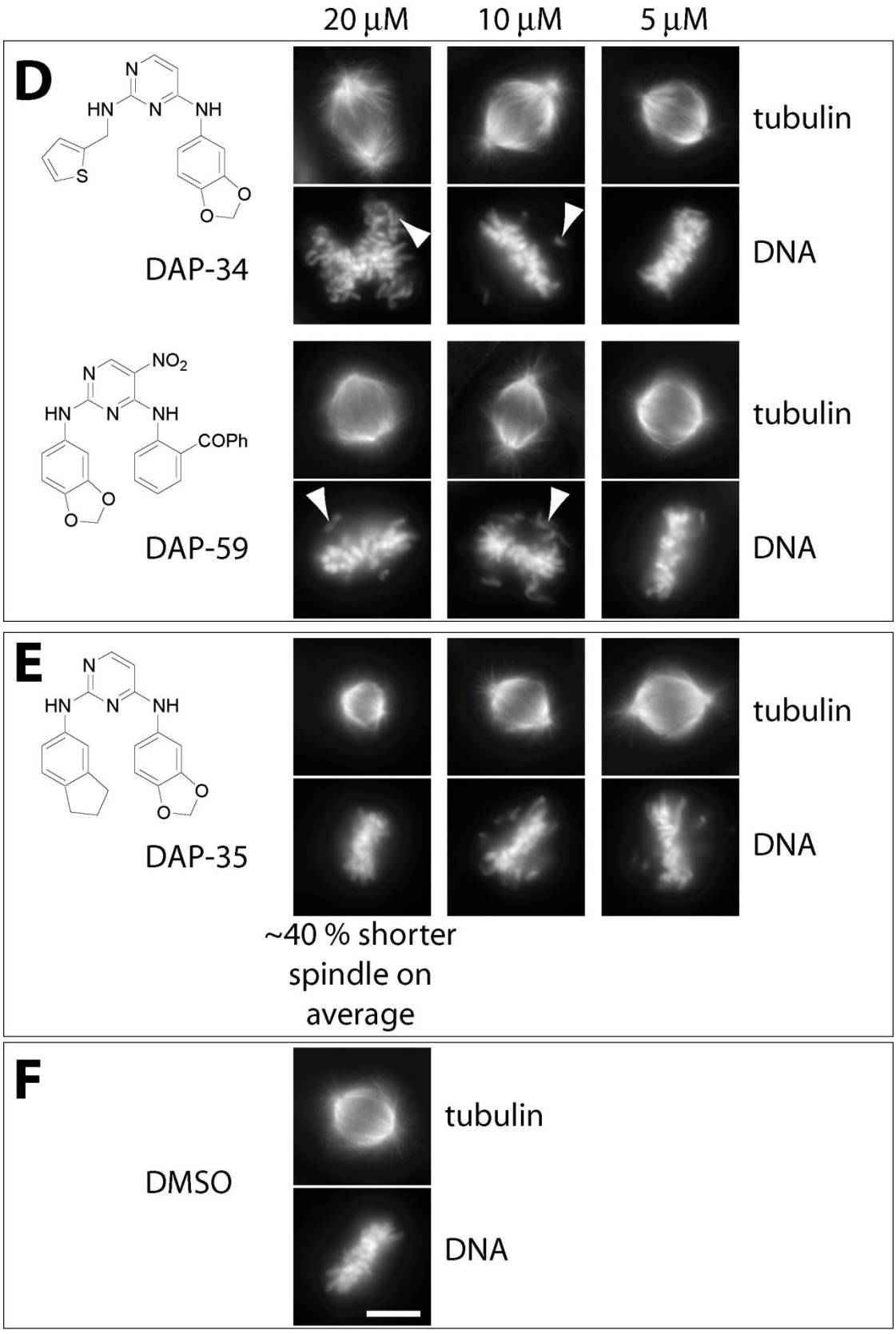

arrowheads: unaligned chromosomes

Figure 37: Mitotic Phenotypes Induced by a Subset of DAPs

A subset of compounds from the screen (**Figure 10**) was analyzed by high resolution microscopy (63x magnification) to characterize mitotic defects. The images show the predominant phenotypes for each DAP at 3 (or more) concentrations. The observed divergence in phenotypes over the titration indicated differences in the mode of action of the compounds. (**A**) DAP-62, DAP-81: Monopolar spindles were observed at 20 μM. At lower compound concentrations, spindle structures observed had a sphere-like organization. (**B**) DAP-49: In addition to monopolar spindles, cells were observed that had two separated astral microtubule arrays without a well-defined overlap zone (20 μM). At lower concentrations these astral microtubules diminished and normal spindles were observed. Quantitation of the phenotypes for this compound is shown in **Figure** 12**C**. (**C**) DAP-83: While monopolar spindles were observed at 20 μM, spindle pole defects, including unfocused poles and additional spindle poles, were also predominant. (**D**) DAP-34, DAP-59: Chromosome-alignment defects predominated, with only minor, if any, spindle perturbations. (**E**) DAP-35: The bipolar spindles observed had pole-to-pole distances that were less than that observed in untreated dividing cells (40% shorter, n = 13). (**F**) Normal bipolar spindle in cells treated with carrier (DMSO).Scale bar, 10 μm.

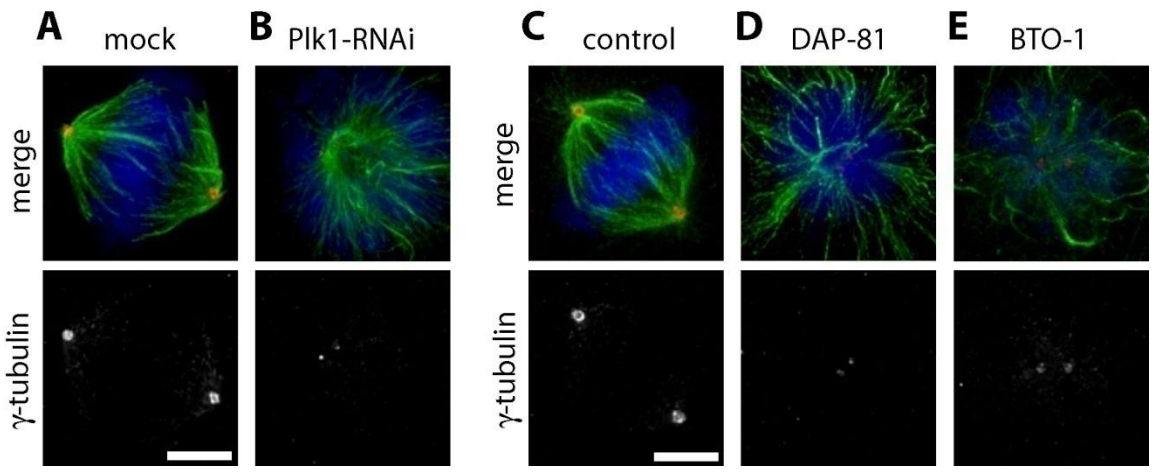

Figure 38: Additional Images for Comparing Plk1-knock-down and Treatment with Chemical Inhibitors

(**A,B**) U20S cells were either mock-transfected , or transfected with RNA-oligos against Plk1 as previously described[94]. After ~45 hours cells were fixed and processed for immunofluorescence. (**C-E**) After treatment of U20S cells for 4 hours with carrier (DMSO), 25 μM DAP-81 or 50 μM BTO-1 the cells were processed as in (**A,B**). Overlays show DNA (blue), α-tubulin (green) and γ-tubulin (red). The distribution of γ-tubulin is shown separately. As compared to images shown in **Figure 17A-E**, with cells undergoing the same treatment condition, the RNAi-experiment as well as treatment with chemical inhibitors can lead to centrosomes that are close together, compared to untreated cells. The images show maximum intensity projections of deconvolved image-series covering cell volumes. Scale bars, 5 μm.

Table 2: Overview of Activity of Synthesized Analogs of 37P11

Formula	Name	DI at 40/10 μM (normalized to DMSO=1)		Note
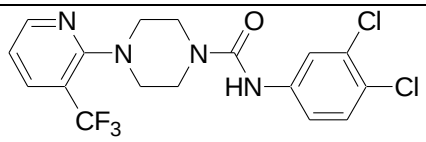	37P11	4.5	2.2	Lead Structure
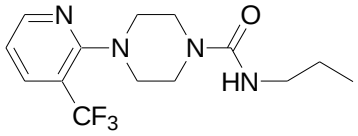	UP-II-89	1.2	0.8	
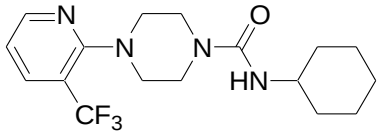	UP-II-90	2.2	0.8	
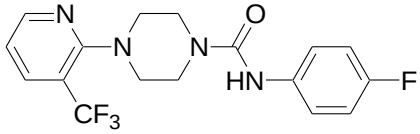	UP-II-91	2.5	1.0	
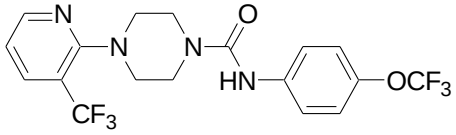	UP-II-92	3.1	1.3	
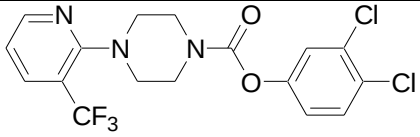	UP-II-95	4.2	2.2	

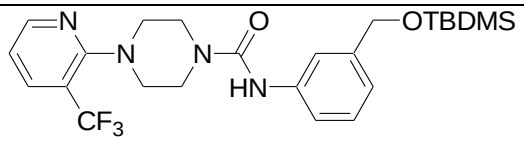	UP-II-103	1.8	0.9	
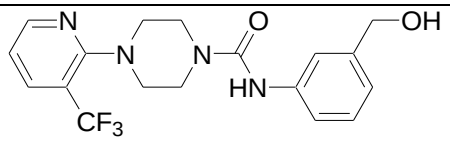	UP-II-105	1.3	0.7	
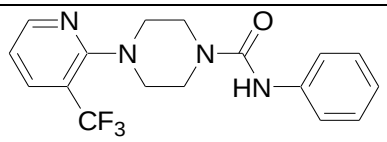	UP-II-113	2.7	0.9	
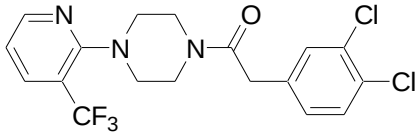	UP-II-115	5.7	2.1	
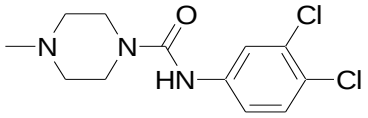	UP-II-116	1.0	1.1	
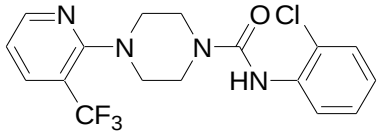	UP-II-120	3.4	1.1	
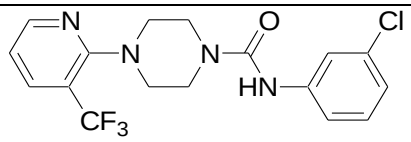	UP-II-121	2.3	1.2	
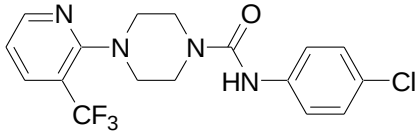	UP-II-122	1.6	1.2	

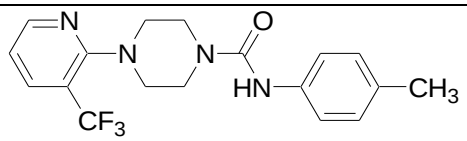	UP-II-123	1.6	1.0	
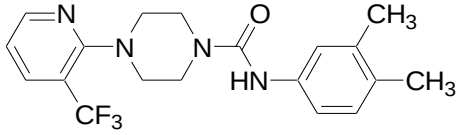	UP-II-124	2.0	1.3	
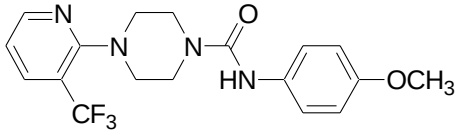	UP-II-125	2.0	1.2	
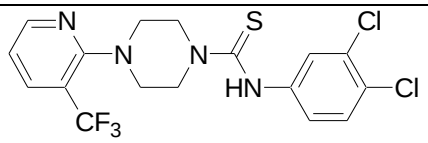	UP-II-126	2.1	1.5	
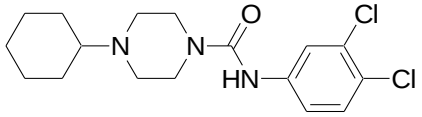	UP-II-127	0.9	0.9	
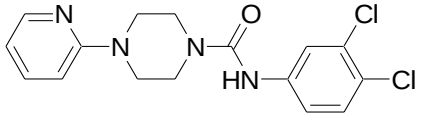	UP-II-128	1.8	0.8	
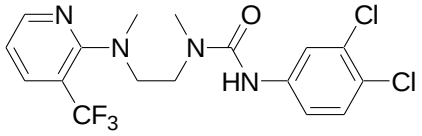	UP-II-131	2.8	1.1	
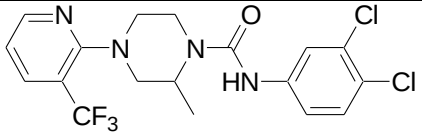	UP-II-132	3.5	2.2	

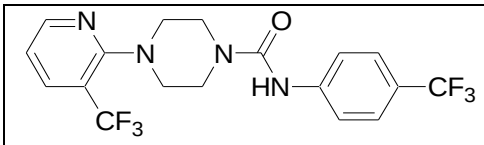	UP-II-133	2.0	1.8	
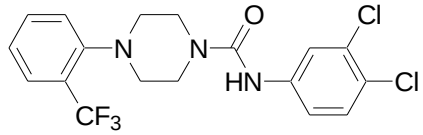	UP-II-134	1.1	0.8	
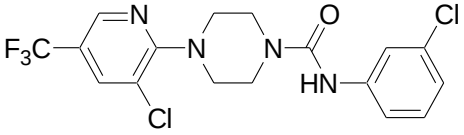	UP-II-138 (37B13)	4.2	2.5	Structure from screen
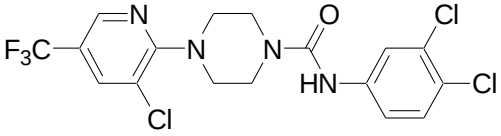	UP-II-139	4.1	2.3	
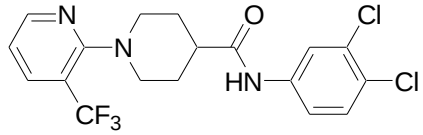	UP-II-141	2.9	1.2	
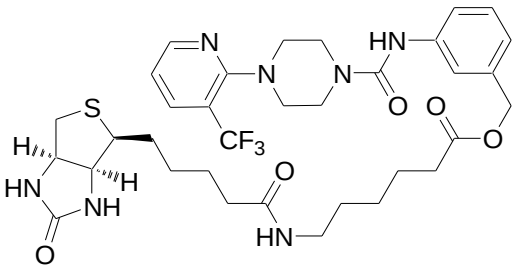	UP-II-148-2	0.9	0.8	
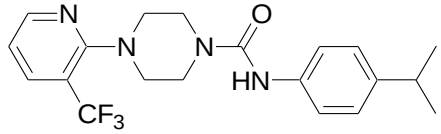	UP-II-152	2.2	1.3	

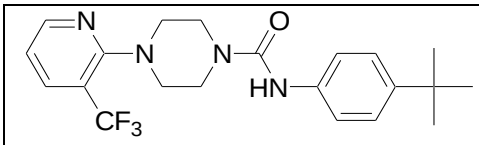	UP-III-8	1.9	1.8	
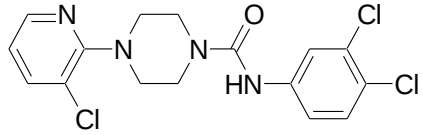	UP-III-12	1.2	1.5	
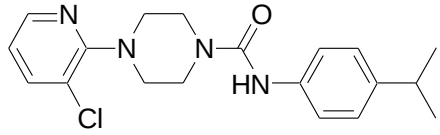	UP-III-13	2.0	1.2	
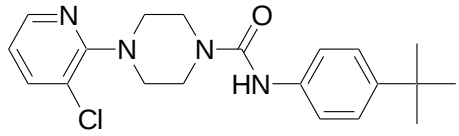	UP-III-14	2.9	1.7	
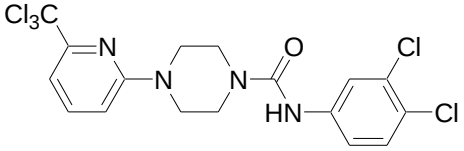	UP-III-23	2.3	1.6	
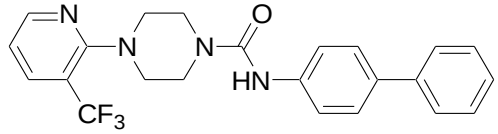	UP-III-24	1.8	1.5	
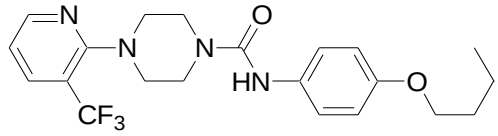	UP-III-25	0.9	1.0	
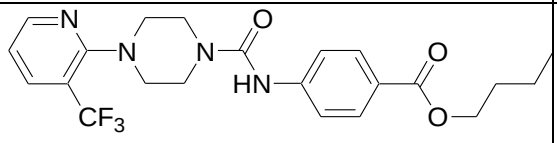	UP-III-26	2.2	1.6	

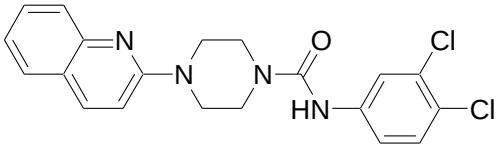	UP-III-30	1.5	1.1	
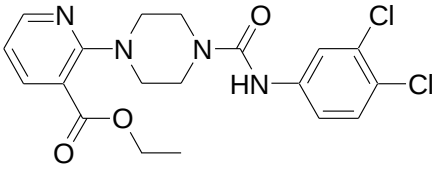	UP-III-31	1.6	1.4	
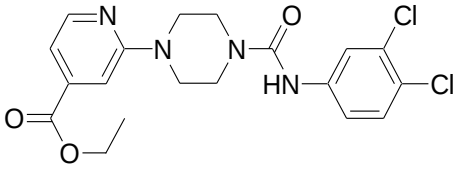	UP-III-40	1.2	1.4	
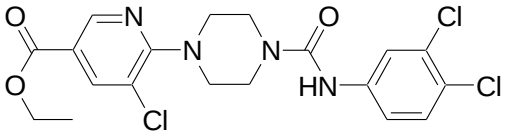	UP-III-41	1.9	1.8	
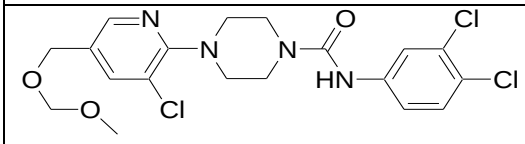	UP-III-48	1.3	1.9	
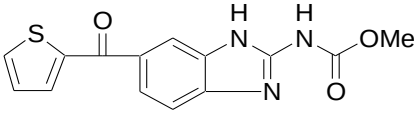	Nocodazole	4.7		control

REFERENCES

1. Rajagopalan, H. & Lengauer, C. Aneuploidy and cancer. *Nature* **432**, 338-41 (2004).
2. Mitchison, T. J. & Salmon, E. D. Mitosis: a history of division. *Nat Cell Biol* **3**, E17-21 (2001).
3. Inoue, S. & Salmon, E. D. Force generation by microtubule assembly/disassembly in mitosis and related movements. *Mol Biol Cell* **6**, 1619-40 (1995).
4. Lampson, M. A. & Kapoor, T. M. Unraveling cell division mechanisms with small-molecule inhibitors. *Nat Chem Biol* **2**, 19-27 (2006).
5. Jordan, M. A. & Wilson, L. Microtubules as a target for anticancer drugs. *Nat Rev Cancer* **4**, 253-65 (2004).
6. Inoue, S. [Polarization optical studies of the mitotic spindle. I. The demonstration of spindle fibers in living cells.]. *Chromosoma* **5**, 487-500 (1953).
7. Inoue, S. The effect of colchicine on the microscopic and submicroscopic structure of the mitotic spindle. *Exp. Cell Res. Suppl* **2**, 305 (1952).
8. Inoue, S. Cell division and the mitotic spindle. *J Cell Biol* **91**, 131s-147s (1981).
9. Borisy, G. G. & Taylor, E. W. The mechanism of action of colchicine. Binding of colchincine-3H to cellular protein. *J Cell Biol* **34**, 525-33 (1967).
10. Chen, R. H., Waters, J. C., Salmon, E. D. & Murray, A. W. Association of spindle assembly checkpoint component XMAD2 with unattached kinetochores. *Science* **274**, 242-6 (1996).
11. Waters, J. C., Chen, R. H., Murray, A. W. & Salmon, E. D. Localization of Mad2 to kinetochores depends on microtubule attachment, not tension. *J Cell Biol* **141**, 1181-91 (1998).
12. Li, Y. & Benezra, R. Identification of a human mitotic checkpoint gene: hsMAD2. *Science* **274**, 246-8 (1996).
13. Lampson, M. A., Renduchitala, K., Khodjakov, A. & Kapoor, T. M. Correcting improper chromosome-spindle attachments during cell division. *Nat Cell Biol* **6**, 232-7 (2004).
14. Peterson, J. R. & Mitchison, T. J. Small molecules, big impact: a history of chemical inhibitors and the cytoskeleton. *Chem Biol* **9**, 1275-85 (2002).
15. Carter, S. B. Effects of cytochalasins on mammalian cells. *Nature* **213**, 261-4 (1967).
16. Wessells, N. K. et al. Microfilaments in cellular and developmental processes. *Science* **171**, 135-43 (1971).
17. Straight, A. F. et al. Dissecting temporal and spatial control of cytokinesis with a myosin II Inhibitor. *Science* **299**, 1743-7 (2003).

18. Yarrow, J. C., Totsukawa, G., Charras, G. T. & Mitchison, T. J. Screening for cell migration inhibitors via automated microscopy reveals a Rho-kinase inhibitor. *Chem Biol* **12**, 385-95 (2005).
19. Corcoran, L. J., Mitchison, T. J. & Liu, Q. A novel action of histone deacetylase inhibitors in a protein aggresome disease model. *Curr Biol* **14**, 488-92 (2004).
20. Pelish, H. E. et al. Secramine inhibits Cdc42-dependent functions in cells and Cdc42 activation in vitro. *Nat Chem Biol* **2**, 39-46 (2006).
21. Kau, T. R. et al. A chemical genetic screen identifies inhibitors of regulated nuclear export of a Forkhead transcription factor in PTEN-deficient tumor cells. *Cancer Cell* **4**, 463-76 (2003).
22. Yam, P. T. et al. Actin-myosin network reorganization breaks symmetry at the cell rear to spontaneously initiate polarized cell motility. *J Cell Biol* **178**, 1207-21 (2007).
23. Klausner, R. D., Donaldson, J. G. & Lippincott-Schwartz, J. Brefeldin A: insights into the control of membrane traffic and organelle structure. *J Cell Biol* **116**, 1071-80 (1992).
24. Mossessova, E., Corpina, R. A. & Goldberg, J. Crystal structure of ARF1*Sec7 complexed with Brefeldin A and its implications for the guanine nucleotide exchange mechanism. *Mol Cell* **12**, 1403-11 (2003).
25. Keeler, R. F. & Binns, W. Teratogenic compounds of Veratrum californicum (Durand). V. Comparison of cyclopian effects of steroidal alkaloids from the plant and structurally related compounds from other sources. *Teratology* **1**, 5-10 (1968).
26. Ingham, P. W. & McMahon, A. P. Hedgehog signaling in animal development: paradigms and principles. *Genes Dev* **15**, 3059-87 (2001).
27. Chen, J. K., Taipale, J., Cooper, M. K. & Beachy, P. A. Inhibition of Hedgehog signaling by direct binding of cyclopamine to Smoothened. *Genes Dev* **16**, 2743-8 (2002).
28. Katano, M. Hedgehog signaling pathway as a therapeutic target in breast cancer. *Cancer Lett* **227**, 99-104 (2005).
29. Alaimo, P. J., Shogren-Knaak, M. A. & Shokat, K. M. Chemical genetic approaches for the elucidation of signaling pathways. *Curr Opin Chem Biol* **5**, 360-7 (2001).
30. Burkard, M. E. et al. Chemical genetics reveals the requirement for Polo-like kinase 1 activity in positioning RhoA and triggering cytokinesis in human cells. *Proc Natl Acad Sci U S A* **104**, 4383-8 (2007).
31. Provance, D. W., Jr. et al. Chemical-genetic inhibition of a sensitized mutant myosin Vb demonstrates a role in peripheral-pericentriolar membrane traffic. *Proc Natl Acad Sci U S A* **101**, 1868-73 (2004).
32. Ubersax, J. A. et al. Targets of the cyclin-dependent kinase Cdk1. *Nature* **425**, 859-64 (2003).

33. Stockwell, B. R. & Schreiber, S. L. Probing the role of homomeric and heteromeric receptor interactions in TGF-beta signaling using small molecule dimerizers. *Curr Biol* **8**, 761-70 (1998).
34. Spencer, D. M. et al. Functional analysis of Fas signaling in vivo using synthetic inducers of dimerization. *Curr Biol* **6**, 839-47 (1996).
35. Schneekloth, J. S., Jr. et al. Chemical genetic control of protein levels: selective in vivo targeted degradation. *J Am Chem Soc* **126**, 3748-54 (2004).
36. Mootz, H. D. & Muir, T. W. Protein splicing triggered by a small molecule. *J Am Chem Soc* **124**, 9044-5 (2002).
37. Schwartz, E. C., Saez, L., Young, M. W. & Muir, T. W. Post-translational enzyme activation in an animal via optimized conditional protein splicing. *Nat Chem Biol* **3**, 50-4 (2007).
38. Thompson, L. A. & Ellman, J. A. Synthesis and Applications of Small Molecule Libraries. *Chem Rev* **96**, 555-600 (1996).
39. Schreiber, S. L. Target-oriented and diversity-oriented organic synthesis in drug discovery. *Science* **287**, 1964-9 (2000).
40. Evans, B. E. et al. Methods for drug discovery: development of potent, selective, orally effective cholecystokinin antagonists. *J Med Chem* **31**, 2235-46 (1988).
41. Gray, N. S. et al. Exploiting chemical libraries, structure, and genomics in the search for kinase inhibitors. *Science* **281**, 533-8 (1998).
42. Chang, Y. T. et al. Synthesis and application of functionally diverse 2,6,9-trisubstituted purine libraries as CDK inhibitors. *Chem Biol* **6**, 361-75 (1999).
43. Lipinski, C. A., Lombardo, F., Dominy, B. W. & Feeney, P. J. Experimental and computational approaches to estimate solubility and permeability in drug discovery and development settings. *Adv Drug Deliv Rev* **46**, 3-26 (2001).
44. Boehm, H. J. et al. Novel inhibitors of DNA gyrase: 3D structure based biased needle screening, hit validation by biophysical methods, and 3D guided optimization. A promising alternative to random screening. *J Med Chem* **43**, 2664-74 (2000).
45. Shuker, S. B., Hajduk, P. J., Meadows, R. P. & Fesik, S. W. Discovering high-affinity ligands for proteins: SAR by NMR. *Science* **274**, 1531-4 (1996).
46. Erlanson, D. A. et al. Site-directed ligand discovery. *Proc Natl Acad Sci U S A* **97**, 9367-72 (2000).
47. Liu, G. et al. Novel p-arylthio cinnamides as antagonists of leukocyte function-associated antigen-1/intracellular adhesion molecule-1 interaction. 2. Mechanism of inhibition and structure-based improvement of pharmaceutical properties. *J Med Chem* **44**, 1202-10 (2001).

48. Arkin, M. R. et al. Binding of small molecules to an adaptive protein-protein interface. *Proc Natl Acad Sci U S A* **100**, 1603-8 (2003).
49. McMillan, K. et al. Allosteric inhibitors of inducible nitric oxide synthase dimerization discovered via combinatorial chemistry. *Proc Natl Acad Sci U S A* **97**, 1506-11 (2000).
50. Last-Barney, K. et al. Binding site elucidation of hydantoin-based antagonists of LFA-1 using multidisciplinary technologies: evidence for the allosteric inhibition of a protein--protein interaction. *J Am Chem Soc* **123**, 5643-50 (2001).
51. Gorczynski, M. J. et al. Allosteric inhibition of the protein-protein interaction between the leukemia-associated proteins Runx1 and CBFbeta. *Chem Biol* **14**, 1186-97 (2007).
52. McGovern, S. L., Helfand, B. T., Feng, B. & Shoichet, B. K. A specific mechanism of nonspecific inhibition. *J Med Chem* **46**, 4265-72 (2003).
53. Spring, D. R. Chemical genetics to chemical genomics: small molecules offer big insights. *Chem Soc Rev* **34**, 472-82 (2005).
54. Kwok, T. C. et al. A small-molecule screen in C. elegans yields a new calcium channel antagonist. *Nature* **441**, 91-5 (2006).
55. Mayer, T. U. et al. Small molecule inhibitor of mitotic spindle bipolarity identified in a phenotype-based screen. *Science* **286**, 971-4 (1999).
56. Kapoor, T. M., Mayer, T. U., Coughlin, M. L. & Mitchison, T. J. Probing spindle assembly mechanisms with monastrol, a small molecule inhibitor of the mitotic kinesin, Eg5. *J Cell Biol* **150**, 975-88 (2000).
57. Kapoor, T. M. & Mitchison, T. J. Eg5 is static in bipolar spindles relative to tubulin: evidence for a static spindle matrix. *J Cell Biol* **154**, 1125-33 (2001).
58. Kwok, B. H. et al. Allosteric inhibition of kinesin-5 modulates its processive directional motility. *Nat Chem Biol* **2**, 480-5 (2006).
59. Canman, J. C. et al. Determining the position of the cell division plane. *Nature* **424**, 1074-8 (2003).
60. Peterson, R. T., Link, B. A., Dowling, J. E. & Schreiber, S. L. Small molecule developmental screens reveal the logic and timing of vertebrate development. *Proc Natl Acad Sci U S A* **97**, 12965-9 (2000).
61. Chan, J., Bayliss, P. E., Wood, J. M. & Roberts, T. M. Dissection of angiogenic signaling in zebrafish using a chemical genetic approach. *Cancer Cell* **1**, 257-67 (2002).
62. Shinya, M., Koshida, S., Sawada, A., Kuroiwa, A. & Takeda, H. Fgf signalling through MAPK cascade is required for development of the subpallial telencephalon in zebrafish embryos. *Development* **128**, 4153-64 (2001).
63. Knight, Z. A. & Shokat, K. M. Features of selective kinase inhibitors. *Chem Biol* **12**, 621-37 (2005).

64. Godl, K. et al. An efficient proteomics method to identify the cellular targets of protein kinase inhibitors. *Proc Natl Acad Sci U S A* **100**, 15434-9 (2003).
65. Fabian, M. A. et al. A small molecule-kinase interaction map for clinical kinase inhibitors. *Nat Biotechnol* **23**, 329-36 (2005).
66. Karaman, M. W. et al. A quantitative analysis of kinase inhibitor selectivity. *Nat Biotechnol* **26**, 127-32 (2008).
67. Bantscheff, M. et al. Quantitative chemical proteomics reveals mechanisms of action of clinical ABL kinase inhibitors. *Nat Biotechnol* **25**, 1035-44 (2007).
68. Weiss, W. A., Taylor, S. S. & Shokat, K. M. Recognizing and exploiting differences between RNAi and small-molecule inhibitors. *Nat Chem Biol* **3**, 739-44 (2007).
69. Cohen, M. S., Zhang, C., Shokat, K. M. & Taunton, J. Structural bioinformatics-based design of selective, irreversible kinase inhibitors. *Science* **308**, 1318-21 (2005).
70. Bettencourt-Dias, M. et al. Genome-wide survey of protein kinases required for cell cycle progression. *Nature* **432**, 980-7 (2004).
71. Kittler, R. & Buchholz, F. Functional genomic analysis of cell division by endoribonuclease-prepared siRNAs. *Cell Cycle* **4**, 564-7 (2005).
72. Fitzgerald, K. RNAi versus small molecules: different mechanisms and specificities can lead to different outcomes. *Curr Opin Drug Discov Devel* **8**, 557-66 (2005).
73. Specht, K. M. & Shokat, K. M. The emerging power of chemical genetics. *Curr Opin Cell Biol* **14**, 155-9 (2002).
74. Tan, D. S. Diversity-oriented synthesis: exploring the intersections between chemistry and biology. *Nat Chem Biol* **1**, 74-84 (2005).
75. Lipinski, C. & Hopkins, A. Navigating chemical space for biology and medicine. *Nature* **432**, 855-61 (2004).
76. De Corte, B. L. From 4,5,6,7-Tetrahydro-5-methylimidazo[4,5,1-jk](1,4)benzodiazepin-2(1H)-one (TIBO) to Etravirine (TMC125): Fifteen Years of Research on Non-Nucleoside Inhibitors of HIV-1 Reverse Transcriptase. *Journal of Medicinal Chemistry* **48**, 1689-1696 (2005).
77. Sorbera, L. A., Castaner, J. & Martin, L. Revaprazan Hydrochloride: Treatment of GERD, H+/K+-ATPase inhibitor, antiulcer drug. *Drugs of the Future* **29**, 455-459 (2004).
78. Breault, G. A. et al. Cyclin-dependent kinase 4 inhibitors as a treatment for cancer. Part 2: identification and optimisation of substituted 2,4-bis anilino pyrimidines. *Bioorg Med Chem Lett* **13**, 2961-6 (2003).
79. Legendre, P. & Legendre, L. *Numerical ecology* (Elsevier, Amsterdam ; New York, 1998).
80. Hotha, S. et al. HR22C16: a potent small-molecule probe for the dynamics of cell division. *Angew Chem Int Ed Engl* **42**, 2379-82 (2003).

81. Feng, B. Y., Shelat, A., Doman, T. N., Guy, R. K. & Shoichet, B. K. High-throughput assays for promiscuous inhibitors. *Nat Chem Biol* **1**, 146-148 (2005).
82. Burdine, L. & Kodadek, T. Target identification in chemical genetics: the (often) missing link. *Chem Biol* **11**, 593-7 (2004).
83. Davis-Ward, R., Mook, R. A., Jr., Neeb, M. J. & Salovich, J. M. in *PCT Int. Appl.* 115 pp. ((SmithKline Beecham Corporation, USA). WO 2004074244, 2004).
84. Barr, F. A., Sillje, H. H. & Nigg, E. A. Polo-like kinases and the orchestration of cell division. *Nat Rev Mol Cell Biol* **5**, 429-40 (2004).
85. Takai, N., Hamanaka, R., Yoshimatsu, J. & Miyakawa, I. Polo-like kinases (Plks) and cancer. *Oncogene* **24**, 287-91 (2005).
86. Compton, D. A. Spindle assembly in animal cells. *Annu Rev Biochem* **69**, 95-114 (2000).
87. Sharp, D. J., Rogers, G. C. & Scholey, J. M. Microtubule motors in mitosis. *Nature* **407**, 41-7 (2000).
88. Sunkel, C. E. & Glover, D. M. polo, a mitotic mutant of Drosophila displaying abnormal spindle poles. *J Cell Sci* **89 (Pt 1)**, 25-38 (1988).
89. Llamazares, S. et al. polo encodes a protein kinase homolog required for mitosis in Drosophila. *Genes Dev* **5**, 2153-65 (1991).
90. Kitada, K., Johnson, A. L., Johnston, L. H. & Sugino, A. A multicopy suppressor gene of the Saccharomyces cerevisiae G1 cell cycle mutant gene dbf4 encodes a protein kinase and is identified as CDC5. *Mol Cell Biol* **13**, 4445-57 (1993).
91. Takizawa, C. G. & Morgan, D. O. Control of mitosis by changes in the subcellular location of cyclin-B1-Cdk1 and Cdc25C. *Curr Opin Cell Biol* **12**, 658-65 (2000).
92. Lane, H. A. & Nigg, E. A. Antibody microinjection reveals an essential role for human polo-like kinase 1 (Plk1) in the functional maturation of mitotic centrosomes. *J Cell Biol* **135**, 1701-13 (1996).
93. van Vugt, M. A. et al. Polo-like kinase-1 is required for bipolar spindle formation but is dispensable for anaphase promoting complex/Cdc20 activation and initiation of cytokinesis. *J Biol Chem* **279**, 36841-54 (2004).
94. Sumara, I. et al. Roles of polo-like kinase 1 in the assembly of functional mitotic spindles. *Curr Biol* **14**, 1712-22 (2004).
95. Nasmyth, K., Peters, J. M. & Uhlmann, F. Splitting the chromosome: cutting the ties that bind sister chromatids. *Science* **288**, 1379-85 (2000).
96. Golan, A., Yudkovsky, Y. & Hershko, A. The cyclin-ubiquitin ligase activity of cyclosome/APC is jointly activated by protein kinases Cdk1-cyclin B and Plk. *J Biol Chem* **277**, 15552-7 (2002).
97. Kraft, C. et al. Mitotic regulation of the human anaphase-promoting complex by phosphorylation. *Embo J* **22**, 6598-609 (2003).

98. Adams, R. R., Tavares, A. A., Salzberg, A., Bellen, H. J. & Glover, D. M. pavarotti encodes a kinesin-like protein required to organize the central spindle and contractile ring for cytokinesis. *Genes Dev* **12**, 1483-94 (1998).
99. Neef, R. et al. Phosphorylation of mitotic kinesin-like protein 2 by polo-like kinase 1 is required for cytokinesis. *J Cell Biol* **162**, 863-75 (2003).
100. Zhou, T., Aumais, J. P., Liu, X., Yu-Lee, L. Y. & Erikson, R. L. A role for Plk1 phosphorylation of NudC in cytokinesis. *Dev Cell* **5**, 127-38 (2003).
101. Niiya, F., Tatsumoto, T., Lee, K. S. & Miki, T. Phosphorylation of the cytokinesis regulator ECT2 at G2/M phase stimulates association of the mitotic kinase Plk1 and accumulation of GTP-bound RhoA. *Oncogene* **25**, 827-37 (2006).
102. McInnes, C., Mezna, M. & Fischer, P. M. Progress in the discovery of polo-like kinase inhibitors. *Curr Top Med Chem* **5**, 181-97 (2005).
103. Winkles, J. A. & Alberts, G. F. Differential regulation of polo-like kinase 1, 2, 3, and 4 gene expression in mammalian cells and tissues. *Oncogene* **24**, 260-6 (2005).
104. Spankuch-Schmitt, B., Bereiter-Hahn, J., Kaufmann, M. & Strebhardt, K. Effect of RNA silencing of polo-like kinase-1 (PLK1) on apoptosis and spindle formation in human cancer cells. *J Natl Cancer Inst* **94**, 1863-77 (2002).
105. Spankuch-Schmitt, B. et al. Downregulation of human polo-like kinase activity by antisense oligonucleotides induces growth inhibition in cancer cells. *Oncogene* **21**, 3162-71 (2002).
106. Cogswell, J. P., Brown, C. E., Bisi, J. E. & Neill, S. D. Dominant-negative polo-like kinase 1 induces mitotic catastrophe independent of cdc25C function. *Cell Growth Differ* **11**, 615-23 (2000).
107. Liu, X., Lei, M. & Erikson, R. L. Normal cells, but not cancer cells, survive severe Plk1 depletion. *Mol Cell Biol* **26**, 2093-108 (2006).
108. Steegmaier, M. et al. BI 2536, a potent and selective inhibitor of polo-like kinase 1, inhibits tumor growth in vivo. *Curr Biol* **17**, 316-22 (2007).
109. Gumireddy, K. et al. ON01910, a non-ATP-competitive small molecule inhibitor of Plk1, is a potent anticancer agent. *Cancer Cell* **7**, 275-86 (2005).
110. McInnes, C., Meades, C., Mezna, M. & Fischer, P. in *PCT Int. Appl.* 43 pp. ((Cyclacel Limited, UK). WO 2004067000, 2004).
111. McInnes, C. et al. Inhibitors of Polo-like kinase reveal roles in spindle-pole maintenance. *Nat Chem Biol* **2**, 608-17 (2006).
112. Lenart, P. et al. The small-molecule inhibitor BI 2536 reveals novel insights into mitotic roles of polo-like kinase 1. *Curr Biol* **17**, 304-15 (2007).

113. Khodjakov, A., Copenagle, L., Gordon, M. B., Compton, D. A. & Kapoor, T. M. Minus-end capture of preformed kinetochore fibers contributes to spindle morphogenesis. *J Cell Biol* **160**, 671-83 (2003).
114. Toyoshima-Morimoto, F., Taniguchi, E. & Nishida, E. Plk1 promotes nuclear translocation of human Cdc25C during prophase. *EMBO Rep* **3**, 341-8 (2002).
115. Cheng, Y. & Prusoff, W. H. Relationship between the inhibition constant (K1) and the concentration of inhibitor which causes 50 per cent inhibition (I50) of an enzymatic reaction. *Biochem Pharmacol* **22**, 3099-108 (1973).
116. Nigg, E. A. Mitotic kinases as regulators of cell division and its checkpoints. *Nat Rev Mol Cell Biol* **2**, 21-32 (2001).
117. Hauf, S. et al. The small molecule Hesperadin reveals a role for Aurora B in correcting kinetochore-microtubule attachment and in maintaining the spindle assembly checkpoint. *J Cell Biol* **161**, 281-94 (2003).
118. Niiya, F., Xie, X., Lee, K. S., Inoue, H. & Miki, T. Inhibition of cyclin-dependent kinase 1 induces cytokinesis without chromosome segregation in an ECT2 and MgcRacGAP-dependent manner. *J Biol Chem* **280**, 36502-9 (2005).
119. Dogterom, M., Kerssemakers, J. W., Romet-Lemonne, G. & Janson, M. E. Force generation by dynamic microtubules. *Curr Opin Cell Biol* **17**, 67-74 (2005).
120. Goshima, G., Wollman, R., Stuurman, N., Scholey, J. M. & Vale, R. D. Length control of the metaphase spindle. *Curr Biol* **15**, 1979-88 (2005).
121. Li, X. & Nicklas, R. B. Mitotic forces control a cell-cycle checkpoint. *Nature* **373**, 630-2 (1995).
122. Waters, J. C., Mitchison, T. J., Rieder, C. L. & Salmon, E. D. The kinetochore microtubule minus-end disassembly associated with poleward flux produces a force that can do work. *Mol Biol Cell* **7**, 1547-58 (1996).
123. Gergely, F., Draviam, V. M. & Raff, J. W. The ch-TOG/XMAP215 protein is essential for spindle pole organization in human somatic cells. *Genes Dev* **17**, 336-41 (2003).
124. Joseph, J., Liu, S. T., Jablonski, S. A., Yen, T. J. & Dasso, M. The RanGAP1-RanBP2 complex is essential for microtubule-kinetochore interactions in vivo. *Curr Biol* **14**, 611-7 (2004).
125. Garrett, S., Auer, K., Compton, D. A. & Kapoor, T. M. hTPX2 is required for normal spindle morphology and centrosome integrity during vertebrate cell division. *Curr Biol* **12**, 2055-9 (2002).
126. Gruber, J., Harborth, J., Schnabel, J., Weber, K. & Hatzfeld, M. The mitotic-spindle-associated protein astrin is essential for progression through mitosis. *J Cell Sci* **115**, 4053-9 (2002).

127. Adams, R. R., Maiato, H., Earnshaw, W. C. & Carmena, M. Essential roles of Drosophila inner centromere protein (INCENP) and aurora B in histone H3 phosphorylation, metaphase chromosome alignment, kinetochore disjunction, and chromosome segregation. *J Cell Biol* **153**, 865-80 (2001).
128. Holt, S. V. et al. Silencing Cenp-F weakens centromeric cohesion, prevents chromosome alignment and activates the spindle checkpoint. *J Cell Sci* **118**, 4889-900 (2005).
129. Zhu, C. et al. Functional analysis of human microtubule-based motor proteins, the kinesins and dyneins, in mitosis/cytokinesis using RNA interference. *Mol Biol Cell* **16**, 3187-99 (2005).
130. Dai, J., Sultan, S., Taylor, S. S. & Higgins, J. M. The kinase haspin is required for mitotic histone H3 Thr 3 phosphorylation and normal metaphase chromosome alignment. *Genes Dev* **19**, 472-88 (2005).
131. McEwen, B. F., Heagle, A. B., Cassels, G. O., Buttle, K. F. & Rieder, C. L. Kinetochore fiber maturation in PtK1 cells and its implications for the mechanisms of chromosome congression and anaphase onset. *J Cell Biol* **137**, 1567-80 (1997).
132. Karsenti, E. & Vernos, I. The mitotic spindle: a self-made machine. *Science* **294**, 543-7 (2001).
133. Nedelec, F., Surrey, T. & Karsenti, E. Self-organisation and forces in the microtubule cytoskeleton. *Curr Opin Cell Biol* **15**, 118-24 (2003).
134. Maiato, H., Rieder, C. L. & Khodjakov, A. Kinetochore-driven formation of kinetochore fibers contributes to spindle assembly during animal mitosis. *J Cell Biol* **167**, 831-40 (2004).
135. Mahoney, N. M., Goshima, G., Douglass, A. D. & Vale, R. D. Making microtubules and mitotic spindles in cells without functional centrosomes. *Curr Biol* **16**, 564-9 (2006).
136. Tanaka, M. et al. An unbiased cell morphology-based screen for new, biologically active small molecules. *PLoS Biol* **3**, e128 (2005).
137. Petronczki, M., Glotzer, M., Kraut, N. & Peters, J. M. Polo-like kinase 1 triggers the initiation of cytokinesis in human cells by promoting recruitment of the RhoGEF Ect2 to the central spindle. *Dev Cell* **12**, 713-25 (2007).
138. Brennan, I. M., Peters, U., Kapoor, T. M. & Straight, A. F. Polo-like kinase controls vertebrate spindle elongation and cytokinesis. *PLoS ONE* **2**, e409 (2007).
139. Vale, R. D. The molecular motor toolbox for intracellular transport. *Cell* **112**, 467-80 (2003).
140. Brunet, S. & Vernos, I. Chromosome motors on the move. From motion to spindle checkpoint activity. *EMBO Rep* **2**, 669-73 (2001).
141. Scholey, J. M., Brust-Mascher, I. & Mogilner, A. Cell division. *Nature* **422**, 746-52 (2003).

142. Allan, V. J. & Vale, R. D. Cell cycle control of microtubule-based membrane transport and tubule formation in vitro. *J Cell Biol* **113**, 347-59 (1991).
143. Rogers, S. L. et al. Regulation of melanosome movement in the cell cycle by reversible association with myosin V. *J Cell Biol* **146**, 1265-76 (1999).
144. Warren, G. & Wickner, W. Organelle inheritance. *Cell* **84**, 395-400 (1996).
145. Welte, M. A. et al. Regulation of lipid-droplet transport by the perilipin homolog LSD2. *Curr Biol* **15**, 1266-75 (2005).
146. Bagnara, J. T. & Hadley, M. E. in *Chromatophores and Color Change: The Comparative Physiology of Animal Pigmentation* 4-45 (Prentice-Hall, New Jersey, 1973).
147. Hadley, M. E. in *Endocrinology* 160-181 (Prentice Hall, New Jersey, 1984).
148. Daniolos, A., Lerner, A. B. & Lerner, M. R. Action of light on frog pigment cells in culture. *Pigment Cell Res* **3**, 38-43 (1990).
149. Rogers, S. L., Tint, I. S., Fanapour, P. C. & Gelfand, V. I. Regulated bidirectional motility of melanophore pigment granules along microtubules in vitro. *Proc Natl Acad Sci U S A* **94**, 3720-5 (1997).
150. McNiven, M. A. & Porter, K. R. Chromatophores--models for studying cytomatrix translocations. *J Cell Biol* **99**, 152s-158s (1984).
151. Rodionov, V. I., Hope, A. J., Svitkina, T. M. & Borisy, G. G. Functional coordination of microtubule-based and actin-based motility in melanophores. *Curr Biol* **8**, 165-8 (1998).
152. Rogers, S. L. & Gelfand, V. I. Myosin cooperates with microtubule motors during organelle transport in melanophores. *Curr Biol* **8**, 161-4 (1998).
153. Wu, X., Kocher, B., Wei, Q. & Hammer, J. A., 3rd. Myosin Va associates with microtubule-rich domains in both interphase and dividing cells. *Cell Motil Cytoskeleton* **40**, 286-303 (1998).
154. Rogers, S. L., Tint, I. S. & Gelfand, V. I. In vitro motility assay for melanophore pigment organelles. *Methods Enzymol* **298**, 361-72 (1998).
155. Nery, L. E. & Castrucci, A. M. Pigment cell signalling for physiological color change. *Comp Biochem Physiol A Physiol* **118**, 1135-44 (1997).
156. Haggarty, S. J. et al. Dissecting cellular processes using small molecules: identification of colchicine-like, taxol-like and other small molecules that perturb mitosis. *Chem Biol* **7**, 275-86 (2000).
157. Feng, Y. et al. Exo1: a new chemical inhibitor of the exocytic pathway. *Proc Natl Acad Sci U S A* **100**, 6469-74 (2003).
158. Heuser, J. Changes in lysosome shape and distribution correlated with changes in cytoplasmic pH. *J Cell Biol* **108**, 855-64 (1989).
159. Kuznetsov, S. A., Langford, G. M. & Weiss, D. G. Actin-dependent organelle movement in squid axoplasm. *Nature* **356**, 722-5 (1992).

160. Morris, R. L. & Hollenbeck, P. J. Axonal transport of mitochondria along microtubules and F-actin in living vertebrate neurons. *J Cell Biol* **131**, 1315-26 (1995).
161. Raposo, G. et al. Association of myosin I alpha with endosomes and lysosomes in mammalian cells. *Mol Biol Cell* **10**, 1477-94 (1999).
162. Valetti, C. et al. Role of dynactin in endocytic traffic: effects of dynamitin overexpression and colocalization with CLIP-170. *Mol Biol Cell* **10**, 4107-20 (1999).
163. Gross, S. P., Welte, M. A., Block, S. M. & Wieschaus, E. F. Coordination of opposite-polarity microtubule motors. *J Cell Biol* **156**, 715-24 (2002).
164. Welte, M. A. Bidirectional transport along microtubules. *Curr Biol* **14**, R525-37 (2004).
165. Reilein, A. R., Tint, I. S., Peunova, N. I., Enikolopov, G. N. & Gelfand, V. I. Regulation of organelle movement in melanophores by protein kinase A (PKA), protein kinase C (PKC), and protein phosphatase 2A (PP2A). *J Cell Biol* **142**, 803-13 (1998).
166. Bingham, J. B., King, S. J. & Schroer, T. A. Purification of dynactin and dynein from brain tissue. *Methods Enzymol* **298**, 171-84 (1998).
167. Bakthavatchalam, R. et al. in *PCT Int. Appl.* 209 pp. ((Neurogen Corporation, USA). WO 2002008221, 2002).
168. Valenzano, K. J. et al. N-(4-tertiarybutylphenyl)-4-(3-chloropyridin-2-yl)tetrahydropyrazine -1(2H)-carbox-amide (BCTC), a novel, orally effective vanilloid receptor 1 antagonist with analgesic properties: I. in vitro characterization and pharmacokinetic properties. *J Pharmacol Exp Ther* **306**, 377-86 (2003).
169. Pomonis, J. D. et al. N-(4-Tertiarybutylphenyl)-4-(3-cholorphyridin-2-yl)tetrahydropyrazine -1(2H)-carbox-amide (BCTC), a novel, orally effective vanilloid receptor 1 antagonist with analgesic properties: II. in vivo characterization in rat models of inflammatory and neuropathic pain. *J Pharmacol Exp Ther* **306**, 387-93 (2003).
170. Swanson, D. M. et al. Identification and biological evaluation of 4-(3-trifluoromethylpyridin-2-yl)piperazine-1-carboxylic acid (5-trifluoromethylpyridin-2-yl)amide, a high affinity TRPV1 (VR1) vanilloid receptor antagonist. *J Med Chem* **48**, 1857-72 (2005).
171. Clapham, D. E., Runnels, L. W. & Strubing, C. The TRP ion channel family. *Nat Rev Neurosci* **2**, 387-96 (2001).
172. Szallasi, A. & Blumberg, P. M. Vanilloid (Capsaicin) receptors and mechanisms. *Pharmacol Rev* **51**, 159-212 (1999).
173. Skibbens, R. V., Skeen, V. P. & Salmon, E. D. Directional instability of kinetochore motility during chromosome congression and segregation in mitotic newt lung cells: a push-pull mechanism. *J Cell Biol* **122**, 859-75 (1993).

174. Cassimeris, L., Rieder, C. L. & Salmon, E. D. Microtubule assembly and kinetochore directional instability in vertebrate monopolar spindles: implications for the mechanism of chromosome congression. *J Cell Sci* **107 (Pt 1)**, 285-97 (1994).
175. Rieder, C. L., Davison, E. A., Jensen, L. C., Cassimeris, L. & Salmon, E. D. Oscillatory movements of monooriented chromosomes and their position relative to the spindle pole result from the ejection properties of the aster and half-spindle. *J Cell Biol* **103**, 581-91 (1986).
176. Ault, J. G., DeMarco, A. J., Salmon, E. D. & Rieder, C. L. Studies on the ejection properties of asters: astral microtubule turnover influences the oscillatory behavior and positioning of mono-oriented chromosomes. *J Cell Sci* **99 (Pt 4)**, 701-10 (1991).
177. Levesque, A. A. & Compton, D. A. The chromokinesin Kid is necessary for chromosome arm orientation and oscillation, but not congression, on mitotic spindles. *J Cell Biol* **154**, 1135-46 (2001).
178. Kim, H. et al. Microtubule binding by dynactin is required for microtubule organization but not cargo transport. *J Cell Biol* **176**, 641-51 (2007).
179. Satir, P. Morphological aspects of ciliary motility. *J Gen Physiol* **50**, Suppl:241-58 (1967).
180. Ling, S. C., Fahrner, P. S., Greenough, W. T. & Gelfand, V. I. Transport of Drosophila fragile X mental retardation protein-containing ribonucleoprotein granules by kinesin-1 and cytoplasmic dynein. *Proc Natl Acad Sci U S A* **101**, 17428-33 (2004).
181. Kural, C. et al. Kinesin and dynein move a peroxisome in vivo: a tug-of-war or coordinated movement? *Science* **308**, 1469-72 (2005).
182. Aronov, A. M. & Murcko, M. A. Toward a pharmacophore for kinase frequent hitters. *J Med Chem* **47**, 5616-9 (2004).
183. Bebbington, D., Charrier, J.-D., Golec, J. M. C., Miller, A. & Knegtel, R. in *PCT Int. Appl.* 335 pp. ((Vertex Pharmaceuticals Incorporated, USA). WO 2002062789, 2002).
184. Wagner, K., Heitzer, H. & Oehlmann, L. Benzothiazole N-oxides. I. Synthesis and reactivity of 2-(alkoxycarbonyl)benzothiazole N-oxides. *Chemische Berichte* **106**, 640-54 (1973).
185. Reddy, P. E., Reddy, R. M. V. & Bell, S. C. in *PCT Int. Appl.* 189 pp. ((Temple University-of the Commonwealth System of Higher Education, USA; Onconova Therapeutics, Inc.). WO 2003072062, 2003).
186. Hoffman, D. B., Pearson, C. G., Yen, T. J., Howell, B. J. & Salmon, E. D. Microtubule-dependent changes in assembly of microtubule motor proteins and mitotic spindle checkpoint proteins at PtK1 kinetochores. *Mol Biol Cell* **12**, 1995-2009 (2001).
187. Qian, Y. W., Erikson, E., Li, C. & Maller, J. L. Activated polo-like kinase Plx1 is required at multiple points during mitosis in Xenopus laevis. *Mol Cell Biol* **18**, 4262-71 (1998).

188. Gross, S. P. et al. Interactions and regulation of molecular motors in Xenopus melanophores. *J Cell Biol* **156**, 855-65 (2002).
189. Kwok, B. H., Yang, J. G. & Kapoor, T. M. The rate of bipolar spindle assembly depends on the microtubule-gliding velocity of the mitotic kinesin Eg5. *Curr Biol* **14**, 1783-8 (2004).
190. Kapoor, T. M. & Mitchison, T. J. Allele-specific activators and inhibitors for kinesin. *Proc Natl Acad Sci U S A* **96**, 9106-11 (1999).